



THE UNIVERSITY OF
WAIKATO
Te Whare Wānanga o Waikato

Research Commons

<http://researchcommons.waikato.ac.nz/>

Research Commons at the University of Waikato

Copyright Statement:

The digital copy of this thesis is protected by the Copyright Act 1994 (New Zealand).

The thesis may be consulted by you, provided you comply with the provisions of the Act and the following conditions of use:

- Any use you make of these documents or images must be for research or private study purposes only, and you may not make them available to any other person.
- Authors control the copyright of their thesis. You will recognise the author's right to be identified as the author of the thesis, and due acknowledgement will be made to the author where appropriate.
- You will obtain the author's permission before publishing any material from the thesis.

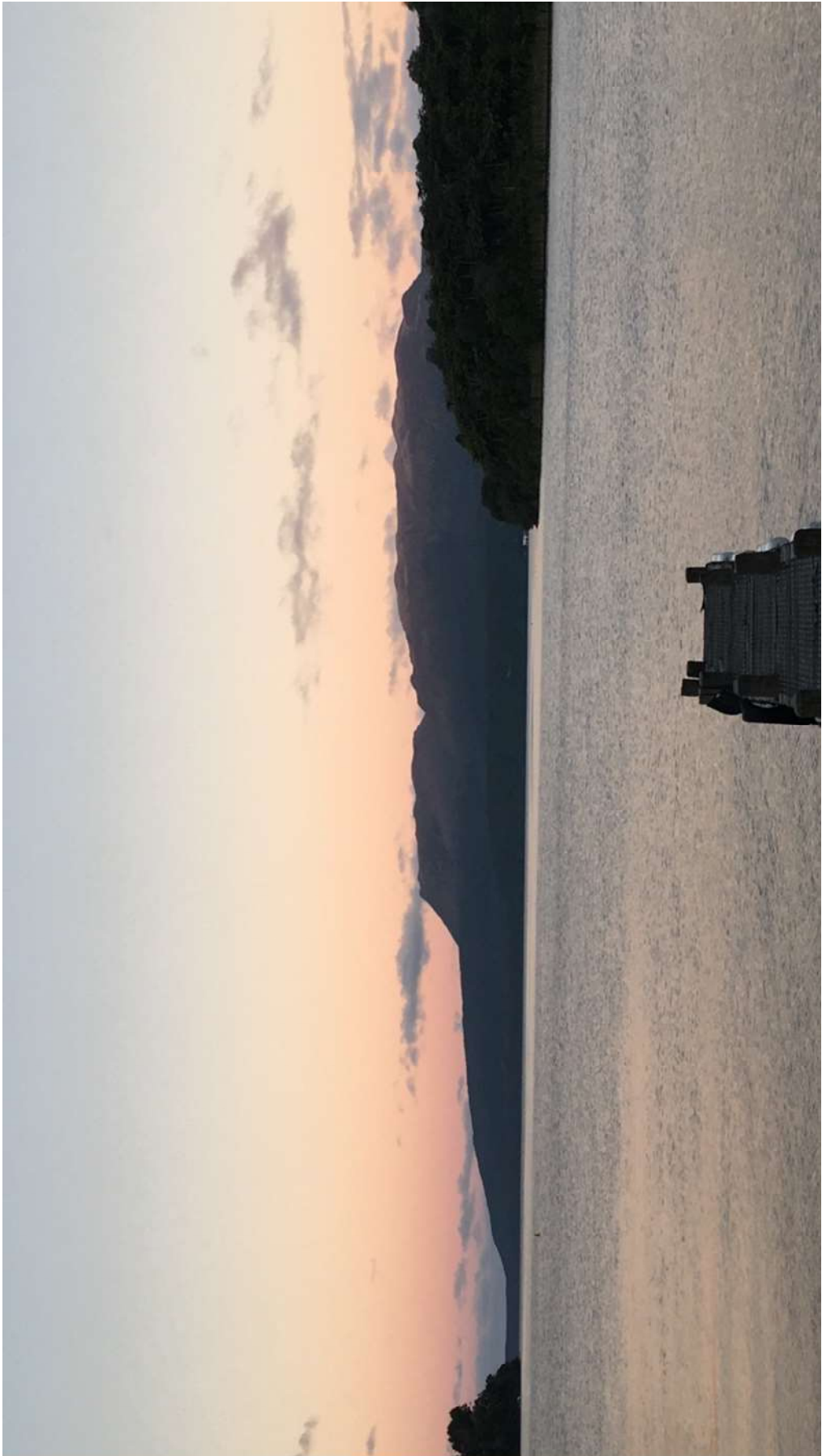
**The Presence, Speciation, and Movement of Arsenic in Lake
Tarawera**

A thesis
submitted in partial fulfilment
of the requirements for the degree
of
Masters of Science
in Chemistry
at
The University of Waikato
by
Kirstie-Lee May Nicole Cochrane



THE UNIVERSITY OF
WAIKATO
Te Whare Wānanga o Waikato

2020



Lake Tarawera at sunset, from the Western ramp. (Photo by Kirstie Cochrane)

ABSTRACT

Arsenic is a naturally occurring element with potential toxicity to humans depending on concentration and chemical state. Contamination of freshwater environments by arsenic has been seen globally, occurring through both natural and anthropogenic sources. This thesis explores the presence, speciation, and movement of arsenic within Lake Tarawera, including the related physical and biogeochemical processes that control the movement and state of arsenic within the water body and from inlet sources.

Lake Tarawera, in the Bay of Plenty Region, North Island, New Zealand is a large deep-water lake in an active volcanic region. Field measurements taken from Lake Tarawera were targeted towards a known localised geothermal area to explore spatial heterogeneity. The results show how the monomictic cycling regime of Lake Tarawera contributes to the retention of arsenic in the water column through increasing concentrations of benthic arsenic during the period of stratification across five open-water sites (196% difference between surface and benthic water As concentrations in March 2020), and homogenous distribution through winter overturning (10% maximum difference in As concentrations, statistically insignificant). The physical and chemical conditions of the lake (temperature and pH) and high solubility of arsenic retain dissolved species in the water column. Oxygen depletion is observed in the deepest part of the lake (2.3 mg L^{-1} at 79 m depth) which corresponds with increased benthic arsenic concentrations ($126 \text{ } \mu\text{g L}^{-1}$).

Inlets in the southern arm of the lake (Wairua Arm) are higher sources of arsenic into the water body than inlets in the main body of the lake, with arsenic concentrations from all sampled Wairua Arm inlets exceeding the World Health Organisation $10 \text{ } \mu\text{g L}^{-1}$ drinking water standard; dissolved concentrations ranging from $41.0\text{-}947 \text{ } \mu\text{g L}^{-1}$. One high volume waterfall (Rotomahana Waterfall) provides a per second arsenic loading of $16,400 \pm 2,660 \text{ } \mu\text{g As s}^{-1}$. The more toxic form of arsenic (As^{III}) was only detected in one instance, from a warm water stream inlet. Iron and manganese concentrations and the partitioning of these transition metals indicates the ratio of arsenic to these binding elements is not of the right order of

magnitude to remove substantial arsenic from the water column, as dissolved arsenic concentrations exceed that of both iron and manganese.

Water isotope ratios and dissolved arsenic concentrations from Rotomahana Waterfall show a complicated mixing regime, including influences such as wind, rainfall, other inlets, and opposing water flows coming from the main water and the high flow waterfall. High temperature and low flow waters from Hot Water Beach demonstrates the influence of inlet water temperature because they alter the movement and concentrations of arsenic heading out towards the open-water inlets. The high temperature of Hot Water Beach creates a localised area of thermal stratification, which causes surface mixing and dilution of the inlet waters with the nearest open-water site. Mixing then occurs with depth closer to the open-water site, passed the point of the hot water induced thermocline. These targeted samples highlight how well arsenic is diluted and buffered by such a large volume of water, and demonstrate the importance of stratification, temperature, and flow rate on the movement of As.

Laboratory and field studies attempted to minimise oxygen introduction to pore water samples using rhizons (pore water filters) and vacutainers. Arsenic speciation was retained in field samples in the vacutainers for up to three months, with concentrations of up to $2,230 \mu\text{g L}^{-1}$ of As^{III} measured; this result which led to laboratory experiments on the long-term storage and retention of As^{III} . However, the data from these laboratory studies were inconclusive for over-time analyses of two experiments; days 2, 26, and 55 after sample spiking for the first experiment, and days 2 and 29 for the second experiment. Vacutainers and rhizons extracted pore waters *in-situ* in attempt to minimise oxygen introduction to low dissolved oxygen samples; however, the methodology for long-term storage requires further research.

Speciation of arsenic occurs in the sediments due to the highly anoxic environment, with pore water As^{III} concentrations ranging exceeding $2,000 \mu\text{g L}^{-1}$ in the surface sediments and decreasing with depth. Sediment concentrations show distinct accumulation boundaries which are indicative of redox boundaries over time.

ACKNOWLEDGEMENTS

I would like to thank my supervisors; Megan Grainger and Amanda French, for your time and patience. You two make a great team; I felt supported, encouraged, and respected every step of the way. I appreciate the knocks on your door that were always welcomed, and your patience when I struggled to verbalise my ideas and questions. Your understanding and support with me trying to balance research with farm and family life has been exceptional, especially through the unprecedented year that 2020 has been.

This project was made possible thanks to Strategic Investment Funding from the University of Waikato.

To the team over in R block; Troy Baisden, Chris Eager, Rachel Murray, and Warwick Powrie, thank you for the help in field, the good conversation, and the action shots captured during field work. To Chris McBride for providing BOPRC data. Terry Beckett for providing samples from his routine Lake Tarawera quarterly sampling and allowing me to analyse them (UoW/BOPRC project), and to Lisa Pearson whose 2012 PhD thesis data has been used. To Danielle Blackwell, John Merring, and Thomas Corbett for your technical support. Annie Barker, for letting me work in your lab and helping me with some field gear. Noel Bates and Holly Harvey-Wishart for allowing me to use the earth science equipment including N₂ gas and vacuum pump. And finally, Matthew, thanks for being a backboard for nutting out concepts, knowing the answers to my computer or software related questions, the tearoom banter, and always having treats in your desk drawer!

To everyone in my life who supported me through this process, particularly through the COVID-19 setbacks which caused delays and left a lot riding on the unknown. James, Mum, Dad and Irene, Stephen and Antionette; if you all hadn't helped me juggle the children, this experience would have been very different. James, your support and encouragement over the past 4.5 years has meant everything. Thank you for all the conversations that meant little to you but helped me process what was going on in my head. To my sweet girls, Dulcie and Harriet; sorry about the long days at daycare, boring weekends at home, and single bedtime stories. I will make it up to you, I promise.

I would also like to acknowledge that I would never had made it here if not for Jo Lane, who let me in to Chem100 as a confused first-year undergraduate student with no science background. Jo, if you had not had faith in me, I may have entirely quit university or, worse, ended up with a psychology degree. I will be forever grateful for the door your class opened for me.

TABLE OF CONTENTS

Contents

ABSTRACT.....	i
ACKNOWLEDGEMENTS.....	iv
TABLE OF CONTENTS.....	vi
List of Figures.....	x
List of Tables.....	xiii
List of Abbreviations.....	1
1 CHAPTER ONE.....	3
LITERATURE REVIEW.....	3
1.1 Introduction.....	3
1.2 Arsenic.....	4
1.2.1 Concentrations of arsenic throughout the world.....	4
1.2.2 Toxicity of arsenic.....	5
1.2.3 Chemistry of Arsenic.....	6
1.3 Reactions of arsenic with other redox sensitive elements.....	9
1.3.1 Iron.....	11
1.3.2 Manganese.....	12
1.3.3 Sulphur.....	13
1.3.4 Other elements.....	13
1.3.5 Implications of redox/complexing molecules on arsenic in lake sediments.....	13
1.4 Chemistry of lake waters and sediments.....	14
1.4.1 Thermal stratification.....	16
1.4.2 Importance of sediment concentrations and physical parameters for elemental cycling in the water column.....	16
1.4.3 Pore Waters.....	18
1.5 Methodology for sampling and analysis of arsenic in water.....	19

1.5.1	In-field sampling methods.....	20
1.5.2	Laboratory analysis for quantification of arsenic.....	22
1.6	Regional geology and chemical history of Taupo Volcanic Zone and Lake Tarawera.....	23
1.6.1	The Rotorua Lakes, Bay of Plenty Region.....	24
1.6.2	Lake Tarawera.....	25
1.6.3	Major inflows to Lake Tarawera.....	26
1.7	Arsenic in Lake Tarawera.....	27
1.8	Summary.....	28
1.9	Aim / research objectives.....	28
2	CHAPTER TWO.....	30
	SITE OVERVIEW AND ANALYTICAL METHODS	30
2.1	Introduction.....	30
2.2	Site overview	30
2.3	Sampling collection	32
2.3.1	Evacuation of O ₂ from vacutainers and HPLC vials.....	32
2.3.2	Water collection of open-water sites and lake inlets.....	33
2.3.3	Sediments and pore water collection.....	33
2.4	Field methods.....	34
2.4.1	In-field instrumentation.....	34
2.5	Analytical and laboratory methods.....	34
2.5.1	Reagents and standards	34
2.5.2	Sediment extrusion from core and preparation for analysis.....	35
2.5.3	Digestion methods.....	36
2.5.4	In-lab validation of vacutainers in arsenic preservation.....	37
2.6	Instrumentation	38
2.6.1	ICP-MS for elemental analysis	38
2.6.2	HPLC for arsenic speciation	39
2.6.3	LGR OA-ICOS for isotope analysis	40

2.7 Data analysis	40
3 CHAPTER THREE	41
PHYSICAL PROPERTIES.....	41
3.1 Introduction.....	41
3.2 Temperature and oxygen profiles	41
3.3 Changes in temperature and dissolved oxygen profiles between 2019 and long-term monitoring programme data	46
4 CHAPTER FOUR	50
ARSENIC AND RELATED REDOX ELEMENTS	50
4.1 Introduction.....	50
4.2 Dissolved arsenic concentrations from Bay of Plenty Regional Council continuous monitoring data (2018-January 2019).....	51
4.3 Investigations into arsenic (speciation, dissolved, and particulate) from February 2019-March 2020.....	56
4.3.1 Arsenic speciation	57
4.3.2 Dissolved arsenic.....	58
4.3.3 Particulate arsenic, iron, and manganese in water samples.....	72
4.4 Summary.....	75
5 CHAPTER FIVE	77
SEDIMENTS AND PORE WATERS	77
5.1 Introduction.....	77
5.2 Method development for pore water sampling.....	78
5.3 In-field collection of pore waters from sediment cores using rhizons and vacutainers.....	85
5.4 Sediment core	88
<i>Core extraction complications</i>	88
6 CHAPTER SIX	93
CONCLUSIONS.....	93
6.1 Thesis summary	93
6.2 Recommendations for future work	96

References	98
Appendix	105

List of Figures

Figure 1-1. The four major species of As found in water. a) As ^{III} as arsenite oxyanion (As ₂ O ₃ ³⁻), b) As ^V as arsenate oxyanion (AsO ₄ ³⁻), c) As ^V as dimethylarsinic acid (DMA), d) As ^V as monomethylarsonic acid (MA).	7
Figure 1-2. Example of the inter-relation of As inputs, lake cycling, sediments, and thermal stratification. a) displays a lake with a redox anoxic/oxic boundary is displayed on the left, with no boundary on the right. b) shows the cycling occurring at the redox boundary, denoted by the star and adapted from Harland <i>et. al</i> (2015). ¹⁸	18
Figure 1-3. Rhizon system including connections for vacuum tubes or syringes. Taken from Seeberg-Elverfeldt et al (2005). ⁵²	22
Figure 1-4. The Taupo Volcanic Zone (red circle) within the North Island of New Zealand.	24
Figure 1-5. Close up map of Central North Island of New Zealand showing; a) Bay of Plenty Region circled in red. b) Closer image of a cluster of lakes, including Lake Tarawera indicated by the red star.....	25
Figure 2-1. a) New Zealand with the Bay of Plenty Region circled in red; b) location of Lake Tarawera, indicated by the red star, in relation to surrounding lakes; c) Red writing indicating the areas of focus for this research; the Wairua Arm and the only lake outlet; d) Sampling locations for all routinely taken samples.	31
Figure 2-2. Core extrusion using a piston and extruder rod to push sediment up through the core barrel into a custom made chamber for transferal into foil trays. a) extruder rod having pushed the piston part-way up through the core; b) the custom-made chamber where sediment is segmented; c) how pushing the plunger segments the sediment for collection.	35
Figure 3-1. CTD casts for temperature (°C) with depth (m) for a) February 2019; b) April 2019; c) August 2019; d) December 2019; e) March 2020, across the five open-water sites TAs1-5. Thermal stratification occurs between 10-25 m depth during the stratified period (a, b, d, and e), and the mixed period is shown by homogenous temperature with depth (c).	42
Figure 3-2 CTD casts for dissolved oxygen (mg L ⁻¹) with depth (m) for a) April 2019; b) August 2019. Seasonal fluctuation is seen between profiles, with the mixed season having more consistent concentration with depth (b), compared with during stratification (a).	43
Figure 3-3. Bay of Plenty Regional Council CTD (temperature) data by depth (m) covering the period 1996 to 2017. White space represents	

missing data, and the scale on the right represents temperature in °C. Note the sampling frequency has increased over time, with sampling increasing from 2 m increments to 1 m.	47
Figure 3-4. Bay of Plenty Regional Council CTD (dissolved oxygen) data covering period 1996 to 2017. White space represents missing data, and the scale on the right represents dissolved oxygen in mg L ⁻¹ . Note the sampling frequency has increased over time, with sampling increasing from 2 m increments to 1 m.	48
Figure 4-1. Geographical location of Lake Rotomahana in relation to Lake Tarawera. Man-made inlet RHMI is represented by the purple dot.	51
Figure 4-2. Location of surface inlets sampled quarterly by the UoW/BoPRC continuous monitoring programme ² (grey circles). Inlet As concentrations were compared between geographical close sites indicated by the red shapes (SE of Wairua Arm, circle; N main body, triangle; NW main body, square).	52
Figure 4-3. Dissolved As concentrations (µg L ⁻¹) for a) inlet sites sampled by UoW monitoring programme ² , excluding HW1, HW2, and Corner Pool; b) for HW1, HW2, and Corner Pool. Note the scale difference between (a) and (b). WHO drinking water standard (10 µg L ⁻¹) is indicated by the dashed line. Inlets correspond to the sample locations in Figure 4-2. Site names with directional labels indicate geographical grouping discussed in this section.	53
Figure 4-4. Dissolved As concentrations (µg L ⁻¹) for; a) inlet sites (excluding HW1); b) HW1 (note the change in y scale); c) across sampling instances (note change in x axis from sample name to date, and change in shape from date to inlet).	59
Figure 4-5. Arsenic concentrations (µg L ⁻¹) for open-water sampling sites TAs1-5. TAs1 is in the Wairua Arm (~20 m depth), close to HW1, with TAs5 in the main water body (80 m depth) and 2- 4 in between.....	63
Figure 4-6. Dissolved As concentrations (µg L ⁻¹) for each grab sample taken around RMHW and out towards TAs3. Samples are grouped by north (green) and south (blue) of the waterfall mouth and out towards open-water site TAs3 (red).	67
Figure 4-7. Water isotopes (per mil (‰)) for grab samples taken from RMHW, including RMHW, TAs3 surface and benthic. Coloured circles correlate to sample locations in relation to waterfall as outlined above: green (north), blue (south), and red out towards open water site TAs3.	68
Figure 4-8. Location and As concentration (µg L ⁻¹) of surface samples taken from HW1. Hot and cold samples were taken from each point due to the difference in temperature between the top and bottom waters (within the depth of a hand).	70

Figure 4-9. Water isotope (per mil (‰)) patterns from HW1 and TAs1, including grab samples in between to determine mixing patterns of the inlet water into the lake.	71
Figure 4-10. Photograph taken from Eastern side of Wairua Arm, near RMHW inlet site. Orange coloured coating appears on rocks and submerged branches.	73
Figure 4-11. Particulate As with Fe (pink) and Mn (blue) concentrations for a) all sites excluding HW1 and RMHW. b) HW1 and RMHW. Ratio of > 1 indicated more As than Fe or Mn.	74
Figure 5-1. Day-2 analysis for pore water concentrations ($\mu\text{g L}^{-1}$) of As^{III} and As^{V} with depth (from March 2020 sediment core), with sediment segment 1 being the surface sediments on the lake bottom. Sediment segment 1, 5, 8, and 11 correspond to depths of 3, 12, 23, and 31 cm, respectively.	87
Figure 5-2. a) Sediment core held in barrel; rhizons are attached for extraction of pore water into vacutainers; b) image from Pylonex website ⁹¹ depicting how the core barrel fits inside the gravity corer casing; c) barrel attached to core extruder with custom made segment extractor attached. Red circle shows where plug was unable to be wound further due to duct tape inside the core barrel.	89
Figure 5-3. Arsenic (As), iron (Fe), and manganese (Mn) concentrations per dry weight (mg kg^{-1}) with depth, 1 being the surface segment of sediment (0-3 cm) and 14 the deepest (~40 cm). a) depicts Fe (circle), Mn (cross), and As (square), and b) blue box from (a) expanded to show the variation in Mn (cross) and As (square) concentrations with depth.	90

List of Tables

Table 1-1. Dissociation constants for As ^{III} and As ^V (as arsenite and arsenate), showing the pH dependence on the charge of the oxide species. Table reproduced from O’Day (2006). ²⁰	9
Table 2-1. Summary of sample locations corresponding to the map in Figure 2-1.....	32
Table 2-2. ICP-MS Optimised Operating Conditions.....	38
Table 4-1. Summary statistics (2018-January 2019 collected by UoW/BoPRC) for clusters of inlet sites which are geographically close and have multiple data points (Figure 4-2).....	54
Table 4-2. Arsenic loading ($\mu\text{g s}^{-1}$) calculated (2018-January 2019) using flow rate (L s^{-1}) and dissolved As concentration ($\mu\text{g L}^{-1}$).....	55
Table 4-3. As loading for RMHW calculated from UoW/BoPRC flow gauging and corresponding dissolved As data ($\mu\text{g L}^{-1}$).	62
Table 4-4. Average As concentrations ($\mu\text{g L}^{-1}$) for open-water sites across all sample dates (February, April, August, December, and March).....	64
Table 4-5. Dissolved arsenic concentrations ($\mu\text{g L}^{-1}$) for equivalent hot and cold grab samples taken from HW1.....	70
Table 5-1. Summary of total As ($\mu\text{g L}^{-1}$) in spiked samples (analysed by ICP-MS) and As ^{III} , As ^V , and total As ($\mu\text{g L}^{-1}$, HPLC-ICP-MS).	79
Table 5-2. Percentage recoveries of As ^{III} in spiked samples for UoW Chapel Lake water and Type 1 water for nitrogen (N) and oxygen (O) vacutainers. DO of the samples is also reported.	81
Table 5-3. Summary of average total As ($\mu\text{g L}^{-1}$, ICP-MS) in spiked samples and As ^{III} , As ^V , and total As ($\mu\text{g L}^{-1}$, HPLC-ICP-MS). n = 3 unless otherwise stated.	83
Table 5-4. Percentage recoveries for As ^{III} spike samples in sediment pore water from core collected in March 2020.	83
Table 5-5. Depth range of sediment core samples segments to compare sediment samples with relevant pore waters.	86
Table 5-6. Concentration of As ^{III} and As ^V in pore waters at corresponding sediment segments.....	87

List of Abbreviations

As ^{III}	Arsenite (As ^{III} O ₃)
As ^V	Arsenate (As ^V O ₄)
BoPRC	Bay of Plenty Regional Council
CTD	Conductivity, temperature, and depth
DGT	Diffusive Gradient Thin-Film
DMA	Dimethylarsenic acid
DO	Dissolved oxygen
DOC	Department of Conservation
EDTA	Ethylenediaminetetraacetic acid
HDPE	High density polyethylene
HCl	Hydrochloric acid
HPLC	High performance liquid chromatography
HG-AAS	Hydride generation atomic absorption spectrophotometry
HW1	Hot Water Beach
ICP-MS	Inductively coupled mass spectrometer
K3(EDTA)	Tripotassium ethylenediaminetetraacetic acid
LGR OA-ICOS	Los Gatos Research Off-axis integrated cavity output spectrometer
MA	Monomethylarsonic acid
MFA	Middle Flax A
NIWA	National Institute of Water and Atmospheric Research
NW	North West
pE	Redox potential
PO ₄ ³⁻	Phosphate
PVC	Polyvinyl Chloride
Redox	Reduction-oxidation reactions
RMHI	Rotomahana Siphon
RMHS	Rotomahana Spring
RMHW	Rotomahana Waterfall
SE	South East

SPE	Solid phase extraction
SWI	Sediment-water interface
TIWA-45 EP	Triple isotope water analyzer
TVZ	Taupo Volcanic Zone
UoW	University of Waikato
WHO	World Health Organisation
WR1	Wairua Hotpool

CHAPTER ONE

LITERATURE REVIEW

1.1 Introduction

Natural water bodies are important ecosystems. There is pressure on aquatic environments through long-term land use changes and population growth. Deterioration in water quality affects aquatic life and drinking water supplies, as well as recreational activities. In Māori culture, water is recognised as a life force - 'Te Māuri o te Wai' denotes our obligation to maintaining the quality of fresh - water environments. This thesis focuses on arsenic (As), a naturally abundant element toxic to humans, and combines long-term water quality monitoring data and point source sampling to explore presence, speciation, and movement of As within Lake Tarawera, a large water body in the Central North Island, Bay of Plenty Region, New Zealand

This introductory chapter focusses on the chemical and physical properties of As and how they relate to the freshwater environment; specifically, mobility and spatial distribution, speciation toxicity, and interactions with other elements. The chemistry of As includes reduction-oxidation (redox) reactions, coordination/surface chemistry, the aquatic electrochemical system (redox potential (pE) and pH), and dissolved oxygen (DO) availability. Adsorption of As to iron (Fe) and manganese (Mn) and the importance of these processes in the cycling of As in deep lakes is discussed.

An overview of the study site, Lake Tarawera, is presented within. The regional geology and historical influences on the presence of As in the region helps to identify a background understanding of As for the lake. There are physical conditions of the water column that contribute to the seasonal variation in the water chemistry of Lake Tarawera. Summer months cause horizontal separation of the water column, into an epilimnion (equilibrating with the atmosphere) and hypolimnion (interacting with the sediments) through thermal stratification (thermocline being the dividing layer). Thermal stratification can affect the speciation and movement of As throughout the water column and sediments. Previous research on Lake Tarawera during 2007/2008¹ has reported As results for

water samples from the deepest part of the lake (near the centre of the lake). This data has been used in conjunction with data collected during this research project for comparison of the As concentrations in Lake Tarawera over time. In addition, an ongoing water quality monitoring programme undertaken by the University of Waikato (UoW) has monitored the inflows to Lake Tarawera since 1996 (unpublished)²; and these data have been provided for this thesis. These data supplement the data collected for this research in dissolved elemental analysis, conductivity, and pH, as well as flow rates used for the calculation of As loading.

1.2 Arsenic

1.2.1 Concentrations of arsenic throughout the world

Arsenic is globally ubiquitous³ occurring naturally in rocks and soils.⁴ The average concentration of As varies depending on the matrix, with an average concentration of 2,000-5,000 $\mu\text{g L}^{-1}$ in the Earth's crust,^{5,6} a median concentration of 6,000 $\mu\text{g L}^{-1}$ in soils,⁷ and an average of 1-2 $\mu\text{g L}^{-1}$ in fresh water environments.⁸

The concentration of As in fresh water environments is related to the surroundings, where fresh waters exceeding this average tend to have a geographical association with As-rich geological regions such as volcanoes, shallow geothermal sources, mines, and landfills⁸; all of which are potential input sources of As into the subsurface environment.^{3,9} Leaching of As into aquatic environments occurs through dissolution of particulate As from rocks and soils into a dissolved form,⁸ where it is often stable in a dissolved phase due to high solubility in most natural water environments. A fresh water environment exceeding 10 $\mu\text{g L}^{-1}$ of total dissolved As (sum of all species) is classified as contaminated by the World Health Organisation⁴ (WHO). Examples of geothermally contaminated fresh waters include As at concentrations of 8,500 $\mu\text{g L}^{-1}$ in surface waters in the Waikato/Bay of Plenty region in New Zealand^{10,11}, 2,000 $\mu\text{g L}^{-1}$ in the Madison River, United States¹², and 6,400 $\mu\text{g L}^{-1}$ in an unspecified fresh water body in Japan.¹³ Contamination of fresh water is difficult to prevent due its mode of transport. The ability for water to transport As from a localised contamination site through both surface and subsurface flows, can significantly broaden the area of contamination.¹²

Large fluctuations in concentration are observed around the world and can also vary within a particular country; for example, concentrations of As ranging between 8 $\mu\text{g L}^{-1}$ and 9,080 $\mu\text{g L}^{-1}$ in 28 different New Zealand geothermal waters in 2012.¹⁰ Drinking water wells studied in Hungary (2013) varied from 7.2 $\mu\text{g L}^{-1}$ to 210.6 $\mu\text{g L}^{-1}$ ($n = 23$).¹⁴ In 1998, it was estimated that 1.5-2.5 million drinking water wells in Bangladesh exceed the local drinking water standard of 50 $\mu\text{g L}^{-1}$, with 35-57 million people exposed to contaminated water.¹⁵ Monitoring of drinking water is important for public health, particularly as As is soluble in water and is both odourless and tasteless when dissolved.⁷

1.2.2 Toxicity of arsenic

The ubiquity of As in the environment is concerning due to As being classified as a Class 1 carcinogen by the International Agency of Research on Cancer.⁴ They state that exposure of 5 $\mu\text{g As/kg/day}$ for up to 14 days is considered acute with 0.3 $\mu\text{g As/kg/day}$ defined as chronic exposure. Potential adverse effects of exposure to As include skin lesions,⁵ vomiting, and diarrhoea⁴ from acute exposure, and neurological or respiratory issues and cancers from chronic exposure¹⁶. The WHO drinking water standard for As was decreased in 1993 from 50 $\mu\text{g L}^{-1}$ to 10 $\mu\text{g L}^{-1}$,¹⁶ in light of this potential toxicity from ongoing exposure.¹²

The studies into the reactivity and biophilicity of As have noted over 100 known compounds and complexes occurring in nature⁹ and trace amounts of As present in most living organisms has been reported.¹⁷ The biological uptake of As has been attributed to phosphate (PO_4^{3-} - an essential molecule for life) being a chemical analogue of a stable As oxide; arsenate ($\text{As}^{\text{V}}\text{O}_4$).¹⁸ The most commonly studied dissolved As compounds present in natural waters are inorganic salts and redox pair arsenite (As^{III}) and arsenate (As^{V}), as well as organic, methylated compounds monomethylarsenic (MA) and dimethylarsenic (DMA). The reactivity of As in the natural environment is further demonstrated through a variety of substituted aromatic compounds, as well as larger organic molecules such as sugar and biomolecules.¹⁹

The toxicity of the four common aqueous species decreases as follows: $\text{As}^{\text{III}} > \text{As}^{\text{V}} > \text{MA} > \text{DMA}$ with regards to potentially adverse effects on human health.²⁰ As^{III} is not only the most toxic, being the most bioactive of the species,²¹ but is also more mobile in aqueous media than As^{V} .⁷ The toxicology of As^{III} to humans is due to chemical reactions with amino acids and enzymes containing sulfur (specifically S-H) groups, such as those with cysteine.^{15,22,23} The formation of kinetically stable S- As^{III} bonds causes interference or inhibition of the biological function of the molecule,¹⁴ thereby justifying the strict WHO standards around As exposure.

1.2.3 Chemistry of Arsenic

The past decade has seen substantial research into As in groundwater, including sources of As, the fundamental processes which control the mobility and speciation of As in various environments, analytical techniques, and remediation of contaminated fresh waters.²⁴ This research has included understanding the chemical differences between the common aquatic As species.

Arsenic has four stable oxidation states. The metallic (0) state is rare due to the high reactivity of the metalloid and As^{III} is highly reduced, gaseous molecule arsine (AsH_3). As^{III} and As^{V} are the most common As species, and a redox vulnerable pair, that in the context of this thesis are considered their respective (hydr)oxides; arsenite ($\text{H}_3\text{As}_2^{\text{III}}\text{O}_3$) and arsenate ($\text{H}_3\text{As}^{\text{V}}\text{O}_4$).^{9,22} However, many other compounds exist containing As in 3^+ or 5^+ oxidation state, such as common sodium arsenite and calcium arsenate salts.⁸ Figure 1-1 depicts the four most common oxide species found in fresh water bodies; As^{III} , As^{V} , and two As^{V} organic metabolites -; dimethylarsinic acid (DMA) and monomethylarsonic acid (MA). The presence of organic species in the aquatic environment is indicative of biological activity.²⁵ MA and DMA are thought to be a successful detoxification mechanism by conversion (through mono- or di- methylation of As^{V}) and excretion²⁵ by bacteria, fungi, and algae in the water column.¹²

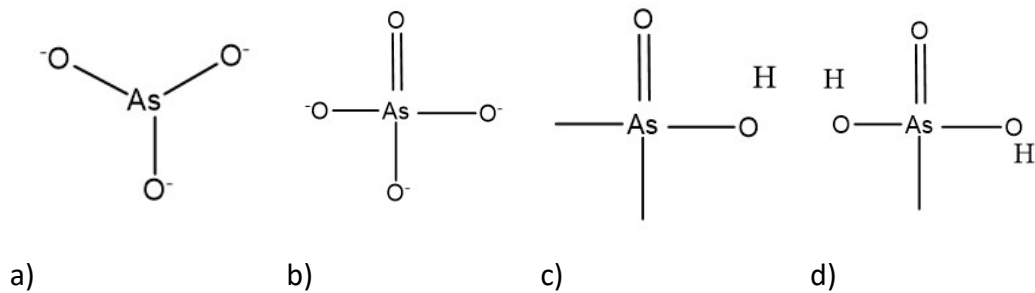


Figure 1-1. The four major species of As found in water. a) As^{III} as arsenite oxyanion ($\text{As}_2\text{O}_3^{3-}$), b) As^{V} as arsenate oxyanion (AsO_4^{3-}), c) As^{V} as dimethylarsinic acid (DMA), d) As^{V} as monomethylarsonic acid (MA).

The chemistry of aquatic As is dictated by the local environment, and great variation has been seen in water chemistry even amongst natural water systems.⁶ The form of As, as well as movement and speciation, is driven by non-constant physical and chemical parameters, such as redox potential (pE). The resolubilising of important As sorbants from the sediments (such as Fe-hydroxides) is controlled by pE.²¹ Decreases in pE (as can occur with depth in a lake from oxygen depletion) leads to increased solubility of these redox sensitive sorbants, thereby providing a seasonal increase of dissolved As into the water column. The partitioning of As between dissolved and particulate phases is therefore important for mobility, reactivity, and toxicity.²⁶ These seasonally driven changes provide complications in the prediction of As movement and speciation, and generalisations about As chemistry within a fresh water body cannot be made without considering these particular parameters about the specific water body.⁶

Particulate As, such as found naturally in rocks and soils, can be readily mobilised through natural processes such as weathering, and can remain in the dissolved phase due to solubility of up to 630 g As per 100 g water.²⁷ This dissolved As can then be transported into in a fresh water body through surface or sub-surface inflows.⁷ Arsenic in a water body, such as a lake, can undergo complex chemical processes including redox reactions, ligand exchange, ion exchange, precipitation and adsorption reactions, as well as biologically induced speciation.^{3,8,22,28} These reactions partition As into multiple forms within the aquatic environment, including hydrated dissolved ions and multiple particulate forms such as colloids, coordination complexes, and adsorbed species.⁶

Of the different aquatic environments (marine, ground waters, and surface fresh waters such as rivers and lakes), lakes are thought to be the most variable in regards to the speciation of As because they have the most significant seasonal fluctuations of physical and chemical parameters.²⁹ Cycling of As in lakes and rivers between dissolved and particulate phases is largely controlled by pE, where high pE values favour particulate As through adsorption to molecules such as Fe- and Mn-(hydr)oxides, and low pE favour dissolved species. These sorbants undergo the same redox based reactivity as As, and partitioning between particulate and dissolved phases. They are largely more abundant in the Earth's crust than As (Fe $3.50 \times 10^7 \mu\text{g L}^{-1}$, and Mn $6.00 \times 10^5 \mu\text{g L}^{-1}$) and are therefore often present in water bodies.⁶ During the period of thermal stratification (which often occurs in lakes) chemical and biological consumption of oxygen in the hypolimnion can reduce pE. This leads to reductive dissolution of redox species from the surface sediments, solubilising and re-dissolving particulate fractions of these redox species with any adsorbed As also being distributed back into the water column.¹⁸ Through lake mixing and reintroduction of oxygen to the system (i.e. increasing pE), these dissolved species can react and settle back into the sediments, thus removing As from the water column. This cycling has been measured in both lakes and rivers. The Hamilton City Water Treatment Station shows an annual seasonal increase of dissolved As ranging from 10-25 $\mu\text{g L}^{-1}$ throughout the summer months (December to February) in the Waikato River¹¹, which also correlates with the increase in solubility of As at higher temperatures.²⁷ As an example of lake cycling, Lake Ngapouri, in the Rotorua Region, shows cycling of As occurring from thermally induced stratification and biological oxygen depletion in the hypolimnion, increasing dissolved concentrations of As, Fe, and Mn by 1-2 orders of magnitude over the period of stratification.¹⁸ The solubilised species were then dispersed throughout the water column during overturning of the lake.

As well as pE, pH is another important factor, contributing to the solubility, oxidation/state, and degree of protonation of aqueous As is pH.⁷ At stable pE values, relatively small changes in pH can have dramatic effect on the reactivity and solubility of both hydrated free As and adsorbed particulate As.⁶ The solubility of free As-(hydr)oxides decrease rapidly as pH decreases; however, complexed compounds may be stable at lower pH values.⁶ Table 1-1 shows the association between charge and pH for As^{III} and As^V.

Table 1-1. Dissociation constants for As^{III} and As^V (as arsenite and arsenate), showing the pH dependence on the charge of the oxide species. Table reproduced from O'Day (2006).²⁰

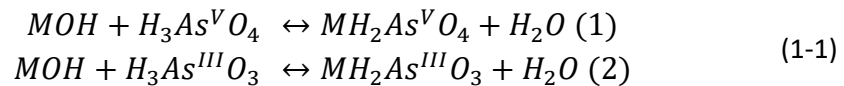
Dissociation Constant (pKa)	As ^{III}	As ^V
1 st	9.23	2.20
2 nd	12.13	6.97
3 rd	13.40	11.54

From a toxicity perspective, the solubility of total As (sum of all species) from pH changes is less significant than the speciation changes (pE/redox) which can occur within fluctuating pE parameters (i.e. how much of the total dissolved arsenic is As^{III}).¹⁶ The approximate fractions of As^{III} and As^V vary within water sources, with most natural waters sitting between pH 6-8²⁰ and pE values are dependent on the water source and seasonal conditions. For example, a thermally stratified lake can have higher pE in surface waters and lower in benthic waters, while maintaining a similar pH with depth. Examples of As fractions include: geothermal waters in New Zealand which contained As^{III} in excess of 70 % of total As (8,590 - 9,080 µg L⁻¹),¹⁰ surface water lakes in Ontario, Canada containing As^{III} between 7- 75 µg L⁻¹, and As^V between 19-58 µg L⁻¹,²⁹ and Bangladeshi groundwaters with approximately equal fractions of As^{III} and As^V.²⁹

1.3 Reactions of arsenic with other redox sensitive elements

Redox drives the speciation of As in the aquatic environment.⁷ In waters where pE favours the oxidised and less soluble species (As^V), pH then controls the coordination/surface chemistry between As and other redox sensitive elements. Surface chemistry reactions dominate the association of As^V with particulate Fe, Mn, and S in slightly acidic waters,^{7,30} whereas dissolved metal cation interactions dominate in neutral and alkaline waters.⁷ Free or hydrated As will remain dissolved; whereas adsorbed As can co-precipitate into particulates which may remain suspended or settle out of the water column into the sediments.^{18,28} The oxidation by, and subsequent adsorption of, As to Fe and Mn is well researched and highly implemented in materials used for the removal of As from contaminated

drinking waters.³¹ The generic reactions for a metal (hydr)oxide (MOH, where M = Fe, Mn, or S) with As^{III} or As^V are shown in Equation 1-1.³⁰

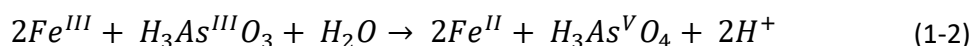


Atmospheric oxygen also oxidises As^{III} to As^V, with reported oxidation rates (under controlled conditions) of no less than 25% oxidation after 72 hours at pH 4, 6, and 8.³⁰ Microbial activity was reported to increase the speed of oxidation of As^{III} by oxygen.¹² Microbial influence is relevant in the speciation of As and is accounted for in the sampling method, but the mechanism of microbial catalysis is beyond the scope of this thesis and will not be discussed in detail.

Fe- and Mn-(hydr)oxides existing primarily as coatings on other minerals, provide large surface area (approximately 200 to 300 m² g⁻¹), and numerous binding sites for As which could adsorb during movement. One researcher estimated up to 50% of total metal transported through rivers is from adsorption to such coated minerals.⁶ Stumm and Morgan (1995)³² studied the relationship between contaminant loading and discharge volume and found that for a continuously flowing source with little to no seasonal variation in physical conditions, an increase in discharge volume did not correspond to an increase in contamination concentration.³² The authors did note, however, that dissolved species predominated with low flow, and particulate constituents with high flow. This was attributed to desorption being the primary mechanism for presence of contaminants in water, the rate for which did not initially increase with discharge volume (effective dilution factor), until the discharge volume was great enough to cause resuspension from sediments, which not only counteracts the dilution effect, it also alters the particulate:dissolved ratio. A discontinuous discharge source is more likely to vary in elemental composition, particularly when the surges of discharge are of high volume.³²

1.3.1 Iron

Iron is widely used in As removal from contaminated waters, due to its adsorptive capacity at known conditions. At a pH of < 8 (isoelectric point of Fe- (hydr)oxides³³), hydrous Fe-(hydr)oxides have a positive surface charge and at this pH As^V is weakly anionic with a strong adsorptive capacity towards the positive surface charge on hydrous Fe-(hydr)oxides.^{18,22} This affinity decreases with increasing pH, as both As^V and Fe-(hydr)oxide become more negative.⁷ The chemical influence of Fe-(hydr)oxides on As has been researched *in-situ* by de Vitre *et. al.*³⁴ Teflon collectors were inserted vertically into shallow water (10 m) sediments known to have oxic conditions. The cores were analysed under controlled conditions to preserve the integrity of the As and Fe species, which was confirmed by spike recovery tests. These results showed oxidation of As^{III} to As^V in the presence of Fe- and Mn-(hydr)oxides (being the redox pairs Fe^{III}/Fe^{II} , and Mn^{IV}/Mn^{II}) with 50-75% of dissolved As^{III} oxidised within 2 days across pH range 4.7-10.2, as well as a greater affinity of As^V over As^{III} to the Fe-(hydr)oxide surfaces.³⁴ An example for this reaction is shown in Equation 1-2.



The relationship between Fe and As has been widely studied to determine necessary pE/pH conditions for maximum adsorption. Ideal conditions for dissolved As to an Fe-based compound has been reported (in laboratory tests) at conditions of pH 7 and 25 °C for 60 minutes.²³ Another study reported similar results for As^{III} , and noted maximum As^V adsorption at pH 4.²⁶ Reaction kinetics for both As^{III} and As^V adsorption to Fe-oxides are biphasic, with adsorption occurring rapidly within the first few minutes and slowing until equilibrium is reached, approximately 60 minutes and 7 days, respectively, for each species.³³ This slowing of adsorption has been attributed to numerous factors including heterogeneous surface binding site energies and the formation of surface precipitates.³³ Adsorption of As to Fe- (hydr)oxides was described as conforming to a Langmuir isotherm (single layer saturation). Under the Langmuir model, the theoretical adsorption of total As to Fe was calculated at 0.18 mol of As adsorbed per mol of Fe, with experimental analyses reporting 0.16-0.25 mol total As per mol of Fe, when the ratio of As to Fe was 1:5.²⁶ A separate study into adsorption for drinking water treatment compared a Langmuir model to a Freundlich isotherm.³¹ This study found that the Freundlich

model proved a better representation due to the heterogeneity of the surface binding sites, which are unaccounted for by the Langmuir model (which assumes equal binding sites, size and shape). Wilkie and Herring (1996)²⁶ noted theoretical modelling is complicated when the matrix contains complex mixtures of trace constituents.

Anderson and Bruland (1991)²⁵ reported the lower adsorptive affinity of As^{III} compared to As^V to Fe- and Mn-(hydr)oxide surfaces; attributing the differences to the neutrality of the As^{III} oxide in most natural waters (pKa = 9.2³⁰). Another study²⁶ agreed with this, whilst noting a higher influence of pH on As^V adsorption than As^{III}. However, other literature stated that at circumneutral pH As^{III} and As^V show equal retention to Fe-(hydr)oxide particulates,^{8,15} with As^{III}-Fe-(hydr)oxide cations being more soluble than the As^V alternative.⁷

1.3.2 Manganese

Manganese is chemically analogous to Fe in common transition metal behaviour; however, their respective oxides differ in chemical behaviour.²⁵ Mn-(hydr)oxides contain a negative surface charge when pH is 1.5 and above (compared with 8.94 for Fe-(hydr)oxide³³).³⁵ Due to this, theoretically adsorption of As^V should not spontaneously occur.^{6,22} However, adsorption to Mn-(hydr)oxides has been measured empirically.²⁵ It has been hypothesised that a net positive charge is created on the Mn-(hydr)oxides through adsorption of other dissolved cations, which anionic As^V can then adsorb to.²⁵ Synthetic experiments showed little to no adsorption of As on hydrous Mn-(hydr)oxides between pH 6-8 (approximate pH of environmental waters) except when in the presence of divalent cations, including Mn^{II}, where adsorption did occur across the same pH range.³⁶ One proposed explanation for this is that the oxidation of As^{III} to As^V consequently reduces Mn^{IV} to Mn^{II}, which can then adsorb to a Mn^{IV}-(hydr)oxide surface providing a more positive binding site for the binding of As^V.^{30,31} A mechanism for catalytic oxidation of As^{III} to As^V was described in Mn^{IV}-(hydr)oxides with a clay mineral structure.¹⁵ This weak adsorption onto the surface site facilitates the oxidation of As^{III} and then releases As^V into aqueous phase due to low affinity for incorporation into the mineral structure, with an approximate reaction rate of a few hours.¹⁵

1.3.3 Sulphur

Due to the strong affinity of As^{III} to S the redox pair sulphate/bisulphide (SO₄²⁻/HS⁻) can be a significant contributor to the oxidation or reduction of the As^{III}/As^V redox pair in natural waters.¹⁵ SO₄²⁻ has also been observed to decrease adsorption of both As^V and As^{III} to Fe-(hydr)oxides, especially at low pH.²⁶ Another study reported significant formation and/or co-precipitation of various As-S molecules with increasing pH (at 90 °C).³⁷ There are also reports that hydrogen sulphide (H₂S) and thiosulphate (S₂O₃) preserve As^{III} speciation in reducing, high pressure environments until the S compounds themselves are oxidised or volatilised.¹²

1.3.4 Other elements

The influence of metal cations on the speciation and mobility of As is greatest for As^V at pH 6 and As^{III} at pH 6-8 depending on the cation.⁷ It has been shown experimentally that in alkaline environments with high levels of As, alkali earth metals such as calcium (Ca) and magnesium (Mg) form soluble ions with As, which could contribute to mobility of As in alkaline environments. The presence of these cations was shown to also enhance adsorption of As^V to Fe-(hydr)oxides as a co-occurring solute⁷, particularly at high pH.²⁶ There is also experimental evidence which links As to other elements which form amphoteric oxides, such as aluminium (Al).⁷

1.3.5 Implications of redox/complexing molecules on arsenic in lake sediments

The distinct redox boundaries which can occur in lake sediments lead to chemical reactions and changes occurring within and between the sediments and the interstitial waters (pore waters). Molecules that are solubilised in deep reducing sediments or geothermal waters can be subjected to changes in the environment through which they are travelling. Oxidic surface sediments, which contain oxidation inducing compounds such as the Fe-, Mn- and S- redox pairs, can alter the speciation of As while it travels through the sediments to the water column.²¹ The oxidation of As by these redox pairs results in the reduction and increased solubility of these molecules from the sediments back into the water system.²⁸ These reduction reactions fit into the redox ladder Mn^{IV}/Mn^{II} > Fe^{III}/Fe^{II} > SO₄⁻/H₂S at

approximate aquatic conditions of pH 7; making Mn the most readily reduced of the three elements.³⁸⁻⁴⁰ The redox potential for the As redox pair ($\text{As}^{\text{V}}/\text{As}^{\text{III}}$) is almost equivalent with the Fe pair.³⁸ This ranking is based on equilibrium and the thermodynamic feasibility for a reaction to occur in ideal conditions.⁴⁰ It assumes a distinct boundary from oxic to anoxic and does not account for the presence of competing reactions, or the reaction rates of each individual reaction. For example, even though Mn oxidation/reduction is thermodynamically more favourable than Fe the reaction occurs more slowly than that of Fe. Free ions such as Fe^{2+} are also oxidised more quickly than hydrated equivalents, ($\text{Fe}(\text{OH})/\text{Fe}(\text{OH})_2$).⁴⁰ Therefore, the vast complexity of the chemical and biological activity occurring in the sediments provides opportunity for deviation from the conceptually expected chemical behaviour of As and the influential redox species.

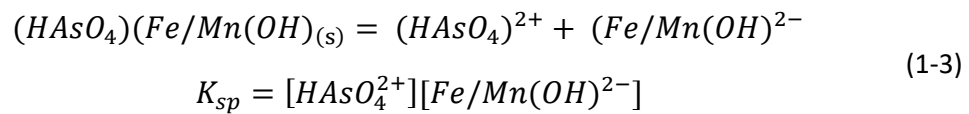
Deep geothermal waters are generally anoxic and significant sources of As.²¹ Geothermal waters can enter lakes through both surface and subsurface inflows. Pore water advection brings dissolved molecules towards the surface of the sediments (i.e. the sediment-water interface (SWI) at the bottom of the lake).²¹ The reduced and solubilised As^{III} may migrate from deep geothermal sources towards the SWI, and when transported through oxic sediments it may be oxidised and present as As^{V} in interstitial and benthic waters, where it can then adsorb, precipitate, and settle out of the water.^{15,25} Long term As accumulation near the surface sediments which exceed seasonal trends can be indicative of these processes.¹⁵

1.4 Chemistry of lake waters and sediments

Lake waters are dynamic, with both chemical and physical influences contributing to the chemical makeup of the water. The concentration, speciation and movement of As is influenced by multiple, and occasionally inter-related factors such as pH, pE, temperature, dissolved oxygen (DO), and thermal stratification.¹ Trends in As within lakes include seasonal variation, high spatial variability, increased concentrations in the benthic waters and sediments of lakes with geothermal inputs, and presence in various molecular forms.^{1,11,18,41} Spatial variability can lead to hot spots of increased As concentrations within both the water column and sediments.

For example Lake Victoria, Africa, had increased concentrations of As at the inlets of the arms of the lake, when compared with the main water body of the lake.⁴²

Equilibrium of the chemical reactions occurring in a fresh water system is convoluted by numerous, simultaneous, and/or competing reactions.⁶ Under reducing conditions the dissolution of particulate As from the sediments to the dissolved phase will form an equilibrium between the solid and dissolved phases. The solubility of As from adsorbed Fe- or Mn-(hydr)oxides is represented by the solubility product (K_{sp}) equilibrium reaction (Equation 1-3):



The presence of competing reactions, such as complexation of the newly dissolved As, can destabilise this equilibrium, forcing further dissolution of As when dissolved As is consumed in complexation reactions.⁶ This broadens the equilibrium equation by adding in the stability constants (K_s) of the complexes. Complexation reactions commonly include organic ligands which were not studied in this current research; however, the impact of competing reactions on this equilibrium system is noted.

Understanding the dynamics of metal chemistry in fresh water systems has often involved bench-top chemistry under controlled conditions, in an attempt to mimic and simplify the natural environment.³² The kinetics and thermodynamics of these reactions under pseudo conditions (potentially closed systems which are well mixed) do not account for the degree of fluctuation that can occur *in-situ*. For example, the above equilibrium (Equation 1-3) may not be reached if the dissolution of As is kinetically slower than the consumption of As through subsequent reactions.^{6,32} Davison (1991)⁴⁰ noted the importance of distinguishing between concentrations of elements in the water column and the contribution of fluxes, i.e. what is cycling through the lake compared with what is being newly added. They also noted that larger precipitates will sink faster than smaller particulates, and the surface layers of the sediments contain the elements which contribute to the flux.⁴⁰

1.4.1 Thermal stratification

Thermal stratification in lake can cause distinct chemical differences within the water column. The development of a thermocline in lakes also leads to spatially distinct mixing boundaries which effectively creates two separate systems, one which equilibrates with the air (“epilimnion”) and one with the sediments (“hypolimnion”).⁴³ With limited (replenishable due to the thermocline) DO in the hypolimnion during thermal stratification, the biological consumption of oxygen leads to an onset of anoxia because oxidised species are stripped and reduced for respiration in the absence of molecular oxygen.^{1,18,44} The degree of DO depletion and annual mixing regime of a lake (i.e mono- or poly-mictic) largely influences the cycling of those species which are controlled by pE; such as Fe, Mn, As, S, nitrogen (N), and phosphorus (P).^{18,43} Not all stratified lakes are completely depleted of oxygen across benthic waters, with some presenting ‘hotspots’ of activity in confined areas in the benthic boundary layer.¹ This is because lakes that are large in size and deeper than 30 metres, which stratify between 20-30 m, require more biological activity to completely deplete such a large area of oxygen than a smaller, shallower lake.⁴⁰

1.4.2 Importance of sediment concentrations and physical parameters for elemental cycling in the water column

While water column research provides short-term data, including seasonal and spatial fluctuations, sediments provide a historical record of the geological periods and changes through time, and together they provide an overview of the system as a whole.¹ Similarly to the water column, sediment profiles display a gradient of oxygen with depth, from the SWI as the ‘surface’.⁴⁴ In sediments and interstitial waters studied by Aggett and Kreigman (1988)⁴⁴, reducing environments such as deep, compact sediment were reported to transport As through molecular diffusion to the SWI. Turbulent diffusion can then transport As into an anoxic hypolimnion, or reprecipitate it at the surface of the sediments in an oxic hypolimnion.^{1,44} Sediments can be considered a source of elemental input into the water column by the mechanism of translocation, for which time-series analysis can show elements or molecules that are cycled through molecular diffusion across the SWI and accumulated at the oxic boundary.^{1,15,45} There is a natural trend of element accumulation at various depths, due to the different solubilities of the dissolved

elements or molecules.¹² Therefore transportation of As through complexation, such as with S, would precipitate deeper (in response to decreasing physical or chemical gradients occurring) than soluble As moving as hydrated As^{III}.¹² The rate of chemical change can also alter the precipitation depth. For example, Mn^{II} oxidises more slowly than Fe^{II}; therefore, can travel higher towards the SWI before precipitating out.

Surface sediment cycling is observed through long-term analysis where this natural zoning pattern is altered by certain elements or molecules (such as As-metal complexes) depleting over time at a certain depth and accumulating in the surface sediments.¹² This has been seen in deep lakes in Japan where As is observed in its greatest concentration in the surface sediments.³⁶ One study has shown surface oxic sediments consist almost entirely of oxidised species such as As^V, with the As^{III}/As^V ratio increasing with depth.³⁸ Alternatively, in reducing environments, reductive dissolution of As^V adsorbed Fe^{III}-(hydr)oxide supplies hydrous and dissolved As^{III} and Fe^{II}-(hydr)oxides to the dissolved system. Subsequent reactions of these reduced and dissolved molecules with S could form authigenic (formed *in-situ*) minerals such as arsenopyrite (FeAsS), which remains stable under reducing conditions and are considered a sink for trace elements such as As.^{15,46} Mineral formation such as FeAsS, however, does not readily occur unless the trace element is in sufficiently high concentration. Therefore, sorption usually dominates the particulate forms of As in the sediments of fresh water environment (i.e. surface chemistry over incorporation as a constituent atom).²⁶

The cycling of As, together with thermal stratification and inputs of As from lake inlets, create a dynamic system, as depicted by Figure 1-2 a. Cycling of As can occur at the oxic/anoxic boundary (Figure 1-2 b), with the reverse processes occurring during the period of stratification. The addition of As from lake inlets provides a continuous source of As to the surface waters, which could cause an over-time increase of concentrations of the elements being cycled in the lake system.

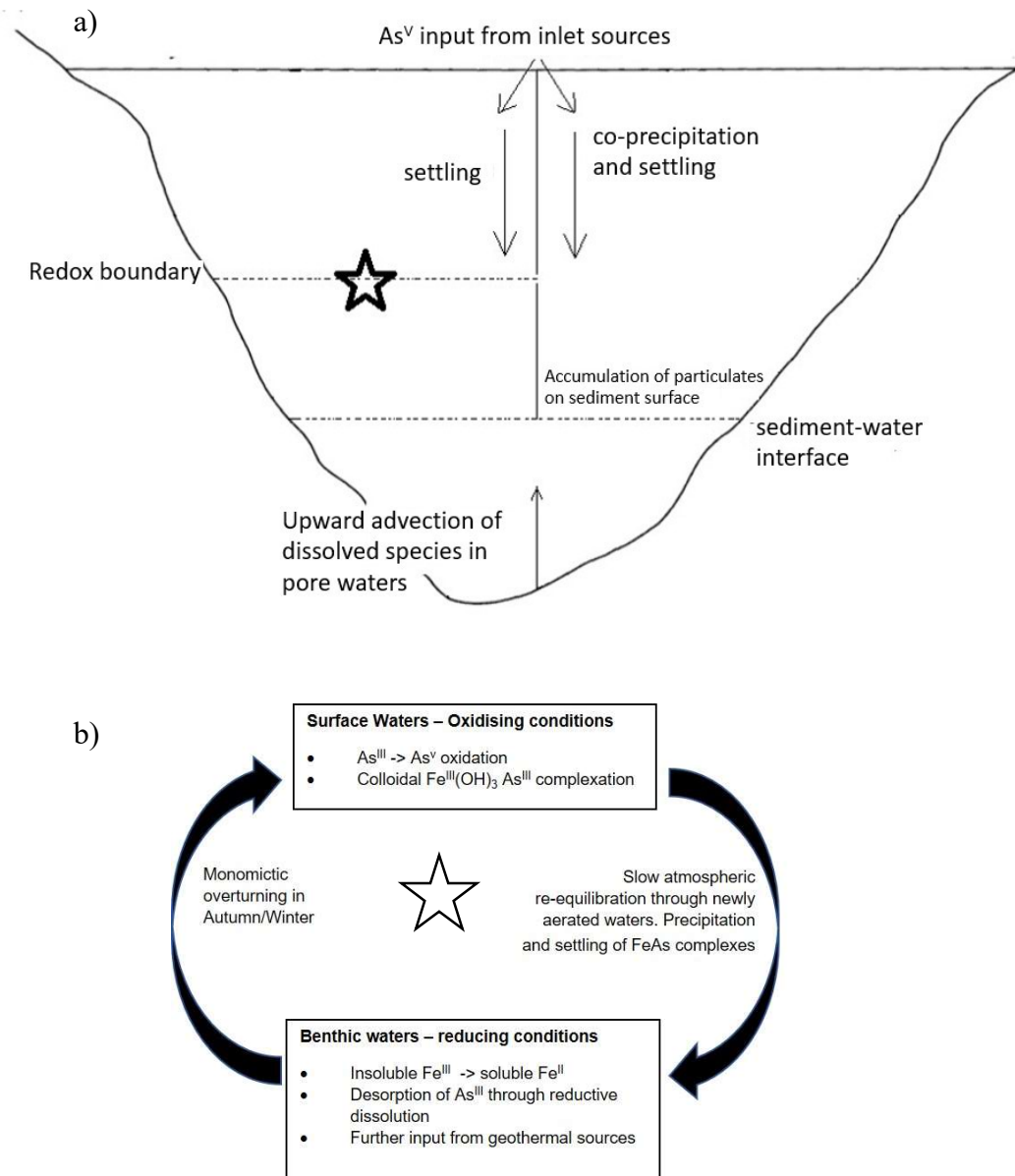


Figure 1-2. Example of the inter-relationship of As inputs, lake cycling, sediments, and thermal stratification. a) displays a lake with a redox anoxic/oxic boundary is displayed on the left, with no boundary on the right. b) shows the cycling occurring at the redox boundary, denoted by the star and adapted from Harland *et. al* (2015).¹⁸

1.4.3 Pore Waters

Pore water is the water that fills the space between grains of sediment.⁴⁷ The gradient of chemical changes of the pore waters/sediments differ to the overlying water column, by having significantly sharper gradients (mm to cm scale).⁴⁸ Therefore, the analysis of pore water chemistry provides data with high spatial resolution. These data provide information on biogeochemical processes and solute fluxes occurring within the sediments, from the SWI with depth.⁴⁸

Pore waters are governed by neither the surface water nor ground water definitions.⁴⁹ They are, however, thought to be in equilibrium with the surrounding sediments and are often used as a measure of sediment contaminants. The most important objective of pore water collection is the preservation of the *in-situ* conditions during transport and analysis, and the method used for pore water collection should be chosen based on the *in-situ* conditions which require maintaining. Exposure of anoxic pore water samples to the atmosphere may result in the precipitation of the less soluble redox species, or dissolve the As bound to sulphide minerals which are stable in reduced conditions, thereby altering the $\text{As}^{\text{III}}/\text{As}^{\text{V}}$ ratio of As species in the natural environment.⁴⁹

1.5 Methodology for sampling and analysis of arsenic in water

With As speciation as the driving force of this research, maintaining the natural environment of the water sample is crucial for sample integrity. Oxidation timeframes for As^{III} to As^{V} is influenced by the constituents in the water sample, which complicates the storage stability of the sample. The presence of Fe and Mn are reported to oxidise As^{III} to As^{V} within approximately 48 hours.³⁴ Oxygen induced oxidation occurs within eight days in surface fresh waters and three days in rain water.¹⁶ Whether this oxidation is partial or complete, it changes the ratio of $\text{As}^{\text{III}}:\text{As}^{\text{V}}$, and the sample is no longer representative of the environment. Changes in temperature, pE, pH, or the addition of oxygen to anoxic samples can also alter the speciation and solubility. Sampling methods need to consider these factors, and be tailored to the environment (geothermal, acidic, marine/fresh, etc.), as well as the timeframe between sampling and laboratory analysis. Sampling locations which are geographically isolated may require more stringent means of preservation than samples which can be transported to a laboratory and analysed within a shorter timeframe.

1.5.1 In-field sampling methods

The collection of untreated (raw) samples are suitable for non-extreme environments or where analysis can occur within 48 hours, if they are treated with precautions such as filtration to remove particulates, overflowing of the sample bottle to ensure no headspace, and storage in dark, cold conditions.¹⁰ For longer-term storage of samples (more than 48 hours between sampling and analysis), use in extreme environments (high or low pH, pE, or temperature), or a combination of the two, sampling methods have been analytically tested for the retention of As species from open-water samples.

The addition of preservative ethylenediaminetetraacetic acid (EDTA), a chelating agent, effectively removes the metal-As binding by complexing oxidising cations, thereby stabilising the sample for transport.³⁹ In-field species separation through solid phase extraction (SPE)¹⁶ is an example of a sequential partial extraction.⁶ SPE cartridges are useful in extreme environments where oxidation is expected to occur more quickly than 48 hours. The cartridges exploit the acid-base properties of As- (hydr)oxide species in water, given the deprotonation of As^V at pH 2.20 and 6.97, compared to As^{III} at pH 9.23.²⁰ These properties allow As^V to be retained on an anion exchange column while As^{III} is eluted through the column and thus the species are separated. The effluent containing As^{III} and elution of As^V from the cartridges allows each fraction to be analysed separately through ICP-MS without concern of interconversion of species, therefore eliminating the need of a separation technique.¹⁶ The co- elution of organic species, DMA with arsenate and MA in the effluent with As^{III}, is one complication of this technique, particularly in waters with high microbial activity. Other precautions that should be undertaken when using SPE is filtration to remove particulates which can obstruct the head of the column¹⁶, dilution of the sample where there is high conductivity (to prevent overloading of the column) or suspected competitive adsorption (such as chemically analogous PO₄³⁻)¹⁸, and conditioning the cartridges prior to use based on the pH of the sample.¹⁶

For the extraction of pore waters, rigorous methodology is required when analysing for elemental speciation due to the impact on the sample integrity from exposure of anoxic waters to the atmosphere during sampling or transport. Gruzalski *et. al.* 2016⁴⁹ reviewed pore water extraction methods, both *ex-situ* and *in-situ*. Vacuum filtration has been used to remove pore waters from sediment samples *ex-situ*; however, it has been reported that there is some difficulty maintaining integrity of the environment (e.g., minimising oxygen exposure during extraction).⁴⁹ Earlier methods of pore water extraction using suction often produced unfiltered samples which required filtration prior to analysis, or used ceramic or glass materials which were prone to adsorption of charged species, both providing sources of sampling error.⁵⁰ Filters themselves can also be a source of error; leading to sorption of charged groups, such as trace metals. Methods such as centrifugation of sediment sub-samples also increases the chance of atmospheric conditions being introduced due to the extra steps involved with segmenting the samples.

Multiple techniques for *in-situ* sample collection have been explored. Porous walled chambers (called Peepers), are filled with water (deionised and deoxygenated if appropriate) and inserted into sediments and left to equilibrate with the pore waters. This method requires the equipment to be deployed in field for a minimum of two weeks before being extracted and analysed. Diffusive Gradient Thin-Film (DGT) also require deployment in field prior to sampling, for periods of days or months, relying on diffusion and adsorption and can be targeted to a specific analyte.⁴⁹

Pore water sampling through the use of rhizons allows for removal of pore waters *in-situ* without disturbing the sediments or contaminating the sample with air.^{51,52} Rhizons contain micron size filters which are considered ‘non-destructive’⁵⁰ due to their overall small size (2.4 mm diameter).⁵² One study concluded rhizons preserved the speciation of redox pair $\text{H}_2\text{S}/\text{HS}^-$ better than sub-sectioning and centrifugation.⁵³ No literature was found specifically for As speciation; however, another source reported higher retention of trace elements such as zinc (Zn), copper (Cu), nickel (Ni), and lead (Pb) on the 0.1 μm filter in soils with higher conductivity and more dissolved cations.⁵⁰ The use of rhizons requires a source of suction to draw the water through the membrane and polyvinyl chloride (PVC) tubing, a

polymer chosen for its low sorption properties.⁵² Luer-lock syringes create a suction by connecting the syringe to the rhizon and drawing the plunger;⁵⁴ and both vacutainers⁵³ and peristaltic pumps⁵² have also been used for suction. An example of a rhizon with vacuum tube or syringe alternatives is depicted in Figure 1-3. These sampling techniques cover a range of water matrices, from neutral waters to geothermal waters, or waters with high conductivity (i.e. marine).

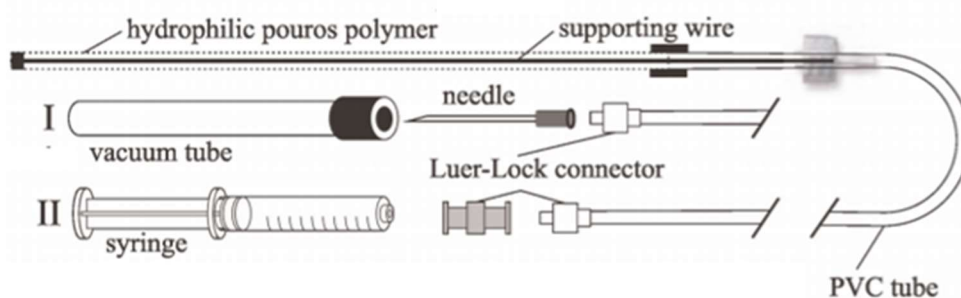


Figure 1-3. Rhizon system including connections for vacuum tubes or syringes. Taken from Seeberg-Elverfeldt et al (2005).⁵²

1.5.2 Laboratory analysis for quantification of arsenic

For unpreserved field samples, laboratory analysis for quantification of As involves multiple steps; first species separation, commonly done through a form of chromatography⁵⁵, followed by a form of high sensitivity detection (e.g. mass spectrometry).¹³ Various methods of chromatography have been used for As speciation, but most commonly a form of liquid chromatography using separation techniques specific to the analyte such as reversed-phase chromatography⁵⁶, or ion-exchange.^{10,19,39,56,57}

High Performance Liquid Chromatography (HPLC) was used in conjunction with hydride generation atomic absorption spectrophotometry (HPLC-HGAAS) up until the mid to late 1980's. Detection limits for HPLC-HGAAS were reported as low as 0.013 μM arsenic (ng L^{-1} order of magnitude).³⁰ This technique has now been superseded by inductively coupled plasma mass spectrometry (ICP-MS) as the leading source of cationic elemental analysis in research;⁵⁸ however, AAS is still used in places where ICP-MS may not be available or affordable.⁴² ICP-MS has high sensitivity, enabling detection of trace elements down to the ng L^{-1} level.¹³ Coupling HPLC to ICP-MS allows elemental species to be separated before

analysis. One problem when using ICP-MS for As quantification is that the carrier gas, argon (Ar), can form a polyatomic interference which overlaps with the monoisotopic ^{75}As signal. This is a complication for samples that contain even moderate concentrations of chloride ions due to the formation of $^{40}\text{Ar}^{35}\text{Cl}$. The development of collision and reaction cells overcame these spectroscopic interferences through either breaking the bond of the interfering molecule or by reacting the analyte and detecting it at a different m/z ratio.¹³ HPLC- ICP- MS detection limits for As analysis have been reported (using a Hamilton PRP-X100 anion-exchange column) as $0.1 \mu\text{g L}^{-1}$ using with a gradient elution (38-75 mM sodium phosphate buffer), and $0.6 \mu\text{g L}^{-1}$ As using isocratic mobile phase (malonate/acetate).¹³

The combination of advanced laboratory technology and high-quality sampling techniques suited to the specific sampling environment allows for accurate As speciation and elemental analysis which is representative of the field environment.

1.6 Regional geology and chemical history of Taupo Volcanic Zone and Lake Tarawera

The Taupo Volcanic Zone (TVZ) is an area encompassing 6000 km^2 in the Central North Island of New Zealand.⁵⁹ It was created through the subduction of the Pacific plate beneath the North Island of New Zealand and contains clusters of volcanic centres and geothermal systems. The geological history has evolved over time, with each volcanic episode physically altering the zone.⁶⁰

The TVZ (Figure 1-4) spans the length of Mt Ruapehu to White Island (southern and northern boundaries).^{3,29} The area contains numerous volcanoes and lakes.³¹ Within the TVZ are a series of geothermal fields; Okataina Volcanic Centre underlies Lake Tarawera, as well as Lakes Rotomahana (South of Tarawera) and Okataina (North of Tarawera). Okataina Volcanic Centre is basaltic in origin, therefore the 1886 eruption of Mt Tarawera introduced significant basaltic (Mg and Fe rich) material to Lake Tarawera, as well as altering the aquatic animal and plant life, and surrounding geology and bush.^{29,61}



Figure 1-4. The Taupo Volcanic Zone (red circle) within the North Island of New Zealand.

1.6.1 The Rotorua Lakes, Bay of Plenty Region

The tourism and aquatic sporting features of the Bay of Plenty region have provided an economic basis for sustaining the health and quality of the Rotorua Lakes, of which Lake Tarawera is apart (Figure 1-5).⁶² The Rotorua Lakes have been subjected to various water quality monitoring programmes since 1990, primarily focusing on nutrient loading and chlorophyll activity.¹ In 2006, developing strategies for restoration of the local lakes became a focus of local and regional councils supported by the New Zealand Government.⁶² Lake health is often described through trophic status, where the nutrient inputs, chlorophyll activity, and water clarity are used in an equation that categorises the overall state of the water body. The trophic status index defines lake water quality as oligotrophic > mesotrophic > eutrophic > hypertrophic, the former being the ideal status; having low nutrient inputs, low chlorophyll activity and high water clarity.⁶³ Consequences of declining lake health include deterioration of native lake plants, increases in cyanobacterial blooms, and depletion of oxygen in hypolimnetic waters through periods of thermal stratification.⁶⁴

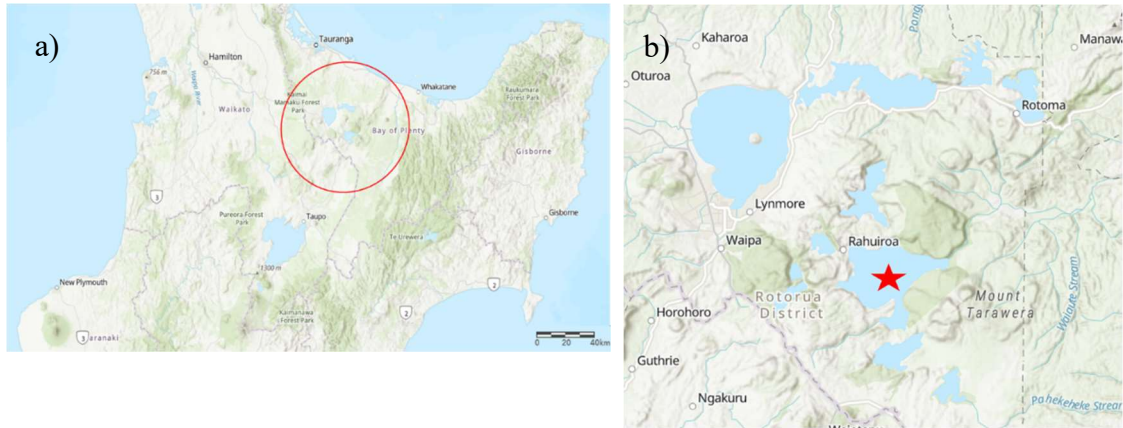


Figure 1-5. Close up map of Central North Island of New Zealand showing; a) Bay of Plenty Region circled in red. b) Closer image of a cluster of lakes, including Lake Tarawera indicated by the red star.

1.6.2 Lake Tarawera

Local council, tourist, and DOC websites describe the appeal of Lake Tarawera through its picturesque landscapes, large size, cultural history, and quality of its rainbow trout.⁶⁵⁻⁶⁸ It is the third largest of the TVZ lakes at 41 km², with an average depth of 57 m and maximum depth of 87 m.²⁹ It also has the lowest elevation at 299 m.⁶⁹ Varying degrees of thermal stratification in Lake Tarawera occur between 15-30 m depth, from August to May, annually, with one mixing episode per year (monomictic regime).¹ The current (2019) lake health status is oligotrophic,⁶⁸ with Secchi depth (average water clarity) of 9.4 m.¹

Lake Tarawera has been a sample location for a variety of studies undertaken on the wider region. For example, a 2008 study on managing lake health from a nutrient perspective.⁶² Lakes Taupo, Rotorua, Rotokakahi, Orareka, Rotoiti, Rotoma, Okataina, Rotoehu, Rerewhakaaitu, Rotomahana, Rotokawa, and the Blue Lake have all been studied in conjunction with Tarawera for water chemistry in a geothermal region,^{1,29} water quality,^{62,64,70} aquatic pollution,³ and regional trends.⁴¹

1.6.3 Major inflows to Lake Tarawera

The 1886 Mount Tarawera eruption was a major point source of chemical input into Lake Tarawera.²⁹ Rhyolitic (silica rich) mud was transferred from Lake Rotomahana (which sits at 335 m above sea level compared with Lake Tarawera at 299 m⁶⁹) and ash of basaltic origin (categorised by $Mg^+ : Ca^+$ ratio > 1 ⁶⁰) as well as tephra (airborne volcanic rocks), and these deposits can be seen in the top 30 cm of Lake Tarawera's sediment.¹ Aside from that isolated event, the main ongoing chemical inputs into Lake Tarawera are other connected lakes, geothermal waters, geothermal steam²⁹, rain water, and weathering.^{29,69} Lake Tarawera is reported to be fed by seven other lakes in the region, with direct inflows coming from Lakes Okareka and Rotokaki through streams, and sub-surface inputs from Lakes Tikitapu and Okataina.⁷⁰ Lake Rotomahana is significantly supplied by geothermal springs, as well as direct inputs from Lakes Okaro and Rerewhakaaitu.⁷⁰ Lake Rotomahana is partially drained into Lake Tarawera during times of heavy rainfall through a man-made gate.⁶⁹

Known surface hot-water geothermal inputs into the southern arm of Lake Tarawera include the Wairua Stream (208 L s⁻¹), Hot Water Beach (0.1 L s⁻¹), and Rotomahana Spring (91 L s⁻¹).⁶⁹ It has been found that these surface inflows only contribute 20% of the total geothermal inputs, being approximately 250 L s⁻¹ of a total estimated 1270 L s⁻² geothermal inflow, estimated from data collected between 2003 and 2006.⁷⁰ Major cold-water inlets include Rotomahana waterfall (173.5 L s⁻¹), Main Twin Creeks (384 L s⁻¹), Waitangi Stream (102 L s⁻¹) which comes from Lake Okareka, and Te Wairoa Stream (310.6 L s⁻¹); with an overall estimated inflow of 1760 L s⁻¹. There is only one surface outlet from Lake Tarawera (7240 L s⁻¹), leading to the Tarawera River.⁶⁹ It was estimated that these surface inputs only made up 42% of the total lake recharge, therefore a large portion of the chemical inputs are unmeasured.⁶⁹ Additionally, considering Lake Tarawera is the lowest elevation in the Okataina Volcanic Complex, there are likely groundwater inputs from Lakes Rotomahana, Okareka, Okataina, and Rotokakahi to Lake Tarawera due to porosity of pumice and other volcanically produced rocks which form the surface layer of the area.⁶⁹ These inflows may be sources of As into Lake Tarawera, although transport of As depends on the pE and pH of the flowing waters. Both dissolved and colloidal fractions are carried with flowing water, and

turbulence may suspend particulates along the flow path, which will then settle out into the sediments of the lake.⁶

1.7 Arsenic in Lake Tarawera

Numerous studies have reported general water quality and conditions of Lake Tarawera, often in relation to biological species. Within some of those studies, As concentrations has been mentioned, or they have reported conditions which influence As, such as thermal stratification and DO levels.

Pearson (2012)¹ collected monthly conductivity, temperature, and depth (CTD) casts from the centre of the lake (~80 m depth) over a 15 month period from September 2007 to December 2008. They reported strong thermal stratification with a temperature gradient of 16 °C at the surface to ~11 °C at depth, and DO profiles showed sharp decline at the thermocline (~30 m) from ~7.5 mg L⁻¹ to ~5 mg L⁻¹.¹ Thermodynamic conditions in sediment pore waters showed pE ranging between 100 and -180 mV and pH, 6.1-6.4.¹ Results for sediment and pore water sampling in the same location showed oxic sediments up to several cm deep; however, they also reported metal-As cycling between sediments and benthic waters through Fe and Mn concentrations. Concentrations of dissolved Fe were low (< 1 mg L⁻¹) in the pore waters to 20 cm below interface, whereas the sediments showed significant quantities of redox sensitive elements (Fe max 80.8 mg g⁻¹ and Mn max 42 mg g⁻¹) bound in particulate form. This was attributed to the reduction of sulphide co-precipitating with Fe as arsenopyrite thereby removing it from the precipitation/dissolution cycling. Fe showed little fluctuation between sediments and overlying water column. Mn showed high levels of flux, suggesting the cycling of As is from adsorption of As^V to Mn-(hydr)oxides. Pore water concentrations for As were reported as 0.2 mg L⁻¹ at the water-sediment interface, ~1 mg L⁻¹ at 20 cm depth, with a peak of ~1.1 mg L⁻¹ at 12 cm.¹

Nutrient loading (P and N) has been noted as detrimental to water quality due to increased biological activity; which subsequently leads to decrease of DO in the hypolimnetic waters during stratification. This loading can cause seasonal change in chemistry of benthic waters and can induce reduction and cycling of As and other redox sensitive elements. Scholes and Hamill (2016)⁷⁰, reported slight degradation

in the overall water quality of Lake Tarawera and a statistically insignificant change in average hypolimnetic DO concentrations across a decade of monitoring nutrient loading. They did, however, note a concern for increased trace element sedimentary internal cycling long-term due to this ongoing nutrient loading.⁷⁰

1.8 Summary

The focus of this thesis is the chemical movement and speciation of As in Lake Tarawera together with an indication of the mass loading and sources. It has been widely recognised that various oxides play a major role in the regulation of trace elements in aquatic environments.³⁴ The greatest transformations in As movement and speciation occur in water bodies with significant oxic/anoxic boundaries.²⁶ Understanding all relevant biogeochemical controls is thus necessary to explain the speciation, mobility, and cycling of As. The physical characteristics of Lake Tarawera are well studied, as are the inlet sources to the lake. Elevated levels of As in Lake Tarawera have been recognised; however, the source and form of this As and how it is transported around the lake has not been addressed.

There are biological processes involved in the movement and speciation of As that are beyond the scope of this thesis including the processes involved in the creation of the organic arsenic species DMA and MA. The uptake of As by fish and plants is not pursued in this study, however measurable amounts of As have been reported in mussels and fish found in Lake Tarawera.³ There are numerous elements which play a role in the redox processes contributing to the speciation and movement of As, however this thesis focuses on the two important ones; Fe and Mn.

1.9 Aim / research objectives

This study aims to determine the presence, chemical form, spatial distribution, and movement of As in Lake Tarawera, focusing on the Wairua Arm of the lake. The relevant fluctuations in redox parameters and geochemical processes are used to reinforce the As findings. The inlets to Lake Tarawera were examined for sources and spatial variation of As being input into Lake Tarawera. The use of previous work and ongoing monitoring data allows investigation and comparison of As concentrations and to estimate As loadings into the lake. Combining long-term with current data provides a basis for examining water quality changes in the lake.

Chapter Two provides field and laboratory methods for water sampling and analysis, digestion, sediment coring and pore water extraction. Chapters Three to Five present and discuss the results for this study. Chapter Three identifies the physical conditions of five open-water sampling sites in Lake Tarawera as they relate to As; such as thermal stratification and dissolved oxygen with depth. Chapter Four describes the presence, movement, and speciation of As and other related redox elements Fe and Mn. Chapter Five provides method development for pore water sampling to minimise oxygen exposure, together with preliminary sediment and pore water concentrations. Chapter Six concludes this study, summarising the findings and recommendations for future work

CHAPTER TWO

SITE OVERVIEW AND ANALYTICAL METHODS

2.1 Introduction

This chapter describes the field and analytical methods for the water, core, and pore water sampling undertaken in Lake Tarawera. Site locations are identified and details for each site are given. Laboratory and instrument specifics are outlined including the digestion and analysis of water samples, and preparation, digestion, and analysis of core samples.

2.2 Site overview

Lake Tarawera sits in a large geologically active region (Taupo Volcanic Zone). The Southern arm of Lake Tarawera, known as the ‘Wairua Arm’, contains many surface inlets, seven of which are included in an ongoing Regional monitoring programme undertaken by the Bay of Plenty Regional Council (BoPRC) and University of Waikato (UoW).^{1,60-62} The sites which were used for this research include those seven shallow/surface water inlets, as well as point samples taken from deeper waters from the Department of Conservation (DOC) camping site (“hot water beach”) out to the monitoring buoy near the centre, which is deepest part of the lake.

Water samples

The sampling location, Lake Tarawera, and more specifically the inlets of the southern arm (Wairua Arm) studied in this thesis are outlined in Figure 2-1. The GPS coordinates for the sample locations and site names which coordinate with abbreviated site names used in maps and discussion are outlined in Table 2-1.

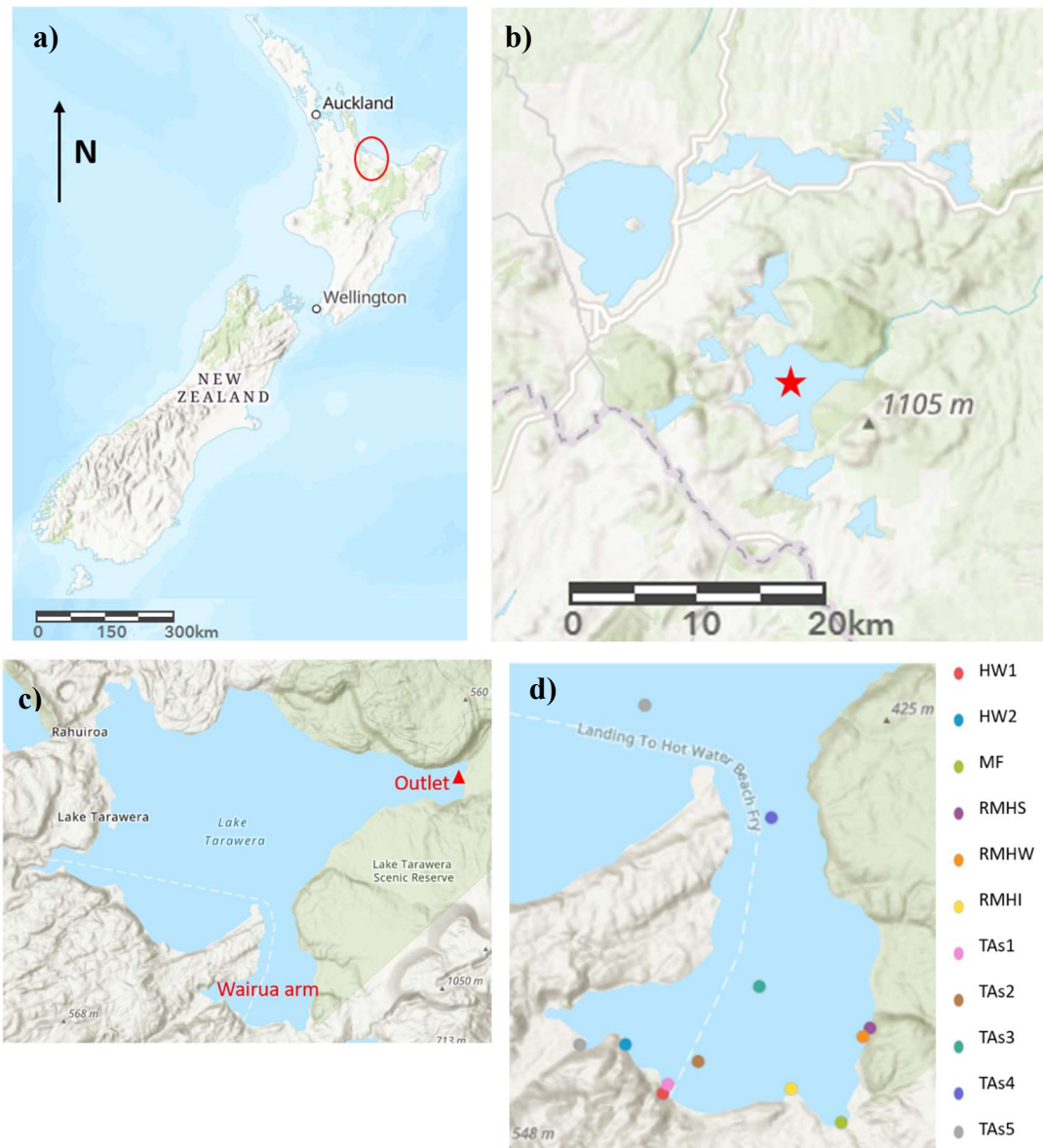


Figure 2-1. a) New Zealand with the Bay of Plenty Region circled in red; b) location of Lake Tarawera, indicated by the red star, in relation to surrounding lakes; c) Red writing indicating the areas of focus for this research; the Wairua Arm and the only lake outlet; d) Sampling locations for all routinely taken samples.

Table 2-1. Summary of sample locations corresponding to the map in Figure 2-1.

Sample ID	Site name	Latitude	Longitude
HW1	Hot water beach	-38.24351167	176.4332033
HW2	Champagne pool	-38.239472	176.429281
WR1	Wairua Stream	-38.23949833	176.4244967
RMHI	Rotomahana Inlet	-38.24313333	176.4466667
RMHW	Rotomahana Waterfall	-38.23883333	176.4541833
RMHS	Rotomahana Spring	-38.23811667	176.4549333
MF	Middle Flax A	-38.245849	176.4519167
TAs1	Open water 1 ~ 20 m	-38.24276833	176.4337217
TAs2	Open water 2 ~ 40 m	-38.24088333	176.4369033
TAs3	Open water 3 ~ 50 m	-38.23469167	176.4433233
TAs4	Open water 4 ~ 60 m	-38.220765	176.4445833
TAs5	Open water 5 ~80 m	-38.21147667	176.4313117

Core samples

Core samples were taken an estimated 5 m off-shore from HW1, at a depth of approximately 10 m, where the lake bed was flat. These samples were taken for pore water sampling and method development.

2.3 Sampling collection

2.3.1 Evacuation of O₂ from vacutainers and HPLC vials

Vacutainers (Greiner Medical Blood Collection Tubes, Thermo Fisher Scientific) and HPLC vials (2 mL, Thermo Fisher Scientific) were flushed with N₂ gas at ~90 Kpa pressure (until the pressure gauge stabilised) using a 30 gauge needle to pierce the vial septa and remove oxygen from the vessels, leaving them under vacuum. A Rocker 600 pump was used to evacuate the containers and vials. Three cycles of N₂ gas flushing and evacuating was undertaken per vial.

2.3.2 Water collection of open-water sites and lake inlets

Open-water site samples were collected using a Van Dorn horizontal water sampler, with surface samples taken at ~5 m depth, and ~5 m above the sediment (for the purpose of this thesis they are known as the benthic samples), depths that were estimated using rope markings and the boat fish finder. A three-way valve was attached to the Van Dorn with a 60 mL luer-lock syringe and 0.45 µm membrane filter to reduce exposure of the samples to oxygen while filtering them directly into 15 mL polypropylene tubes. Sample tubes for As speciation were filled leaving no headspace.

Surface inlet sites were sampled using an open plastic vessel attached to a long wooden handle. The vessel was rinsed twice, gently, to not stir up sediments, before the sample was collected and transferred into labelled 15 mL polypropylene tubes using a 60 mL luer-lock syringe and 0.45 µm membrane filter.

At each site (open water and inlet sites) opaque Astraline HDPE bottles (100 mL) were used to collect unfiltered samples for total elemental analysis. These were also used for grab samples taken while wading off Hot Water Beach and Rotomahana Waterfall.

All water samples were kept in a cooler box on ice in field and for transport, then transferred to a refrigerator at 4°C until analysis.

2.3.3 Sediments and pore water collection

A Gravity Corer was fitted with a plexiglass core barrel. Holes (1.5 mm diameter) were drilled in the plexiglass core barrel at 2 cm increments lengthwise down the barrel, for sampling at multiple depths. A plug was 3D printed at UoW to fit the barrel and prevent leaking. The drilled holes were covered with duct tape prior to sampling to prevent sample leakage once it was obtained. The core was held with a ring stand and clamps to allow for sampling to take place on shore. Pore waters were collected in field, and the core was transported back and stored in the refrigerator at 4°C.

Rhizons (Rhizosphere, The Netherlands) equipped with female luer, 5 cm long 0.58-0.65 μm membranes, and 12 cm PVC tubing were connected to an in-house made male/male adaptor that connected to 27-gauge hypodermic needles (Terumo Corporation, Thermo Fisher Scientific). These were used to collect pore waters from the sediment core(s) taken. Vacutainers were pierced with the needle to create suction and draw the pore waters out of the core through the rhizon. Pore waters were collected at five depths (3, 13, 17, 25, and 33 cm) using vacutainers which drew in differing volumes of water (unmeasured).

2.4 Field methods

2.4.1 In-field instrumentation

At each open-water site (TAs1-5), a water column profile was obtained by a Sea - Bird Electronics 19 plus SEACAT profiler (CTD, Sea-Bird Electronics Inc., Washington) which measured temperature, dissolved oxygen (DO), conductivity, and depth at a frequency of 4 Hz. The DO sensor (Sea-Bird Electronics) had a detection limit of 0.1 mg L^{-1} . DO profiles were not obtained for all sampling dates, due to faulty equipment.

2.5 Analytical and laboratory methods

2.5.1 Reagents and standards

Stock solutions for As^{V} and As^{III} were prepared from $1004 \pm 6 \mu\text{g mL}^{-1}$ As solution containing As^{V} oxide hydrate, and $1002 \pm 4 \mu\text{g mL}^{-1}$ As^{III} oxide (Inorganic Ventures, Christianburg, Virginia, USA). The HPLC mobile phase (phosphate buffer, $\text{pH} = 6$) was prepared using ammonium dihydrogen orthophosphate $(\text{NH}_4)_2\text{H}_2\text{PO}_4$ (2.382 g L^{-1}), Hopkin & Williams Ltd, England and ammonium hydrogen orthophosphate $(\text{NH}_4)_2\text{HPO}_4$, (0.734 g L^{-1}) Ajax Chemicals, Australia. Totals and sediment digestion was undertaken using concentrated HNO_3 (65%) and HCl (37%) (ACS, Iso Reag.), which was double-distilled using Savillex DST-1000 acid purification system. Distilled and deionised (Type 1) water was sourced from a Merck Milli-Q® system at a resistance of 18.2 $\text{M}\Omega/\text{cm}$.

2.5.2 Sediment extrusion from core and preparation for analysis

The sediment core totalling 40 cm depth was extruded into 14 sections. The 3D printed plug was attached to a piston on top of an extruder rod, stabilised with a base plate, and clamped to hold the core barrel on. Four full rotations of the handle on the extruder rod equated to one sample which was then scraped into a foil tray using a custom made chamber (Figure 2-2).

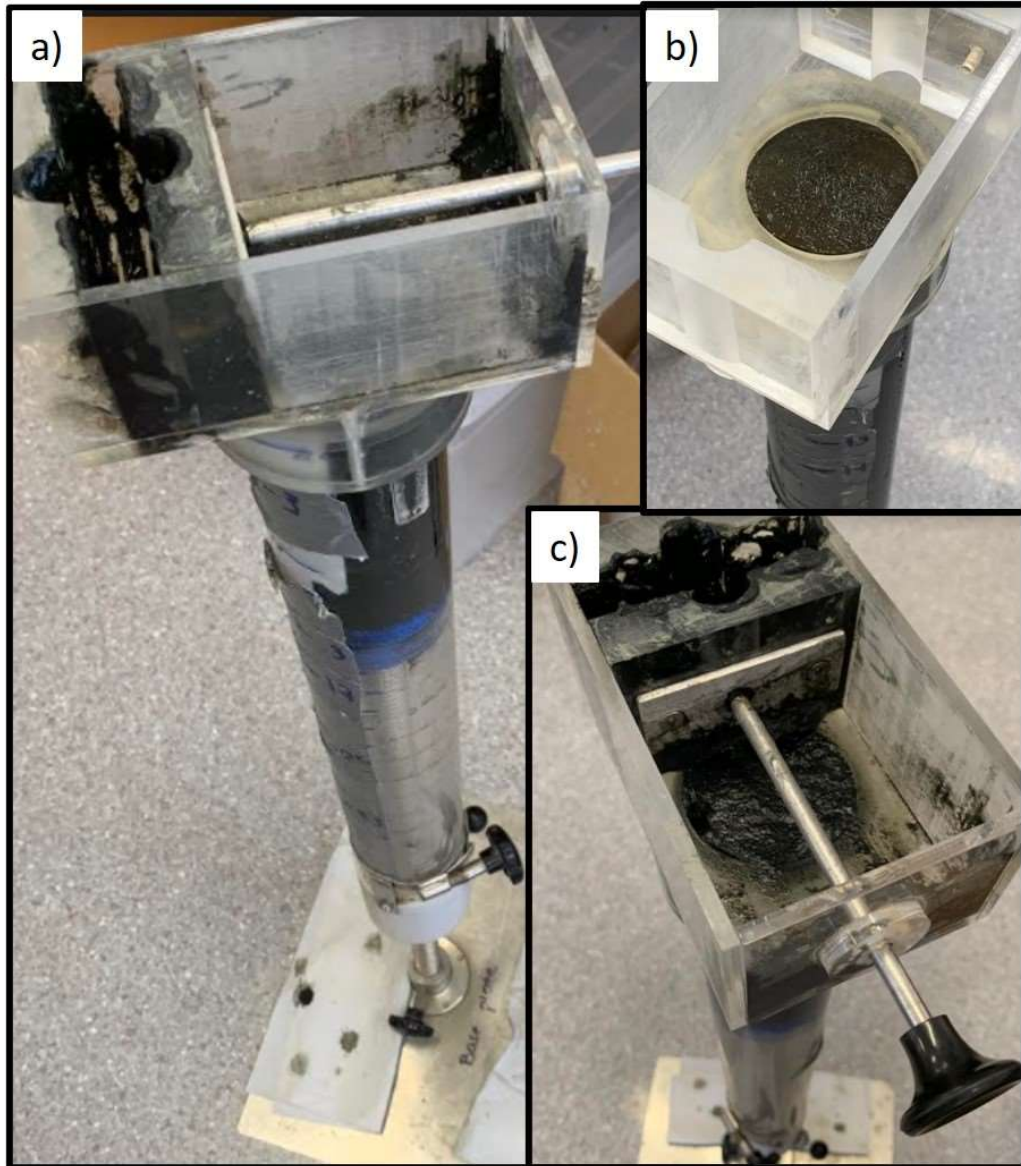


Figure 2-2. Core extrusion using a piston and extruder rod to push sediment up through the core barrel into a custom made chamber for transferal into foil trays. a) extruder rod having pushed the piston part-way up through the core; b) the custom-made chamber where sediment is segmented; c) how pushing the plunger segments the sediment for collection.

The sediments were dried at 105°C for 52 hours in accordance with EPA method 200.2.⁷¹ Wet and dry weights were recorded and used, together with the volume of pore waters extracted to determine the porosity of the sediments, calculated as a vol vol⁻¹ multiplication of water mass to volume.

Due to the soft consistency of the sediments, obtaining equal sample sizes was difficult, particularly once the plug was unable to be wound four full rotations per sample.

2.5.3 Digestion methods

Water – total recovery

The unfiltered water samples were digested based on the SCOPE - Digestion for total metals in water method⁷². Unfiltered water (24.25 mL) maintained at 90°C ± 5°C for two hours on a DigiPrep MS digestion hot block (SCP Science, Quebec, Canada) with HNO₃ (0.5 mL) and HCl (0.25 mL). Type 1 (distilled, deionised and 18 Ω) water used to dilute samples back to a final volume of 25 mL to account for any loss by evaporation (dilution factor of 1). Two quality control samples and one blank were prepared with each batch of samples to ensure reproducibility and limited contamination.

Sediment

EPA method 200.2⁷¹ was used as a guideline for the digestion of the sediments for elemental analysis, with the sample size and reagents volumes halved. Ground sediment (0.5 ± 0.01 g) was weighed into a 50 mL calibrated digestion block cup (Environmental Express, Charleston, South Carolina, USA) with 1:1 HNO₃ (2 mL) and 1:4 HCl (5 mL). The acid solution was left for 48 hours in a fumehood prior to digestion in a heat block at 90°C ± 5°C for 2 hours. The digest was diluted to 25 mL using Type 1 water (dilution factor = 25/sample mass (g)). A sub-sample (0.55 mL) of this diluted digest was aliquoted to a 15 mL falcon tube and diluted using Type 1 water to a final volume of 5 mL (dilution factor 0.09) using a pipette to attain a total acid concentration of 2% v/v. A sediment Certified Reference Material PACS-3 (National Research Council, Canada) was digested and analysed alongside the samples.

2.5.4 In-lab validation of vacutainers in arsenic preservation

Vacutainers were prepared by the method outlined in Section 2.3.1. Retention of As^{III} by vacutainers was tested using Type 1 water and UoW campus Chapel Lake water. DO levels of both water types was tested using a handheld DO probe with 0.003 mg L^{-1} resolution (Einstein). Type 1 or UoW water (49.9 mL, in triplicate) was transferred into 50 mL calibrated digestion block cups (Environmental Express, Charleston, South Carolina, USA), with a lid which had been pre-drilled (1.5 mm diameter) and covered with duct tape. A stock solution of As^{III} oxide ($10,000 \text{ } \mu\text{g L}^{-1}$) was added to the samples (100 μL) to give a total spike concentration of $100 \text{ } \mu\text{g L}^{-1}$. The duct tape was pierced with a needle and the rhizon inserted, mimicking in-field pore water collection methods. A waste vacutainer was used until sample was flowing (removing any oxygen from the rhizon), then the sample vacutainers were used to draw sample. Unspiked samples were also prepared in triplicate for both the Type 1 water and UoW campus lake water. All samples were refrigerated prior to HPLC-ICP-MS speciation analysis.

A second validation procedure was undertaken using the second core collected from off-shore HW1 in March 2020. After pore water samples had been collected in - field the core was transported and stored in the refrigerator until August (~5 months), when it was then used for method validation. Two vacutainers were filled from the same core depth (13 cm; approximately 9 mL in each), of which (5.5 mL) of each was transferred to a fresh vacutainer using a 10 mL syringe luer - lock syringe and 27-gauge hypodermic needles (Terumo Corporation, Thermo Fisher Scientific). The two 5.5 mL samples were spiked with 0.275 mL of As^{III} solution (10 mg L^{-1}) to give a final spike concentration of $500 \text{ } \mu\text{g L}^{-1} \text{ As}^{\text{III}}$. A 1 mL subsample was taken from each ($n = 4$) for ICP-MS elemental analysis. The two samples were then each split into three sub-samples for storage and analysis using a 1 mL luer-lock syringe and 27- gauge needle (total $n = 12$, being 3 spiked and 3 unspiked from each of the two original vacutainers).

2.6 Instrumentation

2.6.1 ICP-MS for elemental analysis

An Agilent 8900 Inductively Coupled Plasma – Mass Spectrometer (ICP-MS; Agilent Technologies, Santa Clara, California, USA) equipped with SPS4 autosampler (Agilent Technologies, Santa Clara, California, USA), a 0.05- 0.1 mL min⁻¹ micromist U-series nebuliser (Glass Expansion, Melbourne, Victoria, Australia), and quartz Scott Type spray chamber and quartz torch with 2.5 mm injector (Agilent Technologies, Santa Clara, California, USA), a nickel sample and skimmer cone, an extraction omega lens (Agilent Technologies, Santa Clara, California, USA), and a triple-quadrupole mass spectrometer was used for elemental analysis of ⁷⁵As as ⁹¹AsO, ⁵⁵Mn, ⁵⁶Fe. N₂O was used as the reaction gas for the reaction of ⁷⁵As with ¹⁶O to produce ⁹¹AsO⁺. General operating parameters are reported in Table 2-2. The instrument was optimised daily ensuing oxides and doubly charged ion concentrations were less than 2%.

Table 2-2. ICP-MS Optimised Operating Conditions.

Condition	Operation setting
Forward (reflected) power (watt)	1550
Gas flows (L/min Ar):	
Plasma	15
Makeup/dilution	0.10
Carrier	1.05
Sampling Depth (mm)	8.0
Lens voltage (V)	7.5 – 10
Detector mode	Pulse counting
Sweep replicates	50
Dwell time (s)	0.1-0.3

For solution analysis, a five-point calibration curve (0.1 – 500 ppb) was used (stock standards obtained from Inorganic Ventures, Christiansburg, VA, USA; IV71-A, for trace elements and single-element standards for major elements; Na, Ca, K, P and S). An internal standard solution containing scandium, gallium, rhodium, indium was pumped inline and diluted 1:1 during analysis. Check standards (1.0 and 10 µg L⁻¹) were analysed every 20 samples and re-calibration was performed every 100 samples. Reagent blank samples (2% HNO₃) were analysed every 10 samples to ensure minimal carryover between samples.

For digested samples which were diluted during sample preparation, final concentrations were back calculated using a dilution factor, as shown in Equation 2 - 1 where C = concentration ($\mu\text{g L}^{-1}$), V = volume of water added (mL) and W = weight of dry sample (g)

$$\text{concentration in mg kg}^{-1} = \frac{C \times V}{W} = \quad (2-1)$$

Single samples were taken from each site across the sample period. For quality control, the reproducibility of As concentrations was tested through aliquots (n = 6) of a 1 L TAs5 surface water sample as a real matrix for replicate analyses. An average As concentration of $41.79 \pm 2.9 \mu\text{g L}^{-1}$ provided an indication of sampling and analytical error across all samples, and this variation is in accordance with general lab standards and is accounted for by the method.⁷² No other samples were taken or analysed in duplicate due to sampling limitations; therefore, all presented concentrations throughout this thesis are subject to this standard deviation.

2.6.2 HPLC for arsenic speciation

High Performance Liquid Chromatography (HPLC) (Agilent 1260 Infinity II, Santa Clara, California, USA) equipped with a pump and autosampler was coupled to the Agilent 8900 ICP-MS for As species separation. A Hamilton PRP-X100 anion exchange column (5 μm particle size, 150 x 4.6 mm) was used for complete separation of species As^{III} , As^{V} and DMA. An isocratic elution was used (20 mM ammonium phosphate at pH 6.0), with an injection volume of 100 μL and 1 mL min^{-1} flow rate.⁷³ The total analysis time was 7 minutes. Vial lids without pre-slit septa were used for As speciation to minimise exposure of the sample to atmosphere oxygen.

2.6.3 LGR OA-ICOS for isotope analysis

A Los Gatos Research Off-axis integrated cavity output spectrometer (LGR OA- ICOS) equipped with Triple Isotope Water Analyzer (TIWA-45 EP) and PAL liquid water auto-injection system was used for hydrogen and oxygen isotopic analysis of water samples, using internal standards ANT-01 ($\delta^2\text{H} = -206.61 \text{ ‰}$, $\delta^{18}\text{O} = -25.87 \text{ ‰}$) and AURORA2 ($\delta^2\text{H} = +1.63 \text{ ‰}$, $\delta^{18}\text{O} = -0.80 \text{ ‰}$) to calibrate. Data was processed with the LIMS for Lasers data management system. Based on long-term data collection of the standards, there is an uncertainty of measurement of $\pm 0.03 \text{ ‰}$ for $\delta^2\text{H}$ and $\pm 0.01 \text{ ‰}$ for $\delta^{18}\text{O}$. Eight measurements were taken for each sample, with the first three injections discarded to remove inter-sample memory.

2.7 Data analysis

ICP-MS data and As speciation data were processed using Agilent Mass Hunter 4.5 Workstation Software (Version C.01.05, Build 588.3) 2018. Statistical analyses were conducted in R (R Core Team, 2014) and Microsoft Excel (2007) and figures were produced using the R package ggplot2 (Wickham, 2009).

The Shapiro-Wilks test⁴² was used to test for normality before statistical analyses were undertaken on data subsets less than $n = 30$. Parametric t-tests were used for normally distributed data. Non-parametric analyses were undertaken for non-normal datasets; Mann-Whitney U tests (pairwise comparisons), and Kruskal-Wallis (analysis of variance) were tested for difference at $\alpha = 0.05$ level of significance.

Single samples were taken at each sampling location, therefore values presented are not an average, unless otherwise stated.

CHAPTER THREE

PHYSICAL PROPERTIES

3.1 Introduction

This chapter examines the physical properties of the water column of Lake Tarawera. The physical response of the lake to seasonal changes in weather, such as thermal stratification, influence the speciation and mobility of As and other redox sensitive elements; including the movement and mixing of these elements from their inlet source to the open-water body. In thermally stratified waters, the hypolimnetic (bottom, cooler waters) cycling system is separated from the regenerating oxygen supply of the surface water-air equilibria; therefore, oxygen depletion (and onset anaerobic conditions) can induce chemical changes, particularly in oxygen bound species such as N-, Fe-, Mn-, and As- oxides. Capturing data seasonally will identify any seasonal differences in the temperature with depth, which will potentially support and help explain the mixing of water coming in from inlets, as well as elemental data, both of which will be discussed in following chapters.

Thermal stratification and DO in the water column were profiled using data from a CTD (measuring temperature and DO with depth) which was deployed each season, in approximately the same five locations according to GPS coordinates. Previous data collected from 80 m depth (approximately TAs5 equivalent) was obtained from BoRPC² was used for long-term temporal comparisons.

3.2 Temperature and oxygen profiles

Five open-water locations were chosen between Hot Water Beach (TAs1) in the Wairoa Arm of Lake Tarawera and the deepest part of the lake (TAs5) (refer to Figure 2-1 and Table 2-1). A CTD was deployed at each of these five sites quarterly throughout 2019 (February, April, August, and December), and again in March 2020, to capture seasonal variation. Figure 3-1 presents the vertical gradient profiles for temperature from each sampling date and site, whereas DO profiles (Figure 3-2) were only obtained for August and April 2019.

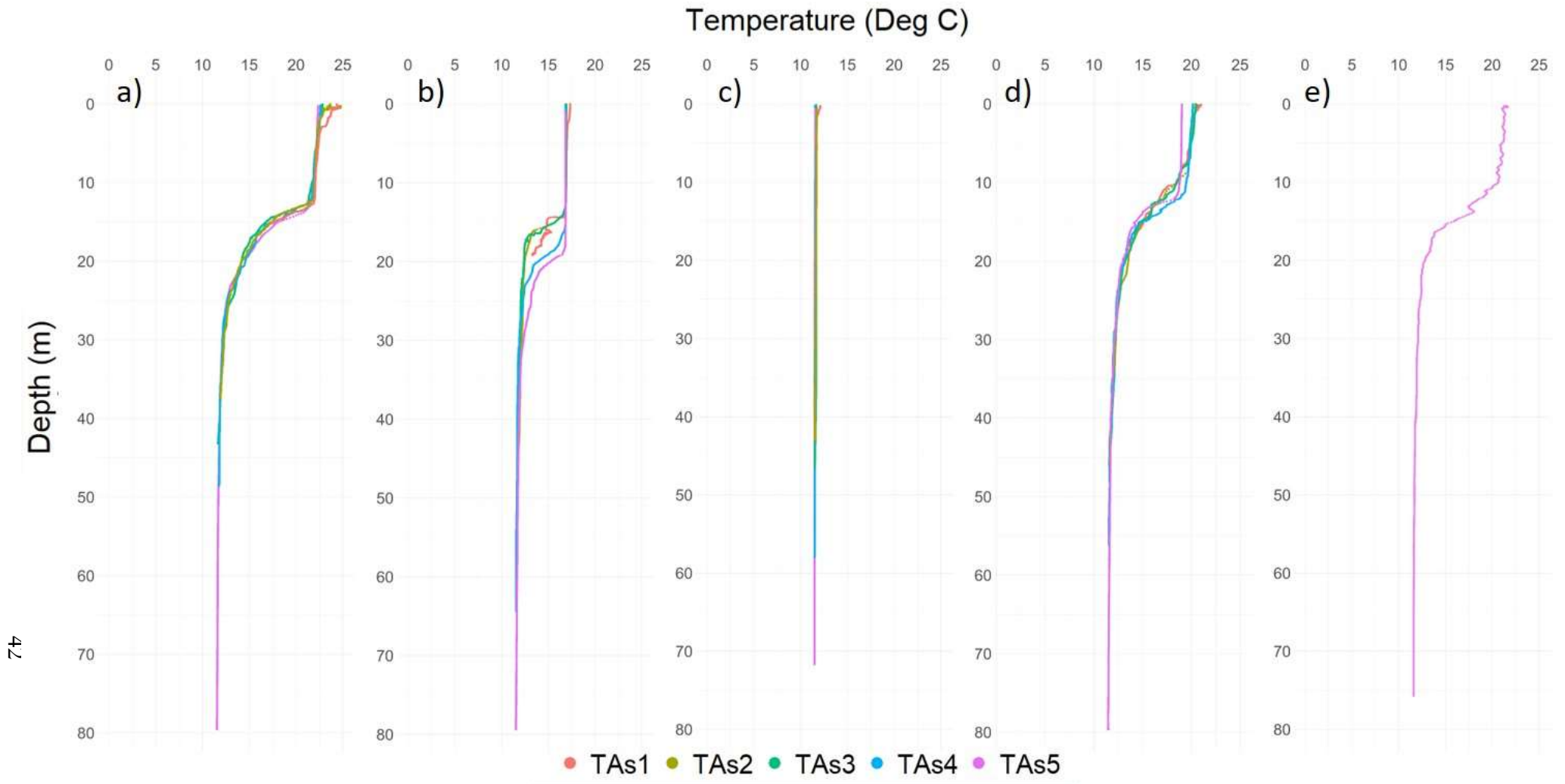


Figure 3-1. CTD casts for temperature (°C) with depth (m) for a) February 2019; b) April 2019; c) August 2019; d) December 2019; e) March 2020, across the five open-water sites TAs1-5. Thermal stratification occurs between 10-25 m depth during the stratified period (a, b, d, and e), and the mixed period is shown by homogenous temperature with depth (c).

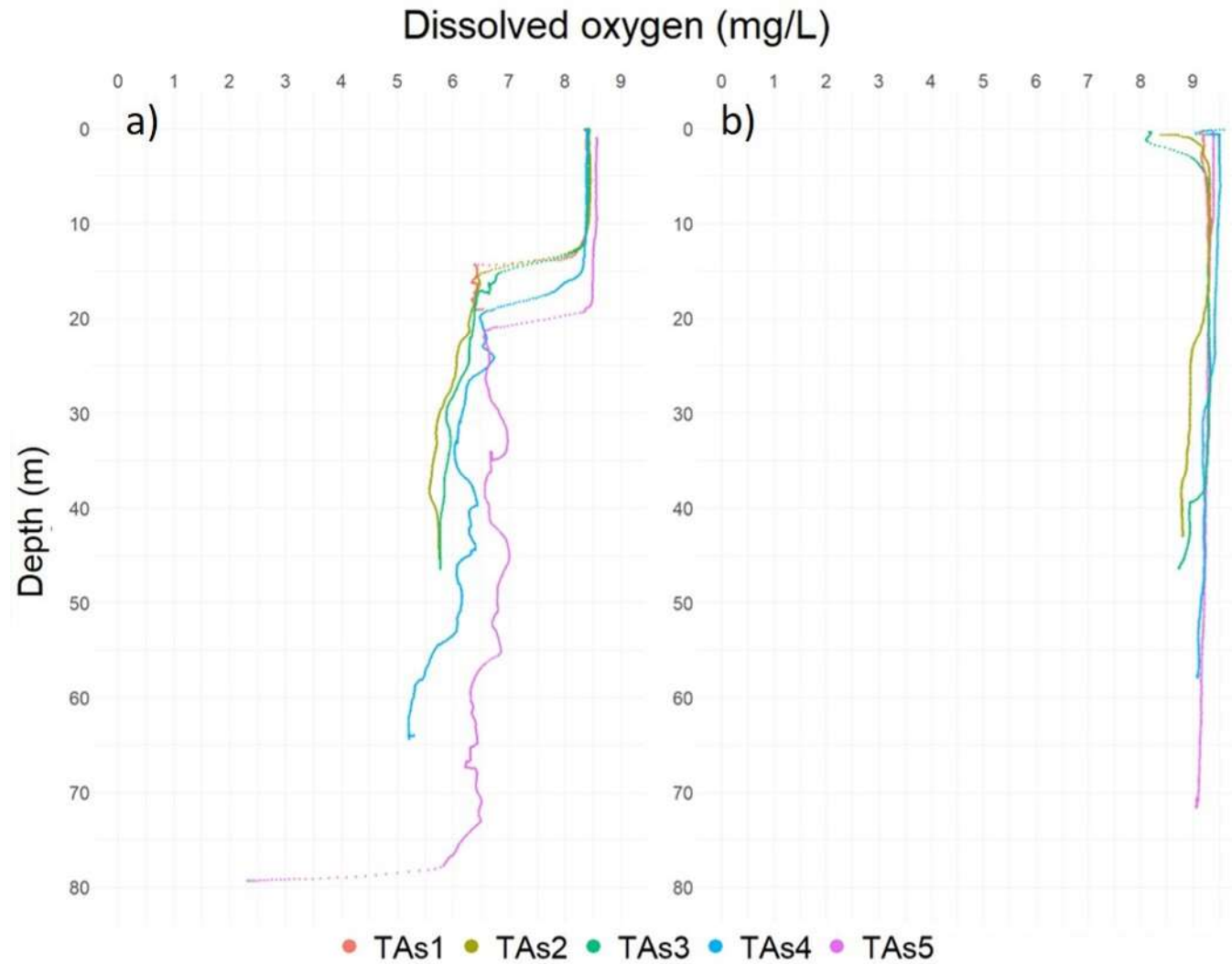


Figure 3-2 CTD casts for dissolved oxygen (mg L^{-1}) with depth (m) for a) April 2019; b) August 2019. Seasonal fluctuation is seen between profiles, with the mixed season having more consistent concentration with depth (b), compared with during stratification (a).

There are clear seasonal trends seen in Figure 3-1 and Figure 3-2 over a 13-month period. In August (winter) the lake was homogenous, with stable temperatures ($< 1\text{ }^{\circ}\text{C}$ variation, Figure 3-1 c) and dissolved oxygen ($< 1\text{ mg L}^{-1}$ variation, Figure 3-2 b). From December (summer) through to April (autumn) varying degrees of thermal stratification can be seen (Figure 3-1 a, b, d, and e) with the most significant vertical gradient being $15\text{ }^{\circ}\text{C}$ in December 2019; where surface waters reached $25\text{ }^{\circ}\text{C}$. The vertical temperature gradient is less significant in April (Figure 3-1 b), with a variation of $5.8\text{ }^{\circ}\text{C}$, and the thermocline depth (separating layer) varies between sites; indicating the lake is preparing to turn over for the winter season.

Overall, there is little seasonal variation ($0.08\text{ }^{\circ}\text{C}$) in the hypolimnetic waters between sites, whereas the surface waters vary by $12\text{ }^{\circ}\text{C}$, with TAs1 being warmer each season, and TAs5 cooler. The shallower sites also stratify higher in the water column than the deeper sites (Figure 3-1 a, b, and d). These subtle stratification differences are reinforced by a more extreme example found in a previous study.^{74,75} Literature comparing stratification between tropical and temperate climates reported higher surface water temperatures (tropical climates) cause thermoclines to form at shallower depths, have thicker bands, form earlier, and last longer than cooler surface waters (temperate climates).^{74,75} Further, it has also been noted that calmer waters create a temperature gradient more quickly than waters which are more turbulent.^{75,76} When comparing the location of the deep-water sites (Figure 2-1 c), TAs1-3 are within the Wairua Arm bay, compared with TAs4 in the neck of the bay and TAs5 out in the main water body; therefore, exposure to winds and currents would be most extreme for TAs5. The overall surface water temperature increase that causes thermocline formation is produced by increasing air temperature and sun exposure during warmer months in temperate regions.⁷⁷ There will be diurnal fluctuations in all surface water temperatures as solar energy (primarily UV⁷⁶) is absorbed during the day and equilibration with cooler air temperatures occurs through the night. One source reported maximum diurnal temperature changes of $2\text{ }^{\circ}\text{C}$ in nearby Lake Rotowhero.⁷⁸ Conversely, TAs1 is offshore from the constant hot water inlet source HW1; therefore, TAs1 has a continuous secondary heat source potentially contributing to the consistently warmer temperature of the surface waters in TAs1. The vertical temperature gradient which occurs during the stratified period will influence the mixing and dispersion of incoming surface waters, depending on the temperature and density

of the water coming from those sources. The movement and mixing of HW1 out towards TAs1 is described in further detail in Chapter 4, describing the specific effects that this may have on As movement.

The variation in temperature occurs within the top 25 m of the water column, a process resulting in the distinct separation of the hypolimnetic waters. During the period of thermal stratification, oxygen regeneration occurring in that top 25 m from waters-air equilibria does not replenish DO in the bottom waters. It has been estimated that 80% of the geothermal inflows are sub-surface.⁷⁰ However, the year - round consistency between benthic water temperatures across the five sites indicates no significant localised heat source captured through this data at any of the sampled sites, as it would influence local water temperature.

The oxygen profiles collected correlate with the temperature in terms of mixing regime. There is a clear decrease in DO with depth and the same between-site variation (Figure 3-2) as seen for temperature. In the deepest part of the lake sampled (~80 m) there is a sharp decline from 6 mg L⁻¹ at 76 m to 2.3 mg L⁻¹ at 79 m, which is approximately 1 m above the SWI.⁷⁴ The CTD deployment to ~1 m above the sediments (estimated in field using boat fish finder depth gauge and the CTD rope with a 5 m increment marks) was to ensure undisturbed water samples and to prevent sediments being pumped through the CTD system. A consequence of the caution taken while sampling is that the final segment of water was not sampled (so as to not disturb the sediments and alter the sample), and the DO concentrations of that final ~1 m of water are speculated based on literature. DO less than 6 mg L⁻¹ has been defined as hyperanoxic,⁷⁹ and 2 mg L⁻¹ as the critical value of onset anoxia.⁷⁴ These conditions are present in TAs5 from 6 mg L⁻¹ at 56 m in April (Figure 3-2 a), with the final recorded measurement of 2.3 mg L⁻¹ at 79 m. It has been reported that if DO is 2 mg L⁻¹ at a height of 1 m above sediment depth, there is likely anoxic conditions at the sediment surface.⁷⁹ Considering this information, together with the gradient of the decrease of DO from 74 m depth (Figure 3-2 a), it is likely that conditions reach anoxia in the last segment of unmeasured water which is an important consideration for As speciation (as discussed in Chapter 4).

3.3 Changes in temperature and dissolved oxygen profiles between 2019 and long-term monitoring programme data

The CTD data collected in 2019/2020 was compared data obtained from BoPRC². Temperature and DO concentrations spanning from 1996 to 2017 were visualised graphically for the purpose of identifying long-term changes in the physical conditions of Lake Tarawera. The BoPRC data was collected at a TAs5 equivalent site and is displayed in Figure 3-3 and Figure 3-4, respectively.

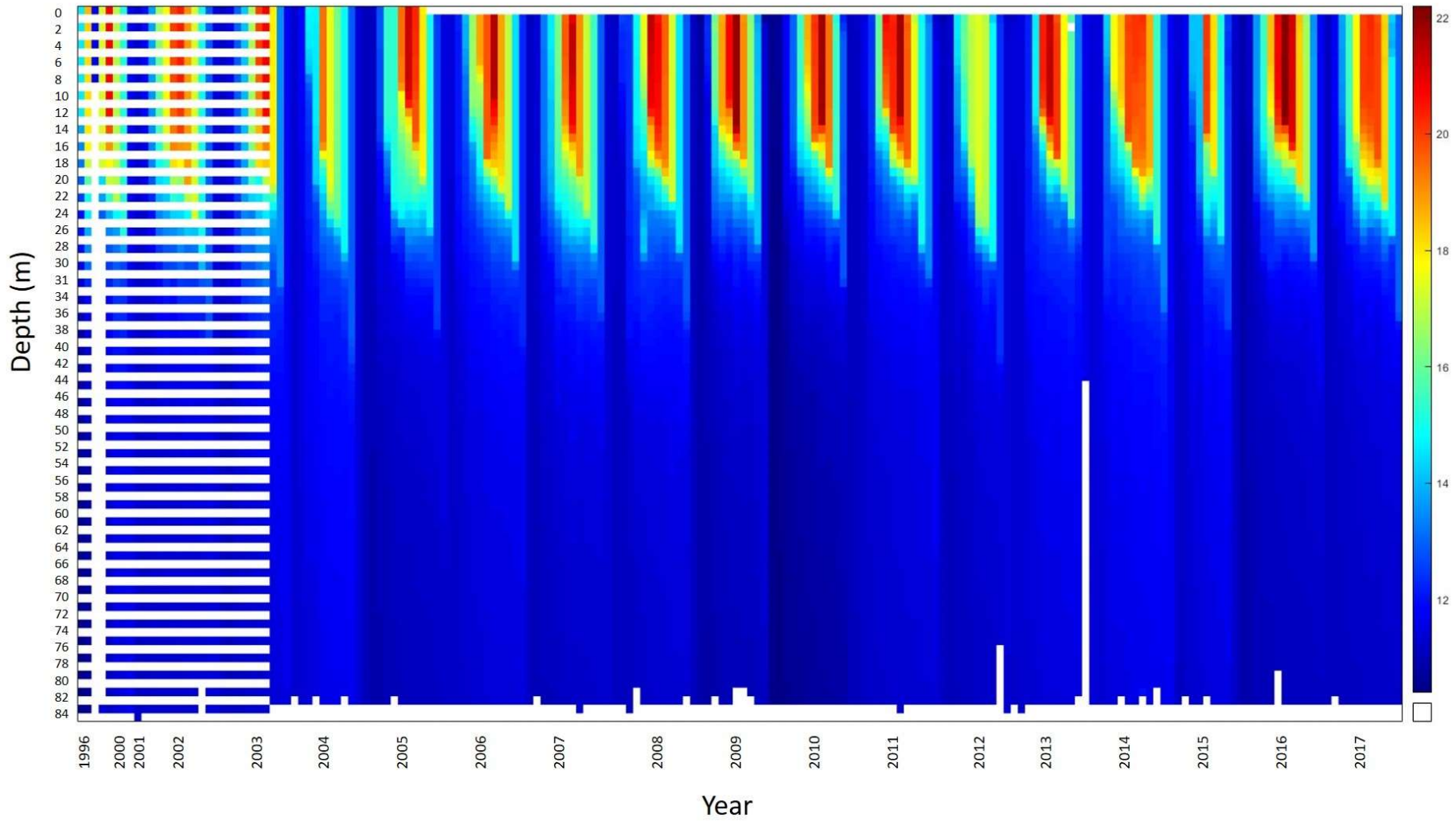


Figure 3-3. Bay of Plenty Regional Council CTD (temperature) data by depth (m) covering the period 1996 to 2017. White space represents missing data, and the scale on the right represents temperature in °C. Note the sampling frequency has increased over time, with sampling increasing from 2 m increments to 1 m.

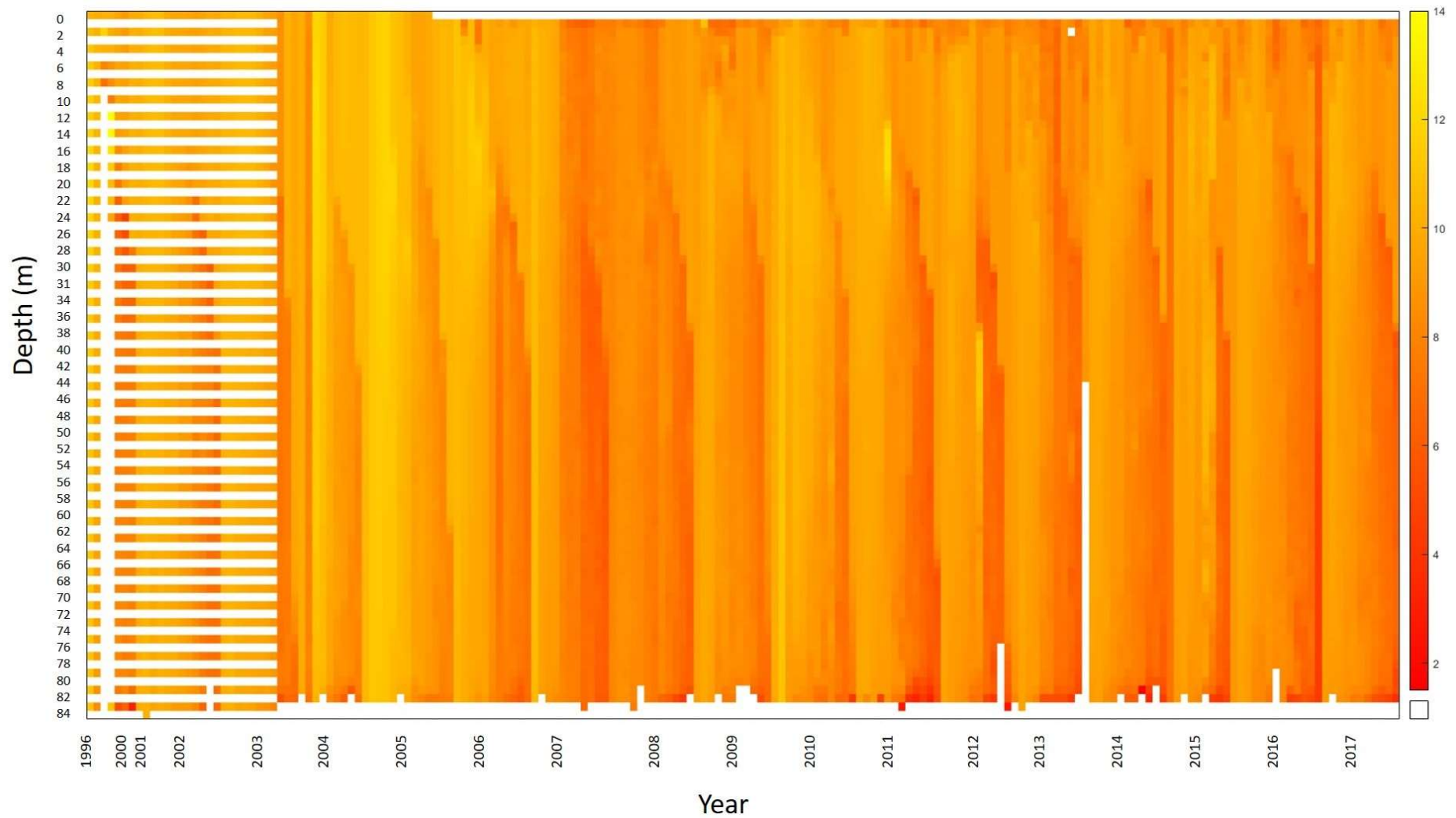


Figure 3-4. Bay of Plenty Regional Council CTD (dissolved oxygen) data covering period 1996 to 2017. White space represents missing data, and the scale on the right represents dissolved oxygen in mg L⁻¹. Note the sampling frequency has increased over time, with sampling increasing from 2 m increments to 1 m.

Figure 3-3 and Figure 3-4 show the regular cycling of temperature and DO that occurs with the annual stratification and turn over based on the inverse relationship between temperature and dissolved gases with winter having the lowest temperatures and highest DO values, reinforcing the findings within this thesis. Stratification occurs higher in the water column in years where the surface water temperatures were higher. It is clear there is variation within and between years for both temperature and DO, as expected. There appears to be a slight decrease in benthic DO from approximately 2010 onwards, however the general trends are consistent with slightly different maximum or minimums. This could potentially correspond to local weather events for specific years.

Surface water temperatures in 1968, when Jolly studied seven lakes over 12 months in the Rotorua-Taupo thermal area, were equivalent to those recorded in Figure 3-1, for both summer (22 °C) and winter (11 °C).⁸⁰ Therefore, there is a possibility of climatic influences on temporal surface water differences. The National Institute of Water and Atmospheric Research (NIWA) reported that the average national temperatures during 2008 were consistent with long-term monitoring; however, they noted extreme conditions throughout the year, including the lowest recorded January temperature for Rotorua and Taupo.⁸¹ NIWA reported 2019 as the fourth warmest year on record (2016 and 2018 being hottest second hottest, respectively), with a maximum of 1.2 °C above average observed across the Bay of Plenty region.⁸² This demonstrates how local weather patterns can affect water temperature.

The temperature and DO reported are consistent with the expectation for a monomictic, oligotrophic, deep lake. A decline of DO over time (a slight decrease in DO is seen from 2011 onwards) is detrimental to water quality, with low DO providing the major requirement for changes in As speciation. The influence of temperature and DO is reiterated throughout Chapter 4, where As concentrations, speciation, and movement is discussed.

CHAPTER FOUR

ARSENIC AND RELATED REDOX ELEMENTS

4.1 Introduction

This chapter focuses on the presence of As in Lake Tarawera; including information on concentration fluctuations within and between inlet sources, the chemical state in which As is entering the lake, and influences driving the movement of As within the lake. The data presented in this chapter is a combination of shallow inlet and open-water samples collected for this research and inlet sampling undertaken for an independent Lake Tarawera inlet monitoring programme.

The chemical state of As coming into Lake Tarawera from each inlet is dependent on the environmental conditions of the source.⁸ Subsurface geothermal waters (reducing and/or acidic) favour conditions for dissolved As, compared to surface (oxic) ground waters which favour the precipitation/co-adsorption and potentially settling out of As.⁶ Lake Tarawera is fed by geothermal waters, through both direct geothermal inlets (e.g. HW1) as well as secondary sources such as any of the seven other lakes that feed Lake Tarawera which themselves have geothermal inlets (e.g. Lake Rotomahana).^{29,69} Of the nearby lakes draining into Lake Tarawera, Lake Rotomahana sits South of the Wairua Arm, making it the closest lake to the area of focus in Lake Tarawera (Figure 4-1). Lake Rotomahana (335 m elevation) is manually discharged into Lake Tarawera (299 m elevation) through a floodgate controlled man-made stream, the inlet site which is called Rotomahana Siphon (RMHI) and could be a source of As to Lake Tarawera. Consequently, the physical and chemical conditions of Lake Rotomahana, including the cycling and distribution of As within the lake, is relevant as an input into Lake Tarawera through the known and suspected inlets.



Figure 4-1. Geographical location of Lake Rotomahana in relation to Lake Tarawera. Man-made inlet RHMI is represented by the purple dot.

4.2 Dissolved arsenic concentrations from Bay of Plenty Regional Council continuous monitoring data (2018-January 2019)

Lake Tarawera is fed by numerous surface inlets. UoW and BoPRC collaborate on a continuous monitoring programme on the known surface inlets into Lake Tarawera (Figure 4-2) on a quarterly basis. Data collected from these samples include ICP-MS dissolved elemental concentrations, water isotopes, conductivity, pH, and flow rate, to monitor lake quality. The elemental and flow rate data from this monitoring programme was used in this thesis for sites located within the Wairua Arm and the only known outlet in Lake Tarawera (Figure 4-2).



Figure 4-2. Location of surface inlets sampled quarterly by the UoW/BoPRC continuous monitoring programme² (grey circles). Inlet As concentrations were compared between geographical close sites indicated by the red shapes (SE of Wairua Arm, circle; N main body, triangle; NW main body, square).

Arsenic concentrations (Figure 4-3) were provided from previous monitoring of the sampling sites (May and October 2018 and January 2019) to give an indication of inlets with concentrations higher than the WHO drinking water standard ($10 \mu\text{g L}^{-1}$)⁴ and also identify inlets with fluctuating As concentrations. Higher concentration inlets with seasonal variation are of interest to further investigate the incoming speciation of As and the distribution of As from these inlets to the greater water body. The known geothermal activity (i.e. hot water inlets such as HW1) in the Wairua Arm was of interest from an As speciation perspective.

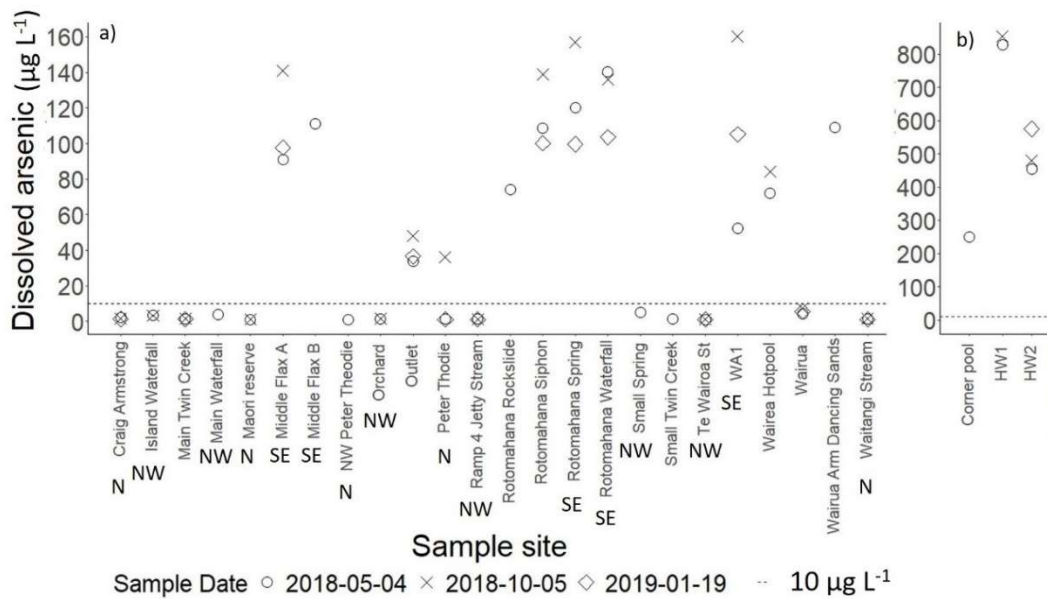


Figure 4-3. Dissolved As concentrations ($\mu\text{g L}^{-1}$) for a) inlet sites sampled by UoW monitoring programme², excluding HW1, HW2, and Corner Pool; b) for HW1, HW2, and Corner Pool. Note the scale difference between (a) and (b). WHO drinking water standard ($10 \mu\text{g L}^{-1}$) is indicated by the dashed line. Inlets correspond to the sample locations in Figure 4-2. Site names with directional labels indicate geographical grouping discussed in this section.

Out of the 27 inlets sampled by UoW/BOPRC (Figure 4-3), 14 (51.9%) exceed the WHO guideline of $10 \mu\text{g L}^{-1}$ dissolved As. The total range across all inlets is $<\text{DL}- 852 \mu\text{g L}^{-1}$, with an average of $97 \pm 181 \mu\text{g L}^{-1}$ ($n = 60$). This average is skewed by the high concentrations of sites HW1, HW2, and Corner Pool which all exceed $200 \mu\text{g L}^{-1}$ (Figure 4-3 b). HW1 exceeds the WHO drinking water standard by 85 times ($851 \mu\text{g L}^{-1}$). Of the inlets exceeding the WHO standard, only two (the Outlet and Peter Thodie) are not located in the Wairua Arm. Only ten samples that exceeded the WHO standard were sampled seasonally (which shows variation), and of those ten, eight had the highest As concentration in October 2018, with HW2 (January 2019) and Rotomahana Waterfall (RMHW, May 2019) being the exceptions.

Rotomahana Siphon (RMHI), Rotomahana Spring (RMHS), and Rotomahana Waterfall (RMHW) had similar January 2019 concentrations of $101 \pm 2 \mu\text{g L}^{-1}$ ($n = 3$). However, different trends between the three sites were observed across other seasons; the Spring was the most variable ($126 \pm 29 \mu\text{g L}^{-1}$, $n = 3$) whereas the Siphon had similar concentrations in May 2018 and January 2019 (108 and $100 \mu\text{g L}^{-1}$, respectively) with greater concentration ($139 \mu\text{g L}^{-1}$) in October 2018 and overall average of $115.7 \pm 20.6 \mu\text{g L}^{-1}$. The Waterfall site had the highest average concentration and least seasonal variation $126.3 \pm 20.3 \mu\text{g L}^{-1}$, with similar As concentrations for May 2018 and October 2018 (140 and $136 \mu\text{g L}^{-1}$) and lower concentrations ($103 \mu\text{g L}^{-1}$) in January 2019.

Inlets which are geographically close to each other (Figure 4-2) were grouped to examine spatial variation and identify localised areas of higher As inputs (Table 4-1). The greatest variation between clustered inlets occurred in the Wairua Arm, which had the highest As concentrations overall, as well as the greatest seasonal variation (Figure 4-3). The variation seen in the Wairua Arm cluster (Table 4-1) includes both between site variation and within site (seasonal) variation. The only data point from Peter Thodie measured $36 \mu\text{g L}^{-1}$, which skews the “NW – main body” average, as all other values in this cluster sit below $2.4 \mu\text{g L}^{-1}$.

Table 4-1. Summary statistics (2018-January 2019 collected by UoW/BoPRC) for clusters of inlet sites which are geographically close and have multiple data points (Figure 4-2).

Geographical location and grouped inlet sites	E – Wairua Arm (6 sites) $n = 17$	NW – main body (7 sites) $n = 12$	N – main body (7 sites) $n = 12$
Maximum ($\mu\text{g L}^{-1}$)	160	4.9	36.0
Range ($\mu\text{g L}^{-1}$)	108	3.9	35.1
Average ($\mu\text{g L}^{-1}$)	116	2.1	4.0
Standard deviation ($\mu\text{g L}^{-1}$)	27.0	1.4	10.0

The loading of As ($\mu\text{g s}^{-1}$) into Lake Tarawera through inlet sources was calculated (where flow rates were available) to examine the impact of various sources based on the volume of water together with dissolved As concentration (Table 4-2). The largest and most consistent source of As into Lake Tarawera was Rotomahana Waterfall, with both consistently high flow rates ($130 \pm 3 \text{ L s}^{-1}$, $n = 3$) and high dissolved As concentrations ($126 \pm 20 \mu\text{g L}^{-1}$, $n = 3$). WA1 had the second highest As loading, having a low flow rate ($7.3 \pm 3.8 \text{ L s}^{-1}$, $n = 3$) combined with high As concentrations ($105 \pm 54 \mu\text{g L}^{-1}$, $n = 3$). Te Wairua St had the greatest flow rate of all measured sites ($539 \pm 182 \text{ L s}^{-1}$, $n = 3$), yet As concentrations were low ($1.10 \pm 0.06 \mu\text{g L}^{-1}$, $n = 3$), resulting in a smaller As loading relative to most other sites. The variation seen across the inlets reinforce the findings of Stumm and Morgan (1995)³² who reported that concentration of contaminants is not a direct result of discharge volume. Thus, these results indicate that while volume of water moving is an important factor, the source-based As conditions of the inlets has the most impact on the concentration of As moving through the inlet into Lake Tarawera.

Table 4-2. Arsenic loading ($\mu\text{g s}^{-1}$) calculated (2018-January 2019) using flow rate (L s^{-1}) and dissolved As concentration ($\mu\text{g L}^{-1}$).

Site	As loading ($\mu\text{g s}^{-1}$) (2018 data)			
	May	October	January	Average
Ramp 4 Jetty	42	45.6	38.9	42.2 ± 3.3
Rotomahana Waterfall	18,500	17,300	13,400	$16,400 \pm 2,660$
Wairua	1,200	N/C*	1,340	$1,270 \pm 101$
Te Wairua St	746	455	501	567 ± 156
Waitangi Stream	323	427	238	329 ± 95.0
Main Twin Creek	506	842	568	639 ± 179
Small Twin Creek	263	N/C*	N/C*	N/C*
Peter Thodie	27.3	55.5	58.3	47 ± 17
NW Peter Thodie	24.3	N/C*	N/C*	N/C*
WA1	4,730	N/C*	10,500	$7,630 \pm 4,090$
Rotomahana Siphon	N/C*	9,313	4705	$2,380 \pm 3,290$

*N/C = flow rate not calculated

This UoW/BoPRC monitoring programme identified a difference in As concentrations between the Wairua Arm and the main water body. The main water body had inlet As concentrations less than $10 \mu\text{g L}^{-1}$ year-round, with the exception of two sites (Peter Thodie, and the Outlet). In contrast, the Wairua Arm displayed overall higher As concentrations, with no inlets containing less than $10 \mu\text{g L}^{-1}$ As, as well as seasonal variability within these inlets. The southern boundary of the lake/Wairua Arm appears to be a localised pocket of As within the lake and thus a focus for biogeochemical influences on the distribution of this As throughout the year.

Time and resources were a factor in reducing the number of inlet sites for this research. Therefore, sites for ongoing monitoring (2019/2020) were chosen based on location (Wairua Arm) from both a speciation perspective (due to hot water inlets such as HW1 and Wairua Hotpool) and having higher and more variable As concentrations. The sites HW1, HW2, Middle Flax A (MFA), Rotomahana Waterfall (RMHW), Rotomahana Spring (RMHS), Rotomahana Siphon (RMHI), Wairua Hotpool (WR1), and the Outlet to the Tarawera River were chosen, Figure 2-1 d shows the chosen sampling locations, and a summary of all sites including who they were sampled by and what for is in the Appendix; Table A-1.

4.3 Investigations into arsenic (speciation, dissolved, and particulate) from February 2019-March 2020.

Water samples from the eight inlet sites identified in Section 4.2 were collected five times between February 2019 and March 2020. These samples were analysed by HPLC for As speciation, ICP-MS for both dissolved and total elemental concentration, and LGR for water isotope analysis (refer to Chapter 2 for methodology). The dissolved elemental data was supplemented with the interspaced UoW/BoPRC monitoring data to provide approximately bi-monthly dissolved As concentrations.

The state, speciation, solubility, and movement of As in the water column of Lake Tarawera is strongly related to the DO and temperature conditions that were presented and discussed in Section 3.2. Where relevant, the data presented in Section 3.2 is discussed throughout the following sections.

4.3.1 Arsenic speciation

The presence of As^{III} in Lake Tarawera was the driving force of this research, because As in its reduced form (As^{III}) is more biologically toxic and water soluble than the oxidised form (As^V).⁴ Two mechanisms for the presence of As^{III} in Lake Tarawera were identified (Refer to Section 1.4). Biogeochemical conditions such as thermal stratification and subsequent reduction of DO in the benthic waters can lead to reductive dissolution of As^V to As^{III}.^{18,29,43} Direct input of As^{III} into Lake Tarawera could also occur through geothermal waters (e.g., inlets HW1 and WR1), as the extreme conditions of geothermal waters often favour As^{III} over As^V.^{29,70}

All water samples were analysed by HPLC for As speciation; samples were collected as outlined in Section 2.3.2. Only one incidence of As^{III} was detected, in WR1 (14 µg L⁻¹, March 2020), which accounted for 13.5% of the total As in the sample (total 104 µg L⁻¹, the remaining 86.5 % was present as As^V). WR1 is a shallow, slow moving stream located in a small cove in the SE of the Wairua Arm (Figure 2-1 d). This site contains recreational man-made dammed hot pools of geothermal waters, with overflow exiting through the shallow stream into the lake. The lakebed in the cove contains large amounts of lake weed compared with the other inlet locations. The vegetation has a diurnal DO cycle of photosynthesis and sequestering, and could deplete DO to the point of As^V reduction. Because As^{III} was only detected in one sample this result was not considered evidence for a continuous supply of As^{III} to the system.

Lake Tarawera is a popular location for recreational activities, including camping, swimming and fishing.⁶² The absence of the more toxic species, As^{III}, reflects the chemical conditions of the lake and is advantageous from a human health perspective. The presence of DO in benthic waters (refer to Figure 3-2) favours the more oxidised species, As^V; therefore, the As^{III} cycling observed in lakes with anoxic hypolimnions (refer to Figure 1-2 b) is not detected in Lake Tarawera. Although As^V is less toxic than As^{III}, the WHO drinking water standard is 10 µg L⁻¹ total As (sum of all species) and there are still health risks associated with exposure to As^V (refer to section 1.2.2). Therefore, in addition to As speciation, elemental analysis was undertaken on all water samples for quantification of dissolved As concentrations.

4.3.2 Dissolved arsenic

4.3.2.1 Inlets to Lake Tarawera as a source of arsenic

The inlets sampled were inter-spaced with the UoW/BoPRC monitoring programme sampling, providing a total of nine sampling instances across the inlets. The only exception was RMHI, with only January and May 2019 data, due to this site being a discontinuous, manually controlled flow used to prevent flooding of farmland surrounding Lake Rotomahana. The combined dissolved As data for the eight inlet sites are displayed in Figure 4-4 (a and b) which show seasonal variation between and within inlet sites, while Figure 4-4 c shows As concentration variation across sampling instances.

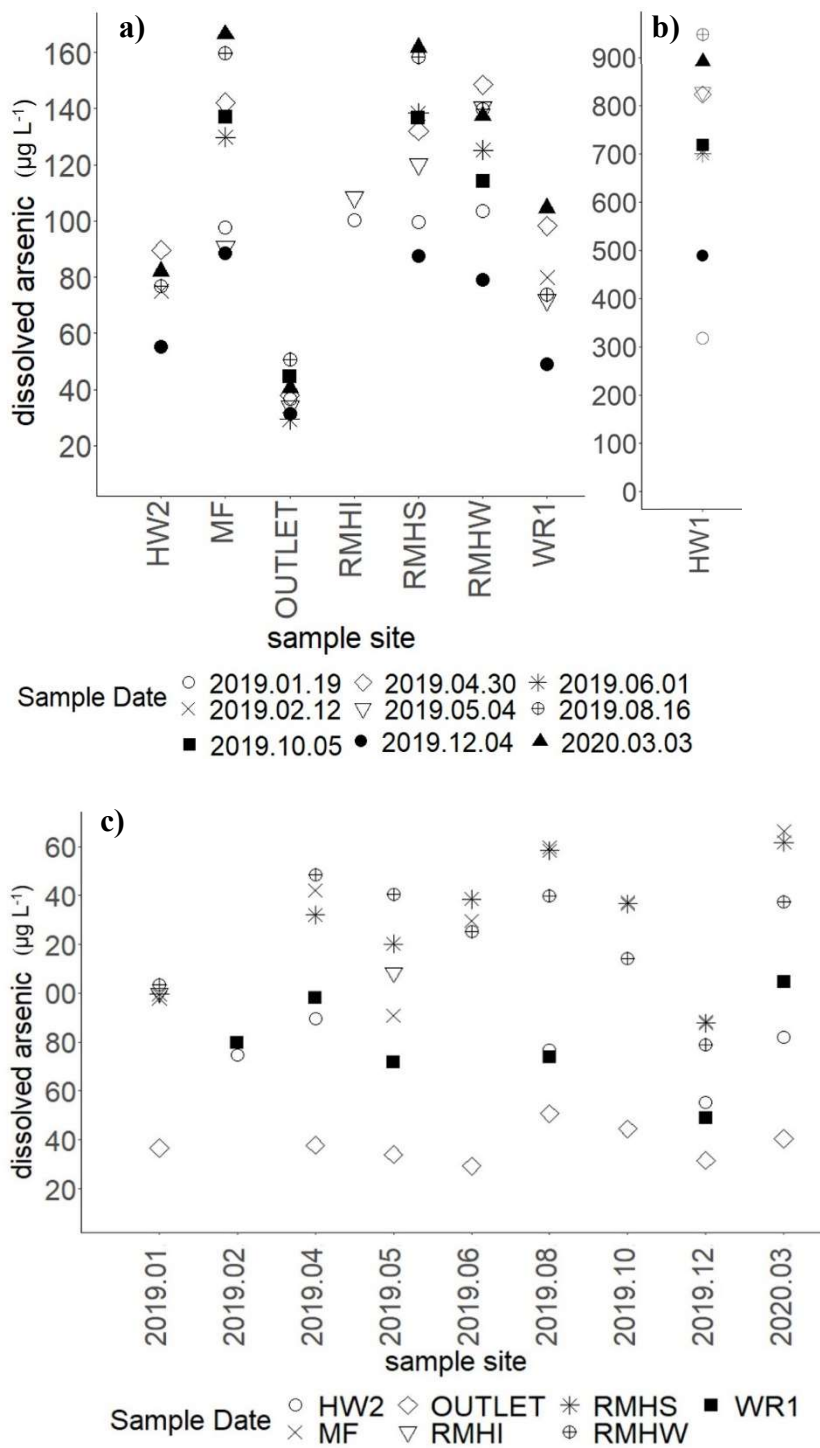


Figure 4-4. Dissolved As concentrations ($\mu\text{g L}^{-1}$) for; a) inlet sites (excluding HW1); b) HW1 (note the change in y scale); c) across sampling instances (note change in x axis from sample name to date, and change in shape from date to inlet).

The concentration of dissolved As varies both between and within sites across the inlets. The Outlet shows both the lowest As concentration and the least seasonal variability ($38.1 \pm 7.0 \mu\text{g L}^{-1}$, $n = 8$), and HW1 the greatest concentration with the most variability ($714 \pm 200 \mu\text{g L}^{-1}$, $n = 9$). Within the Wairua Arm, there was both

between site and within site variation. For example, dissolved As concentrations between the inlets ranged from $41.0 \mu\text{g L}^{-1}$ (WR1, December) to $947 \mu\text{g L}^{-1}$ (HW1, August). Seasonal trends were observed across all inlets, with December and/or January displaying the lowest concentrations for all sites except the Outlet, which is lowest in June. The highest concentration inlets were more variable seasonally; however, the (relative) expected increase of dissolved As with increased temperature^{11,27} were not observed at all sites. The lowest recorded concentrations for each site occurred in December, early summer, which contradicts the theoretical increased solubility of As with increased temperature.¹¹

Some inlets display similar concentrations within seasons, such as HW1 where Autumn months (April and May) averaged $826 \mu\text{g L}^{-1}$ ($n = 2$) and winter and summer concentrations were $707 \pm 8 \mu\text{g L}^{-1}$ ($n = 3$). HW2 displayed similar concentrations across seasons, with $81 \pm 7 \mu\text{g L}^{-1}$ ($n = 4$) excluding December (early summer) with $55 \mu\text{g L}^{-1}$. RMHW had two instances of similar concentrations across seasons; with $139 \pm 2 \mu\text{g L}^{-1}$ ($n = 3$) measured across March (summer), May (autumn), and August (winter), and $114 \pm 11 \mu\text{g L}^{-1}$ ($n = 3$) across January (summer), June (winter), and October (spring), with the lowest recorded As concentration of $78 \mu\text{g L}^{-1}$ in December. There were three distinct across-season clusters at MF, with similar concentrations $136 \pm 7 \mu\text{g L}^{-1}$ ($n = 3$) in April, June and October, $92.0 \pm 4.6 \mu\text{g L}^{-1}$ ($n = 3$) in January, May, and December, and $163 \pm 5 \mu\text{g L}^{-1}$ ($n = 2$) in August and March. While temperatures of the inlets are unknown, surface temperatures from the open-water sites in December (reported in Chapter 3) were 40% warmer than August temperatures, and 20% warmer than April temperatures. Therefore, the decrease in dissolved As concentrations in December, indicates source based geochemical processes causing the changes in solubility of As rather than a major influence of temperature.

As discussed in Section 1.6.3, flow rate can alter elemental concentration, particularly when the water is subjected to a change in physical conditions (e.g., temperature).³² A continuous flow is less likely to resuspend settled particulates along the flow path compared with a discontinuous flow and warmer waters have a higher capacity for retaining dissolved elements. The flow of the Outlet was estimated at 7240 L s^{-1} by Gillon *et al* 2009⁶⁹, and the water exiting

through the Outlet comes from the main water body; which has an approximate 10 year residence time (i.e. is well mixed).⁸³ In contrast, HW1 has a flow rate of 0.1 L s^{-1} , and is a naturally high temperature inlet, with temperatures recorded between 78 and 83 °C by the UoW/BoPRC 2018 data. Based on these two extreme conditions, it is appropriate that the Outlet has the least seasonal variation, and HW1 the most.³²

The three Rotomahana sites (RMHS, RMHI, and RMHW), all exceed $100 \mu\text{g L}^{-1}$ As year-round and had low concentrations in December and January, and highest in October, March, April, and August, displaying similar trends to each other, but unexpected based on As solubility and temperature relationship. Lake Rotomahana is the inlet water source for RMHI and it has been suggested as the source for the RMHS and RMHW sites⁸⁴. There were only two occasions when RMHI was flowing for sample collection. Stumm and Morgan (1995)³² reported that discontinuous flows vary significantly in elemental composition compared to continuous flow sources, which makes this data difficult to interpret in terms of comparing elemental data between these three sites. However, assuming that Lake Rotomahana is the inlet source for all three lakes, seasonal and/or yearly changes in flow could also explain the observed inter-year variation, with smaller scale biogeochemical changes occurring at the inlet source or along the flow path. RMHW provides a continuous large volume of water with an average flow rate of 173 L s^{-1} (2003-2006)⁷⁰ and $130 \pm 2.52 \text{ L s}^{-1}$ (2018/January-2019). The corresponding As loading for each sample instance is displayed in Table 4-3, demonstrating how small changes in flow and/or concentration can have large effects on overall As inputs into the lake. Considering that data shows low variation in flow rate across three different seasons, the As loading is controlled by variability in RMHW dissolved As concentrations which is source-based variation.

Table 4-3. As loading for RMHW calculated from UoW/BoPRC flow gauging and corresponding dissolved As data ($\mu\text{g L}^{-1}$).

Date	Flow (L s^{-1})	As ($\mu\text{g L}^{-1}$)	Loading ($\mu\text{g As s}^{-1}$)
2018-05	132	140	18,480
2018-10	127	136	17,300
2019-01	130	103	13,400
Average	130 ± 3	126 ± 20	$16,400 \pm 2,660$

Lake Rotomahana displays seasonal trends, such as thermal stratification and benthic pE changes, which favour As dissolution.⁸⁵ Furthermore, Lake Rotomahana is on average 3-4.5 °C warmer than the waters of Lake Tarawera due to geothermal inflows.⁸⁵ Therefore, the inverse of the expected temperature/dissolved As concentration relationship seen across the three suspected Lake Rotomahana source sites could be attributed to the increase of As in the hypolimnion of Lake Rotomahana during the stratified period (September through May annually). This would then correlate the spike in As concentrations in April for RMHW with mixing of the waters in Lake Rotomahana. Another explanation could be that due to the porous sediments surrounding the lake (volcanic nature)⁶⁹ and the difference in elevations between the two lakes (299 m Tarawera vs 337 m Rotomahana), the waters from these inlets may not be entirely surface waters, and/or the discharge could cause a local area of mixing by disruption of the thermocline.

4.3.2.2 Arsenic concentrations in open-water sites from Wairua Arm out to main body of Lake Tarawera

Yearly thermal stratification occurs in Lake Tarawera (Figure 3-1) and based on the influence that stratification has on redox parameters samples were collected from both surface (~5m from surface) and benthic (~1 m from bottom) water As concentrations for each open-water site; TAs1-5 (Figure 4-5). These samples were collected pursuant to methods Section 2.4. This depth separation allows comparison between seasons (i.e. thermally stratified and mixed waters) and helps identify deviations in As concentration with depth.

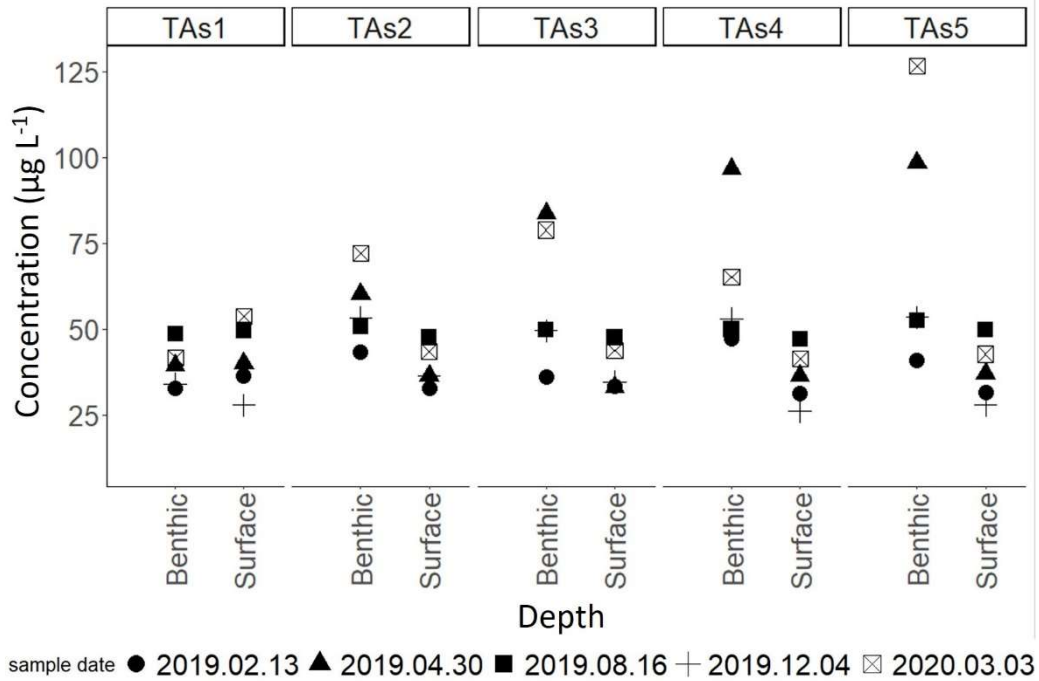


Figure 4-5. Arsenic concentrations ($\mu\text{g L}^{-1}$) for open-water sampling sites TAs1-5. TAs1 is in the Wairua Arm (~20 m depth), close to HW1, with TAs5 in the main water body (80 m depth) and 2- 4 in between.

Dissolved As concentrations, are consistent between sites and with depth during the mixed season (August). Concentrations range from $46.9 - 52.4 \mu\text{g L}^{-1}$ across all five sites (TAs1-5) with an average of $48.3 \pm 1.3 \mu\text{g L}^{-1}$ (surface) and $50.2 \pm 1.4 \mu\text{g L}^{-1}$ (benthic), $n = 5$. Overall, TAs2- 5 contained the highest surface water As concentrations in August; however, the seasonal maximum for TAs1 was March. The largest variation between sites occurred in March for both surface waters ($45.0 \pm 4.9 \mu\text{g L}^{-1}$, $n = 5$) and benthic waters ($76.8 \pm 31.1 \mu\text{g L}^{-1}$, $n = 5$). Benthic water concentrations increased with site depth (TAs1 < TAs5), except for TAs4 which was lower than TAs3 and TAs5. For each site, surface concentrations were less variable than benthic concentrations, excluding TAs1 surface waters, which were more variable than the benthic equivalent (Table 4-4).

Table 4-4. Average As concentrations ($\mu\text{g L}^{-1}$) for open-water sites across all sample dates (February, April, August, December, and March).

Site	Surface ($\mu\text{g L}^{-1}$)	Benthic ($\mu\text{g L}^{-1}$)
TAs1	41.5 \pm 10.4	39.3 \pm 6.4
TAs2	39.2 \pm 6.05	55.9 \pm 10.8
TAs3	38.5 \pm 6.7	59.6 \pm 20.7
TAs4	36.4 \pm 8.3	62.3 \pm 20.4
TAs5	37.8 \pm 8.7	74.4 \pm 36.5

There was a clear difference in As with depth; all benthic concentrations exceed the equivalent site surface concentrations. When comparing overall surface to benthic concentrations (non-normal data Shapiro-Wilks test $p = 4.54 \times 10^{-7}$), a Wilcoxon Rank Signed test ($p = 5.96 \times 10^{-8}$) indicated there was a significant difference between surface and benthic concentrations across the sampling period. A lake with such a large degree of thermal stratification is expected to have observable differences between surface and benthic waters, due to the separation of layers by the thermocline for an extended period of time allowing a build-up of As in the deeper waters.^{11,18,86}

The spike in benthic April As concentrations correlates with the lowest DO concentrations recorded in Chapter 3. All five sites recorded $< 6 \text{ mg L}^{-1}$ DO concentrations, with the lowest measurement at TAs5 of 2.3 mg L^{-1} (79.4 m). As discussed in Section 2.2.1, DO levels beneath 6 mg L^{-1} are considered suboxic, and that levels lower than 2 mg L^{-1} in the last metre of water are likely to reach anoxic conditions at the SWI.^{74,79} These increased concentrations could; therefore, be a consequence of low DO values and reduction/desorption from Mn- or Fe- minerals. The accumulation of As from the inlets could also be contributing to the higher concentrations of benthic As.

The period of overturning (August) provides dissolved As to the surface waters. This can be seen from the highest As concentrations for the surface waters during the mixed period (i.e. after the period of overturning). Dissolved As is evenly distributed throughout the open-water sites (t-test p-value = 0.065) through overturning of the lake, and that the mixed period represents a homogenous distribution of As throughout the lake. Therefore, the fluctuations in As

concentration with depth appear to be influenced primarily by thermal stratification, with the highest benthic water concentrations corresponding to stratified months (refer to Chapter 3).

Seasonal changes are most significant in TAs1 and TAs5. TAs1 is the nearest open-water site to HW1; a hot water and high As concentration inlet ($714 \pm 200 \mu\text{g L}^{-1}$, $n = 9$). The incoming concentrations at HW1 and the movement of this water are discussed in the next section, to elucidate whether this inlet is contributing to the seasonal As fluctuations in the water column at TAs1.

TAs5 is the deepest open-water site (~ 80 m) and is located in the main water body of the 41 km^2 lake.²⁹ TAs5 sits on the edge of the large 80 m plain (bathymetry map attached in Appendix as Figure A-1). The mixing and water flow of this plain is not known. Therefore, the increase in benthic As concentration during the period of thermal stratification (196 % difference between surface and benthic concentrations in March) could be attributed to multiple factors. One such factor could be the gravity-based settling from Wairua Arm out towards the main body of the lake, due to the change in depths (20 to 80 m) from TAs1-TAs5 and the difference in density between geothermal and mixed lake waters. Alternatively, there could be a localised increase in As, such as an area of low horizontal mixing which accumulates As, that is then well diluted and buffered by the large volume of water at TAs5 during lake turnover. A third possibility is that there may be a large area at this depth which has seasonally high As concentrations which is distributed through lake overturning, and may cause the increase in As concentration in the surface waters in August (from $37 \mu\text{g L}^{-1}$ in April to $49 \mu\text{g L}^{-1}$ in August).

The retention of As in oxic waters means that pH influences the dominant type of chemistry undertaken; such as surface chemical reaction (adsorption/desorption) in slightly acidic waters compared with dissolved metal interactions in neutral to alkaline waters.^{7,30} Surface water pH values were recorded for August, December, and March; ranging from 7.1-8. Due to the solubility of As^{V} in water (630 g in 100 g of water),²⁷ it is likely that As is undergoing dissolved metal interactions in waters with such a complex elemental concoction. The adsorption and

co - precipitation of As to transition metals such as Fe and Mn was discussed in Section 1.3; such as Fe-(hydr)oxides having the most significant adsorptive capacity at pH of 8. However, measured Fe concentrations are equal to and/or lower than the corresponding As concentration. For example, TAs1-5 sites (surface and benthic) have an average concentration of $16.4 \pm 15.9 \mu\text{g L}^{-1}$ Fe and $60.9 \pm 26.9 \mu\text{g L}^{-1}$ As for March 2020 ($n = 5$). The ideal ratio of As adsorption has been experimentally determined (using an Fe based compound at 25°C and pH 7) to be $1:1 \times 10^{-6}$ Fe:As.²³ The concentrations of Mn are lower than both Fe and As, with the only detectable Mn being in March 2020 Mn ($20.4 \mu\text{g L}^{-1}$, TAs1) with that concentration being approximately 50% lower than the corresponding As concentration ($41.7 \mu\text{g L}^{-1}$). It is unlikely that the concentrations of dissolved As in Lake Tarawera are controlled by Fe or Mn and adsorption chemistry due to the low measured concentrations of these redox metals in the water column.

The retention of As in the water column throughout the year could be due to conditions favouring dissolved metal interaction over adsorption chemistry, or that surface chemistry is occurring but at a low likelihood due to low concentrations of Fe and Mn. There could also be an influence from a continuous supply of As through the inlets, which have been shown to input As into the lake on a large scale. To further understand the influence of the inlets on the main water body, the movement and mixing of incoming waters from two inlets was studied through a series of additional grab samples. RMHW was chosen for its high As loading ($16,400 \pm 2,660 \mu\text{g As s}^{-1}$) and HW1 for its consistently high As concentrations ($714 \pm 200 \mu\text{g L}^{-1}$ $n = 9$, 2019/2020, Figure 4-4).

4.3.2.3 Movement and mixing from RMHW and HW1 inlets into open-waters

RMHW

Samples from RMHW were analysed for dissolved As during the stratified period (samples collected in March) to investigate how dilution occurs through mixing and movement to the deeper water sites (Figure 4-6). These data are supported by water isotope ratios to determine mixing of inlet waters with lake waters (Figure 4-7). The direction of TAs3 is noted in Figure 4-3, with the proximity of RMHW to TAs3 shown in Figure 2-1 d.

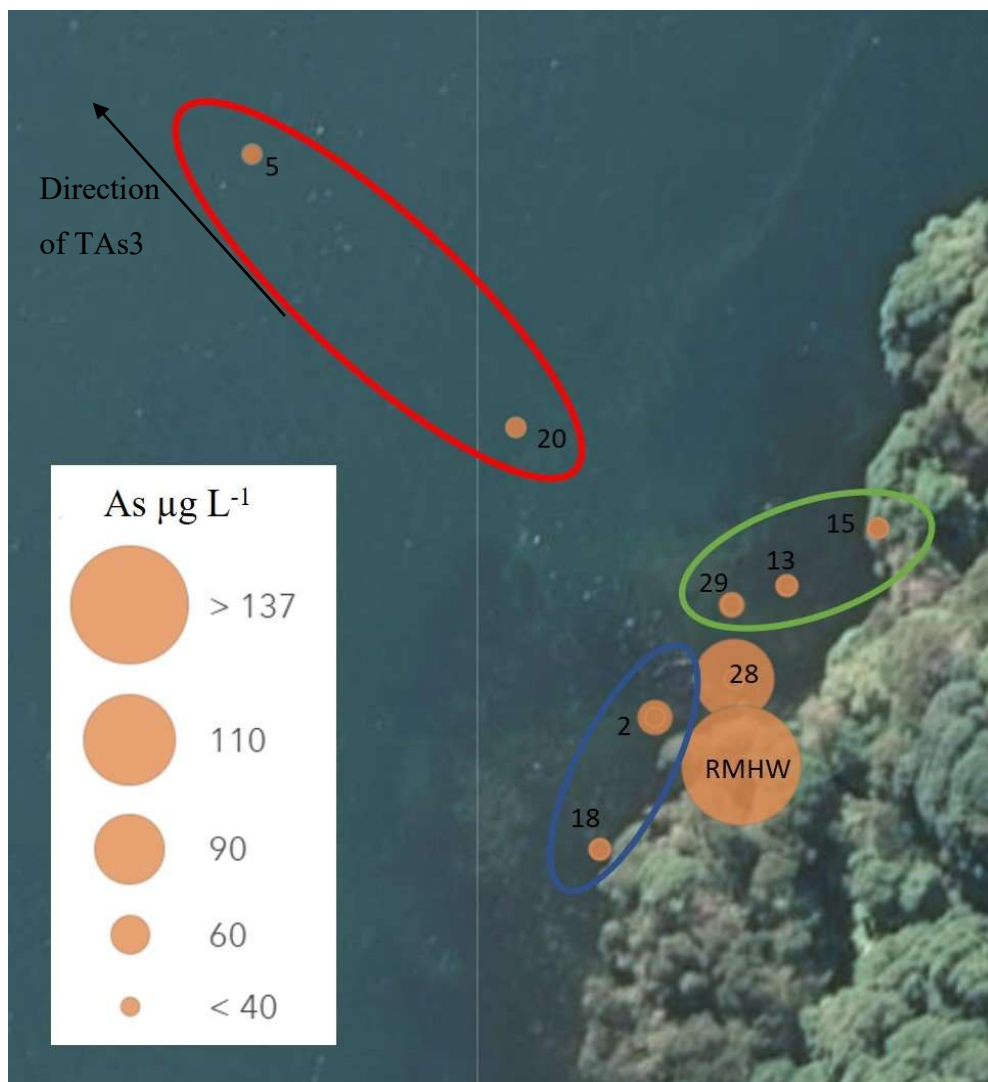


Figure 4-6. Dissolved As concentrations ($\mu\text{g L}^{-1}$) for each grab sample taken around RMHW and out towards TAs3. Samples are grouped by north (green) and south (blue) of the waterfall mouth and out towards open-water site TAs3 (red).

The dissolved As concentration for RMHW was $137 \mu\text{g L}^{-1}$ and the concentration decreases in all samples north (green), south (blue), and further off-shore (red) with the next largest concentration being directly out of the waterfall mouth (sample 28) with a concentration of $100 \mu\text{g L}^{-1}$ (Figure 4-6). The concentrations of all other samples range from 41 to $56 \mu\text{g L}^{-1}$ As ($n = 7$) with an average of $45 \pm 5 \mu\text{g L}^{-1}$, which gives an indication that mixing/dilution of As is occurring not far from the shoreline.

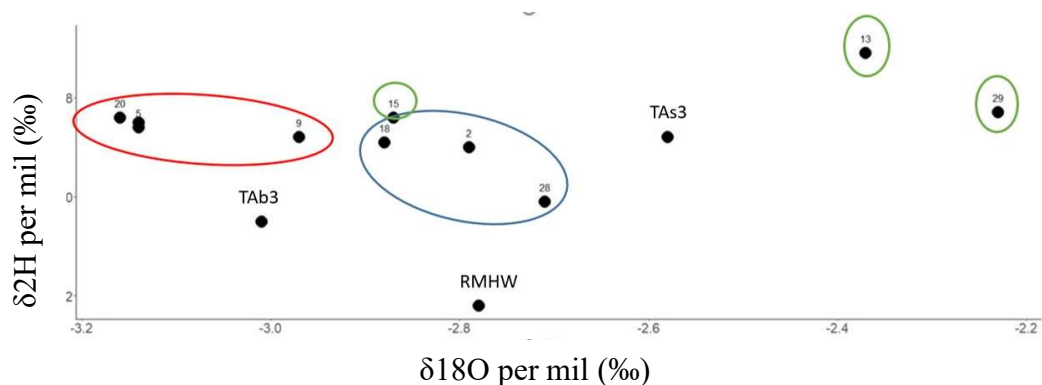


Figure 4-7. Water isotopes (per mil ‰) for grab samples taken from RMHW, including RMHW, TAs3 surface and benthic. Coloured circles correlate to sample locations in relation to waterfall as outlined above: green (north), blue (south), and red out towards open water site TAs3.

There are three clearly distinct water isotope ratios ($\delta^2\text{H}/\delta^{18}\text{O}$) for RMHW, TAs3 (surface) and TAs3 (benthic; Figure 4-7). The difference between the surface and benthic samples indicate that the deep waters are influenced by different factors/sources than the surface waters during the period of stratification. In general, samples collected from sites of proximity have a similar water isotope composition. The surface samples taken leading out towards TAs3 (red circle) fall closer to TAb3 than TAs3, indicating that the inlet water is mixing with the benthic waters rather than the surface waters during stratification. The southern samples (blue circle) fall in between the inlet and TAs endpoints, indicating that RMHW is mixing in the southern direction. The northern samples (green circles) appear to have separate apparent sources. Samples #15, #13, and #29 are all taken along the northern coastline, yet show the most variable isotope ratios of the three geographical clusters (Figure 4-7). Multiple factors could explain the variation in isotope ratios across these samples, such as the wind and current direction at the time of sampling

and evaporation, or there may be groundwater or another inlet influencing these ratios. The Lake Tarawera monitoring buoy was damaged and during this sampling period no exact wind data was available; however, the nearest city (Rotorua) on March 3rd 2020 averaged 11.1 kmh winds, with 34% westerly, 30% northerly, 23% easterly, and 13% southerly across the course of the day.⁸⁷ Based on these wind patterns, it is likely that mixing occurred on the eastern shoreline in a southerly direction. This is reinforced by the water isotope ratios found for the southern grab samples taken. There are also four other known inlets surrounding RMHW (the closest being RMHS) and mixing could be occurring from other inlet sources, particularly if the current was southerly.

The RMHW site falls near the Lake Rotomahana water isotope signature (Appendix Figure A.2), providing evidence that the source of water for the RMHW inlet is Lake Rotomahana. The hypothesis of southerly mixing occurring from RMHW is supported by the grab samples outlined in blue (Figure 4-7), which also sit closer to the Lake Rotomahana water isotope pattern than the Lake Tarawera isotopic patterns (which the red circled samples sit within).

HW1

The naturally hot waters coming from HW1 cause distinct thermal stratification within the shallow (wadable) waters, hence the name Hot Water Beach. Consequently, at each site a ‘hot’ and a ‘cold’ sample were taken and are paired as equivalent sites (Table 4-5) to determine whether the temperature difference has an effect on how the As is moving and mixing from this inlet. Care was taken to disturb the water as little as possible by remaining still for the waters to settle both when wading to a new sampling location and when reaching down to the cold waters to collect a sample.

Table 4-5. Dissolved arsenic concentrations ($\mu\text{g L}^{-1}$) for equivalent hot and cold grab samples taken from HW1.

sample # (hot)	As ($\mu\text{g L}^{-1}$)	sample # (cold)	As ($\mu\text{g L}^{-1}$)
34	231	33	112
24	329	22	80.0
17	309	25	103
27	340	31	67.0
06	204	12	82.0
07	375	16	61.0
32	242	23	76.0
01	149	13	113

Dissolved As concentrations are higher in the surface waters than the equivalent bottom water samples for every instance, with the largest difference being 83% (sites 07 and 16) and the smallest 24% (sites 01 and 13). Figure 4-8 graphically shows the distribution of arsenic across the samples.

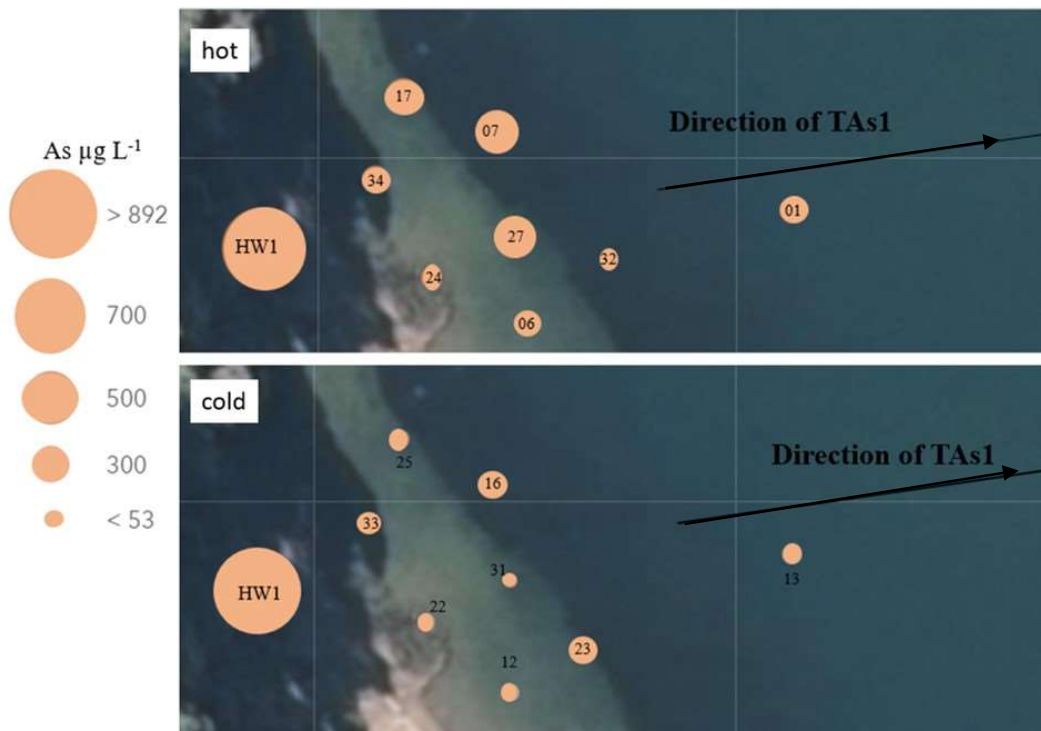


Figure 4-8. Location and As concentration ($\mu\text{g L}^{-1}$) of surface samples taken from HW1. Hot and cold samples were taken from each point due to the difference in temperature between the top and bottom waters (within the depth of a hand).

There are significant (Wilcoxon Signed Rank p - value = 0.0078) concentration differences between the hot and cold samples (Table 4-5 and Figure 4-8). For the hot water samples, dilution occurs relatively evenly along the shoreline, from $892 \mu\text{g L}^{-1}$ at HW1 to $231 \mu\text{g L}^{-1}$ (34) and $329 \mu\text{g L}^{-1}$ (24), with higher concentrations sitting further offshore, $341.3 \pm 33.0 \mu\text{g L}^{-1}$ (sites 17, 07 and 27). The overall average surface (hot water) concentration is $272.4 \pm 77.6 \mu\text{g L}^{-1}$ ($n = 8$). The cold water samples all sit below $113 \mu\text{g L}^{-1}$ with an overall average of $86.8 \pm 20.1 \mu\text{g L}^{-1}$ ($n = 8$). These trends indicate surface mixing is occurring between the warmer surface waters and the high temperature inlet waters, with the strength of this thermal stratification declining further out towards TAs1. The water isotopes for these samples are in Figure 4-9.

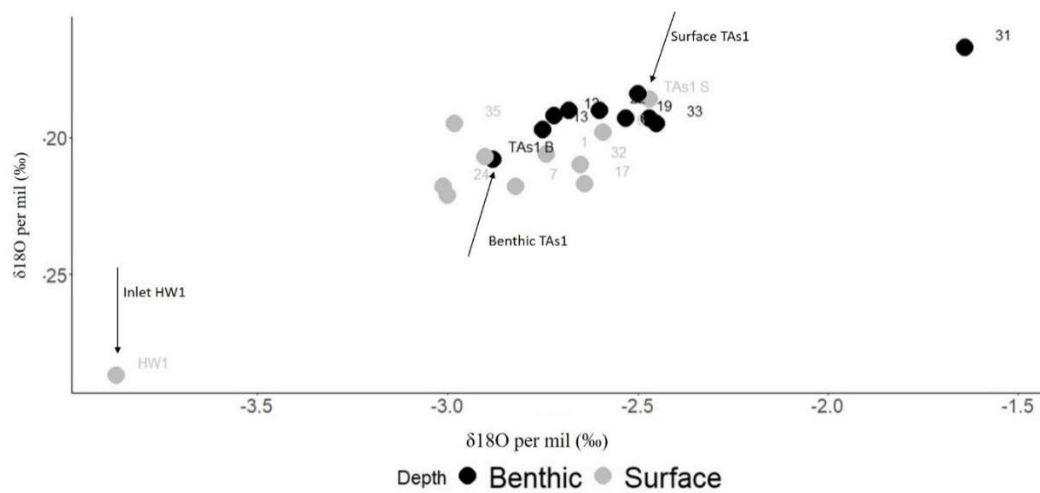


Figure 4-9. Water isotope (per mil ‰) patterns from HW1 and TAs1, including grab samples in between to determine mixing patterns of the inlet water into the lake.

This surface data shows the expected trend of mixing between two end members (HW1 and TAs1) with both $\delta^{18}\text{O}$ and $\delta^2\text{H}$ increasing towards TAs1; however, HW1 is distinctly different. This data reinforces the decrease in thermocline strength out towards TAs1, as the cold water samples sit within the TAs1 and TAb1 isotope ratios. This indicates that mixing of waters with depth occurs further towards the open-water site than the shore. Thus, there is essentially a plume of As remaining in the warm surface waters after flowing from the HW1 inlet. Sample 31 was the exception to this benthic trend and appears to be an outlier entirely. It was noted while in field that bubbling was occurring at various points along the shoreline, suggesting an input of water (unknown source) which could be

contributing to the different isotope ratio in this sample. While the As concentration and temperature of water coming in from HW1 is high, the flow rate is low (0.1 L s^{-1}); therefore, it is reasonable to assume that incoming water is not mixing with the cooler waters and is instead creating a distinct layer of high temperature and high As until diluted and cooled enough to mix with cooler waters.

The isotopic signature of the additional HW1 samples have a slope similar to the evaporation line for lakes, sitting between the lake waters for Tarawera and Rotomahana, as well as rainfall recharge (Appendix Figure A.2). This combination of isotope patterns indicates that the waters coming from TAs1 towards the shore at HW1 are well mixed and that the low flow from HW1 is being diluted into this water without noticeably influencing the isotope patterns. Grab sample #31 sits close to the isotopic signature of Lake Rotomahana surface water (Appendix Figure A-2), so this grab-sample may have included waters from a sub- surface inflow to Lake Tarawera.

4.3.3 Particulate arsenic, iron, and manganese in water samples

An orange coating was observed on the eastern shoreline of the Wairua Arm (Near RMHW and RMHS – Figure 4-10), including rock faces and both submerged and overhanging branches and leaves. This indicated that Fe precipitation is occurring in the surface waters and may be present as suspended solids/colloids in the water column. Total elemental concentrations for As, Fe, and Mn are therefore presented and discussed. The obvious Fe coating and oxic conditions of the lake water, together with high concentrations of dissolved As present in all samples, led to questioning whether there is any appreciable particulate/suspended As adding to the overall system.



Figure 4-10. Photograph taken from Eastern side of Wairua Arm, near RMHW inlet site. Orange coloured coating appears on rocks and submerged branches.

For August and December 2019, and March 2020, unfiltered samples were collected at all sampling locations and total As concentrations were determined using the methods outlined in Section 2.5.3. These digested samples (“totals”) were then compared to the filtered (“dissolved”) samples to determine the suspended fraction of total As. Fe and Mn concentrations were also investigated as the transition metals are known to bind and co-precipitate As. The difference between the total and dissolved concentrations of each Fe, Mn, and As are presented in Figure 4-11.

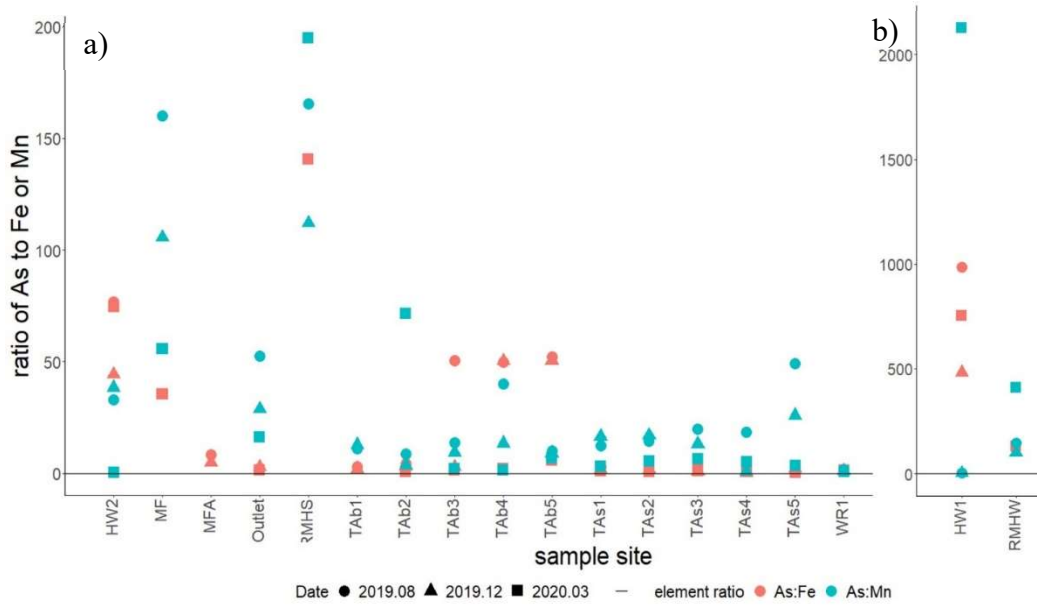


Figure 4-11. Particulate As with Fe (pink) and Mn (blue) concentrations for a) all sites excluding HW1 and RMHW. b) HW1 and RMHW. Ratio of > 1 indicated more As than Fe or Mn.

90% (n = 100) of the samples in Figure 4-11 had a As:Mn or As:Fe ratio above one, indicating a higher suspended fraction of As compared with both Fe and Mn across all samples. Iron and Mn- hydrous(hydr)oxides are known to adsorb As^V , which is the dominant form of As in Lake Tarawera. The oxic waters of Lake Tarawera, which have a circumneutral pH (ranging between 6 and 8) provide suitable conditions for surface-chemistry relationships between As and Fe/Mn.^{18,22,33} However, considering the ideal ratio of Fe:As (which has been reported as $1:1 \times 10^{-6}$ at $25^\circ C$ pH 7)²³ compared with the average 73:1 As:Fe ratio found in these samples it may be that the particulate As is binding to Fe or Mn particulates, but due to the lower concentrations of Fe and Mn in the water column than As, this isn't a significant mechanism for removal of As from the water column

4.4 Summary

The investigations into past inlet data concluded a high contribution of dissolved As came from the Wairua Arm. Seasonal variation were observed across inlet sites, which is not fully explained by the expected temperature-As relationship, such as the Rotomahana sites. Source-based conditions explaining the anomalies in the seasonal trends were suggested, such as overturning of Lake Rotomahana (which has an anoxic hypolimnion during stratification) causing spikes in As concentrations during winter months. Inlet sites with greater As concentrations also displayed larger seasonal variations in concentrations.

The surface and benthic waters in April (during stratification, before overturning) were significantly different from each other indicating an accumulation of As in the benthic waters. Due to the oxic conditions of Lake Tarawera and somewhat stable As concentrations throughout the lake, the reducing - dissolution, mixing, oxidising - adsorption cycling may be occurring, particularly at TAs5, but not to a substantial level. The low contribution of overall As through sediment fluxing/reductive dissolution is also supported through the lack of As^{III} present in deep-water samples when DO reaches hyperanoxic concentrations; however, this is based on samples taken approximately 5 metres from the SWI. The increase in benthic As is considered to be more from travelling out from the Wairua Arm than from anoxic fluxes.

Physical and chemical changes may be occurring within the inlet sources which contribute to seasonally changing concentrations of As, such as for sites HW1 and RMHW. The loading of As into the water column through the inlets depends on both inlet flow rate and concentration (positive correlation between the two parameters), with the mixing of these inlet waters into the main water body depending on inlet flow rate and temperature. The mixing of RMHW to the deeper waters is complicated by suggested factors such as wind direction, evaporation, nearby inlets, and the velocity of the water appears to cause both benthic and surface water mixing. Conversely, HW1 contributes dissolved As to the surface waters of TAs1, with a clear difference in concentrations caused by the localised thermocline;

however, with such a low flow rate the isotope signature of this inlet is quickly diluted by the volume of water into which it is mixed. This continuous inflow of As and surface mixing reinforces the higher As concentrations seen in TAs1 than the other open-water TAs sites during the period of thermal stratification (Figure 4-5).

It is not unexpected that As^V remains dissolved in the water column, based on the physical and chemical properties of the open-waters as well as the concentrations of common adsorbates (Fe and Mn) not being present in high enough concentrations to remove such large quantities of As from the water column.

CHAPTER FIVE

SEDIMENTS AND PORE WATERS

5.1 Introduction

This chapter presents the development of a method for pore water collection used to obtain pore waters from Lake Tarawera sediment cores. Results for the speciation and elemental data from those pore waters, along with digested sediment concentrations, are presented within to ascertain whether a redox boundary occurs in the sampled sediments.

As previously discussed in Section 3.2, a potential redox boundary is observed in the water column of Lake Tarawera. The last three metres of measured data (76 - 79 m) at the TAs5 site showed DO decreased by 62% to hyperanoxic levels (from 6 mg L⁻¹ to 2.3 mg L⁻¹). In comparison, the redox boundary in sediments occurs over a much smaller distance, often only centimetres.³⁹ Therefore, it is possible to capture the redox boundary within the top 40 cm of the sediments. Due to the absence of As^{III} in the water column across all seasons, but high overall As concentrations entering through inlets (e.g. HW1 947 µg L⁻¹ in August 2019), the presence and speciation of As in the pore waters was examined and the depth of any distinct species change was of interest.

Two sediment cores were collected (December 2019 and March 2020) using a gravity corer (methods described in Section 2.4) from which pore water samples were extracted while in field. Pore water extraction occurred in field initially (December 2019); however, instrument malfunctions delayed analysis of these samples until March 2020. The March 2020 analysis of samples stored in vacutainers from December 2019 showed As^{III} retention in the pore waters stored in vacutainers, which prompted the research on the long-term stability of As^{III} in the vacutainers.

5.2 Method development for pore water sampling

The most important consideration for extraction of pore waters is maintaining the integrity of the sampling environment throughout sample collection and storage (refer to Section 1.4.3 for sampling discussion) because exposure to atmospheric conditions can result in speciation changes and precipitation of As and other redox sensitive species, such as Fe and Mn.⁴⁹ The use of rhizon filters for pore water extraction has been described as a rapid method which removes complicated field and technical efforts (such as a glove box to control sampling environment).⁵² A combination of rhizons and vacutainers have been used for collection of pore waters, with vacutainers providing the source of suction required to pull the water through the rhizon filter and tubing as well as sample storage.^{52,88} There is no standardised method for collection and preservation of dissolved As species using rhizon samplers and vacutainers; however, vacutainers have been shown to preserve As^{III} from field samples (length of storage was not reported).⁸⁹ Hence the aim of this experiment was to ascertain what fraction of As^{III} is preserved in rhizon collected samples over time when stored in vacutainers.

Experiment One – Type 1 and UoW lake water samples

Bench-top vacutainer species preservation experiments were undertaken using an As^{III} spike (100 µg L⁻¹) into Type 1 water and Chapel Lake water, UoW campus. To account for vacutainers containing residual oxygen (i.e. not completely evacuated), a set of vacutainers were flushed with N₂ (Section 2.3.1) for comparison to factory prepared vacutainers. These two vacutainer types are hereafter denoted as the N and O samples, respectively. For each water type and vacutainer set triplicate samples were prepared (Section 2.5.4). Samples were analysed via HPLC-ICP-MS on days 2, 26, and 55 of storage, as well as by ICP-MS at the start of the experiment and the results are summarised in Table 5-1. Percentage recoveries for As^{III} (Table 5-2) were calculated using Equation 5-1 and are reported in Table 5-2.

$$\text{Percentage recovery}_{(As)} = \frac{As_{(\text{spiked sample})}(\text{ug L}^{-1}) - As_{(\text{unspiked sample})}(\text{ug L}^{-1})}{As \text{ spike concentration } (\text{ug L}^{-1})} \times 100 \quad (5-1)$$

Table 5-1. Summary of total As ($\mu\text{g L}^{-1}$) in spiked samples (analysed by ICP-MS) and As^{III}, As^V, and total As ($\mu\text{g L}^{-1}$, HPLC-ICP-MS). n = 3 unless otherwise stated.

Sample	Day-2			Day 26			Day-55			
	Total As ($\mu\text{g L}^{-1}$)	As ^{III} ($\mu\text{g L}^{-1}$)	As ^V ($\mu\text{g L}^{-1}$)	Total As ($\mu\text{g L}^{-1}$)	As ^{III} ($\mu\text{g L}^{-1}$)	As ^V ($\mu\text{g L}^{-1}$)	Total As ($\mu\text{g L}^{-1}$)	As ^{III} ($\mu\text{g L}^{-1}$)	As ^V ($\mu\text{g L}^{-1}$)	Total As ($\mu\text{g L}^{-1}$)
ICP-MS				HPLC-ICP-MS						
Type 1 (N)	104	75.3 ± 14.2	43.3 ± 15.8	119	40.5 ± 11.8	127 ± 34	167	32.4 ± 6.3	50 ± 30	82.4
Type 1 (O)	104	88.1 ± 19.5	44.7 ± 21.5	133	54.8 ± 7.7	115 ± 40	169	39.6 ± 2.6	59.8 ± 37.0	99.4
Chapel Lake (N)	107	112 ± 5	27.0 ± 8.5	139	N/A*	N/A*	N/A*	83.0 ± 26.7	10 ± 8.1	93.0
Chapel Lake (O)	107	109 ± 2	18 ± 10	139	69.2 ± 3.7	16.1 ± 10.2	85.3	83.0 ± 29.6	37.0 †	120

* Not analysed

† Standard deviation not calculated when n < 2.

Comparison of total As concentrations between the ICP-MS and HPLC-ICP-MS analyses showed variation both between analyses and between triplicate samples. Day-2 HPLC-ICP-MS results show all samples are within 30% of the ICP-MS data. Day-26 data illustrates inconsistencies between the samples; Type 1 (N) and (O) exceed 60% deviation from the ICP-MS totals, while Chapel Lake (O) is within 20%. For Day-55, Type 1 (N) is within 21% of the ICP-MS data, while Type 1 (O), and Chapel Lake (N) and (O) fall within 15%. The total As concentrations for day-26 are the most inconsistent between ICP-MS and HPLC. The larger deviation for day-26 suggests that there was likely an analytical error for this analysis and the data is less reliable. The conversion of As^{III} to As^V was investigated further to explain any analytical issues as well as determine the stability of As^{III} during sample storage.

Overtime, it is expected that As^{III} concentrations will decrease, with a proportional increase in As^V; however, in this experiment the loss from As^{III} is not equivalent to the increase in As^V. For example, Chapel Lake (O) recorded a decrease in both As^{III} and As^V. While the day-55 HPLC and ICP-MS concentrations fall within 21% of each other, the decrease in As^{III} from day-2 to day-55 and corresponding increase in As^V are not equivalent. This inconsistency between the decrease in As^{III} and the increase in As^V could be attributed to the analytical variation seen for total As concentration.

Spike recoveries for As^{III} were investigated to provide further information on the amount of oxidation occurring over time. Initial (day-2) As recovery for Type 1 samples were lower than Chapel Lake recoveries for both sets of vacutainers, with a larger variation in the Type 1 water samples (Table 5-2). There was a sequential decrease in As recovery for Type 1 samples in both the N and O vacutainers. This is in contrast to the Chapel Lake water (O) vacutainers, which had higher initial recoveries (day-2) than the Type 1 water and exhibited a greater degree of oxidation at day-26, followed by an increase in As^{III} after day-55. This is an unexpected result but aligns with the inconsistencies discussed above for total As concentrations and the oxidation of As^{III} to As^V. Chapel Lake (N) samples were not analysed at day-26, so whether these samples follow the same trend is unknown. However, when

comparing day-2 to day-55 data, recoveries at day-55 indicate As^{III} was recovery was greater than those of the Type 1 water samples. This suggests a higher degree of oxidation occurring in the Type 1 water samples, likely due to the higher concentrations of DO (Table 5-2).

Table 5-2. Percentage recoveries of As^{III} in spiked samples for UoW Chapel Lake water and Type 1 water for nitrogen (N) and oxygen (O) vacutainers. DO of the samples is also reported.

As ^{III} percentage recovery (%)						
	Day-2	Day-26	Day-55	Day-2	Day-26	Day-55
Sample	Type 1 water (DO = 8.3 mg L ⁻¹)			Chapel Lake water (DO = 4.8 mg L ⁻¹)		
N # 1	91.8	28.6	25.4	105	N/A*	97.9
N # 2	58.9	40.9	37.6	110	N/A*	99.0
N # 3	71.9	52.2	34.3	110	N/A*	52.3
Mean	74.2 ± 16.6	40.7 ± 11.8	32.4 ± 6.3	108 ± 3	-	83.1 ± 26.7
O # 1	92.9	62.4	36.7	102	64.9	48.7
O # 2	65.8	54.8	40.6	104	71.3	102
O # 3	100	47.1	41.6	109	71.4	97.9
Mean	83.4 ± 18.2	54.7 ± 7.6	39.7 ± 2.6	105 ± 3	69.2 ± 3.7	82.9 ± 30.0

*N/A = not analysed

The initial (day-2) recovery rates for Type 1 water were lower than reported in the literature⁸⁹, where 95 – 103% of As^{III} was recovered using empty vacutainers. The authors collected samples into a beaker (without a rhizon) and then transferred water to a vacutainer using a syringe and 0.45 µm filter. The previous study reported DO values, ranging from 2.1 – 3.9 mg L⁻¹ (lower than the DO in this current study - 4.8 mg L⁻¹ and 8.3 mg L⁻¹ for UoW Chapel Lake water and Type 1 water respectively) which will influence the higher recovery rates reported. They also reported higher recovery rates in empty vacutainers using deionised water compared with field water samples, with 103.8 % recovery in Type 1 water compared with an average of 96 ± 3 % (n = 3) in field water samples. This contradicts the results presented in (Table 5-2), which show higher recoveries in field samples (Chapel Lake) compared to Type 1 water.

The decrease in As^{III} over time during storage in the vacutainers indicates oxidation of As^{III} is slowly occurring. Both water types were oxic, and molecular oxygen has been reported to oxidise no less than 25% of As^{III} to As^V in 72 hours at pH 4, 6, and 8.³⁰ The day-2 (~ 48 hours) results show oxidation of up to 25.8 ± 16.6 % of As^{III} to As^V, indicating the DO presence in the samples influenced the oxidation from the time of sample collection.

This experiment was undertaken at ambient temperature and atmospheric oxygen levels, using oxic water samples which were collected directly prior to spiking and sampling. It was suggested that these factors have caused higher levels of oxidation after the As^{III} spike was added; however, the unexpected trends and inconsistency in total As concentrations between sampling complicate the results making it difficult to come to a conclusion. Thus, a subsequent spike experiment was undertaken using pore waters from a stored Lake Tarawera sediment core (collected in March 2020 and expected to have low DO values) to try to further limit the introduction of oxygen.

Experiment Two – pore water samples

A sediment core was obtained in March 2020 and was previously used for pore water collection in field. It was stored at 4 °C, with all pierced holes re-taped to prevent leakage until August 2020 when it was used for the second As recovery experiment. Two factory conditioned vacutainers (V1 and V2) were filled from a core depth of 13 cm (refer to Section 2.5.4). To ensure the spiked and unspiked samples were from the same water source each vacutainer was halved to give a spiked and un-spiked pair. The samples were spiked to a final concentration of 500 µg L⁻¹ As^{III}. Samples were analysed via HPLC-ICP-MS on days 2, and 29 of storage for As^{III} and As^V, as well as at the start of the experiment by ICP-MS for total As; the results are summarised in Table 5-3.

Table 5-3. Summary of average total As ($\mu\text{g L}^{-1}$, ICP-MS) in spiked samples and As^{III} , As^{V} , and total As ($\mu\text{g L}^{-1}$, HPLC-ICP-MS). n = 3 unless otherwise stated.

Sample	Day-2			Day-29			Total As ($\mu\text{g L}^{-1}$)
	Total As ($\mu\text{g L}^{-1}$)	As^{III} ($\mu\text{g L}^{-1}$)	As^{V} ($\mu\text{g L}^{-1}$)	Total As ($\mu\text{g L}^{-1}$)	As^{III} ($\mu\text{g L}^{-1}$)	As^{V} ($\mu\text{g L}^{-1}$)	
	ICP-MS	HPLC-ICP-MS		HPLC-ICP-MS		ICP-MS	
V#1	732	455 *	21 *	476	1.58 *	928 *	930
V#2	1,220	1,120 \pm 34	31 \pm 2	1,150	2.6 \pm 1.3	958 \pm 2	961

* No standard deviation calculated when n < 2

Day-2 V#2 total As concentrations (Table 5-3) vary by 5.7% between ICP-MS and HPLC-ICP-MS analyses; however, all others exceed 20% difference for total As. The decrease in As^{III} does not correspond to the proportional increase in As^{V} , however this is likely due to the differences between analysis types. Overall, these results for the sediment pore waters suggest that there was complete oxidation of As^{III} to As^{V} between day-2 and day-29. Percentage recoveries for As^{III} were calculated for day-2 and day-29 (Table 5-4).

Table 5-4. Percentage recoveries for As^{III} spike samples in sediment pore water from core collected in March 2020.

Sample	As^{III} recovery (%)	
	Day-2	Day-29
V1 # 1	N/A*	0
V1 # 2	128	0
V1 # 3	22.2	0
Mean	74.9 †	-
V2 # 1	124	0
V2 # 2	124	0
V2 # 3	115	0
Mean	121 \pm 5	-

* Not analysed due to insufficient sample volume

† No standard deviation calculated due to only two samples

Initial (day-2) percentage recovery averages were similar to the UoW campus lake water results ($108 \pm 3 \%$, N, and $105 \pm 3.3 \%$, O), suggesting a lower DO content in the pore waters. Complete oxidation of As^{III} to As^{V} occurred by day-29. Note that V1 #1 did not contain enough sample for analysis after allocating sufficient volume to V1 #2 and #3, due to low sample volume expressed from the core. DO was not measured in these samples due to the anoxic nature and limited sample volume.

Changes in pE can occur through the introduction of oxygen to anoxic waters and can alter the chemical behaviour of redox sensitive constituents such as As, Fe, Mn, S, and Al. Introduction of oxygen through sample collection and/or through oxygen leaking into containers during storage could alter the environment and cause oxidation. It has been reported in literature that the rate of oxidation and subsequent adsorption of As^{III} by both Fe^{3+} ($377 \mu\text{g L}^{-1}$ in V1 and $1,440 \mu\text{g L}^{-1}$ in V2) and Al^{90} (undetectable in V1 & V2 samples) is biphasic, with an initial spike in oxidation followed by a decrease in rate; with equilibrium occurring within 60 minutes for Fe, and up to 1 year for Al. However, as discussed in Section 1.3.5, the rate of oxidation of As can vary, depending on the constituent oxidising it, with $\text{Fe} > \text{Mn} > \text{O}_2$. If these processes were the cause of the loss of As^{III} ; however there would be a decrease in total As through loss from dissolved phase to particulate phase, which was not observed, as total As remained stable through to day-29.

Summary

Overall, oxidation of As was observed in vachutainers during storage for each sample type analysed (Type 1, Chapel Lake water, and Lake Tarawera pore water), even when exposure of samples to oxygen was minimised in sampling as much as possible through the use of rhizons. Varying rates of oxidation across the different matrices appears to be related to DO concentrations, with higher As oxidation in Type 1 water than Chapel Lake (lower DO) and pore waters (assumed low DO) after 2 - days. Complete oxidation occurred by day-29 in the sediment pore water As recovery analysis. This outcome cannot be explained without further experimentation considering As^{III} was preserved in the original December field samples that were stored for three months prior to analysis.

In conclusion, the use of rhizons did not prevent chemical changes occurring within the sample in the vacutainer over time. The results presented in this section do not give a clear indication of what is causing the oxidation and could be due to a combination of sample preparation as well as analytical error. Further experimentation should be performed to verify the extent of oxidation occurring overtime and the mechanisms causing this oxidation.

5.3 In-field collection of pore waters from sediment cores using rhizons and vacutainers

Pore water samples were collected in field from a core collected in December 2019 and March 2020 for analysis of As speciation (methods described in Sections 2.3.1 and 2.3.4). For both pore water and sediment analysis, a scale of segments (Table 5-5) was used to enable direct comparison between sediment and pore waters elemental concentrations. Overlying water was present in both sediment cores that were collected. Steiner (2018)⁵⁴ noted rhizons preferentially sample from above the insertion point when overlying water is not drained from the sediment core, meaning that pore water concentrations reported may be from shallower depths in the water column than reported or intended.

Table 5-5. Depth range of sediment core samples segments to compare sediment samples with relevant pore waters.

Sediment segment	Approximate depth (cm)
1	0-3
2	4-6
3	7-9
4	10-12
5	13-15
6	16-18
7	19-21
8	22-24
9	25-27
10	28-30
11	31-33
12	34-36
13	37-39
14	40

December 2019 pore waters

The pore waters sampled using rhizons and vacutainers from December 2019 were stored for three months prior to sample analysis, due to complications with the HPLC. As the results from Section 5.2 report, As^{III} was not stable in samples stored in the vacutainers (either N₂ flushed or factory prepared) for this length of time. Therefore, even though there was As^{III} present when the samples were analysed after three months, this data is not considered representative of the sample and this pore water data has not been presented in this thesis.

March 2020 pore waters

A second sediment core collected in March 2020 had pore water extracted and sediment samples were segmented and digested (Section 5.4 below). The pore water results are presented as the corresponding sediment segments (Table 5-5). The concentrations of both As^{III} and As^V with depth are displayed in Figure 5-1 and outlined in Table 5-6. There is a trend of decreasing concentration with depth for

both As species. As^{III} decreases by 82.9% with depth, compared with 66.8 % for As^V.

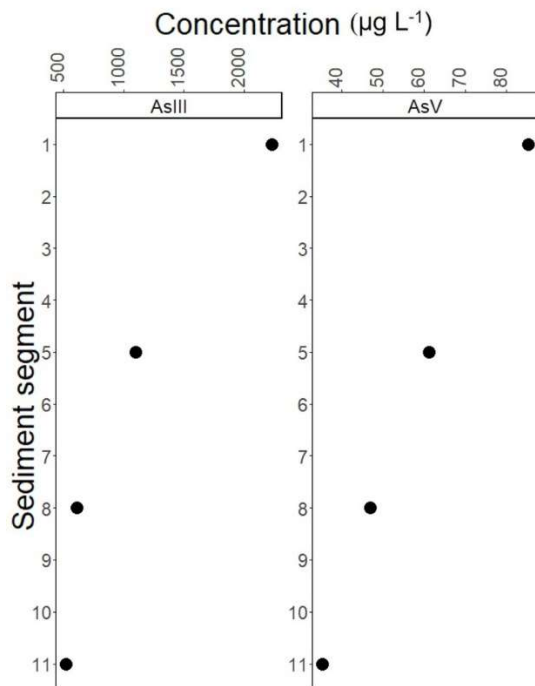


Figure 5-1. Day-2 analysis for pore water concentrations ($\mu\text{g L}^{-1}$) of As^{III} and As^V with depth (from March 2020 sediment core), with sediment segment 1 being the surface sediments on the lake bottom. Sediment segment 1, 5, 8, and 11 correspond to depths of 3, 12, 23, and 31 cm, respectively.

Table 5-6. Concentration of As^{III} and As^V in pore waters at corresponding sediment segments.

Segment	As ^{III} ($\mu\text{g L}^{-1}$)	As ^V ($\mu\text{g L}^{-1}$)
1 (3 cm)	2740	85
5 (13 cm)	1102	61
8 (23 cm)	609	46
11 (31 cm)	523	35

Based on the DO concentrations obtained for Lake Tarawera (discussed in Section 3.2.1 Figure 3.2 a), where the deep-water site closest to the coring location (TAs1) displayed DO values of 6.5 mg L^{-1} at 19 m depth, it would be expected that the SWI is still oxic. Thus, it is hypothesised that DO would decrease with increasing depth in the sediments, corresponding to an increase of As^{III} and decrease of As^{V} with depth based on the expected pE changes which occur with oxygen depletion.³⁸ However, a maximum concentration of both As^{III} and As^{V} is observed in the surface of the sediments (Table 5-6), with decreasing concentrations for both species and total As. This could be due to the different concentrations of As in the equivalent sediment layers (discussed below), whereby the pore waters would be in equilibrium with the surrounding sediments. The greater As^{III} concentration observed in pore waters near the surface of the sediments could be attributed to advection of soluble reduced species (As^{III} being more soluble than As^{V})⁷.

Approximately 61 mL was extracted from the pore waters during sample collection and the sediment surface had dropped by ~ 2 cm. This could have altered the pore water concentrations of some of the last samples (deeper) drawn by effectively sucking surface waters deeper into the core with sampling.

5.4 Sediment core

Core extraction complications

The set-up for pore water extraction is displayed in Figure 5-2, showing how the corer casing fits onto the barrel and how the sediment core was segmented. Originally duct tape was placed on the outside of the core barrel to cover the predrilled holes for sampling (Figure 5-2 a), but this prevented the barrel from being inserted into the corer in field (example of corer casing in Figure 5-2 b). Therefore, duct tape was put on the inside of the top section of the barrel, which is held by the corer frame. This made it difficult to extrude the core sample from the barrel (Figure 5-2 c), as the plug jammed once it reached the duct tape and was unable to wind/push further. The remaining sample had to be extracted using force with a hammer and steel plate moving the barrel down over the plug. This resulted in fragments of duct tape contaminating the samples and they required removal to prevent contamination through the digestion process.

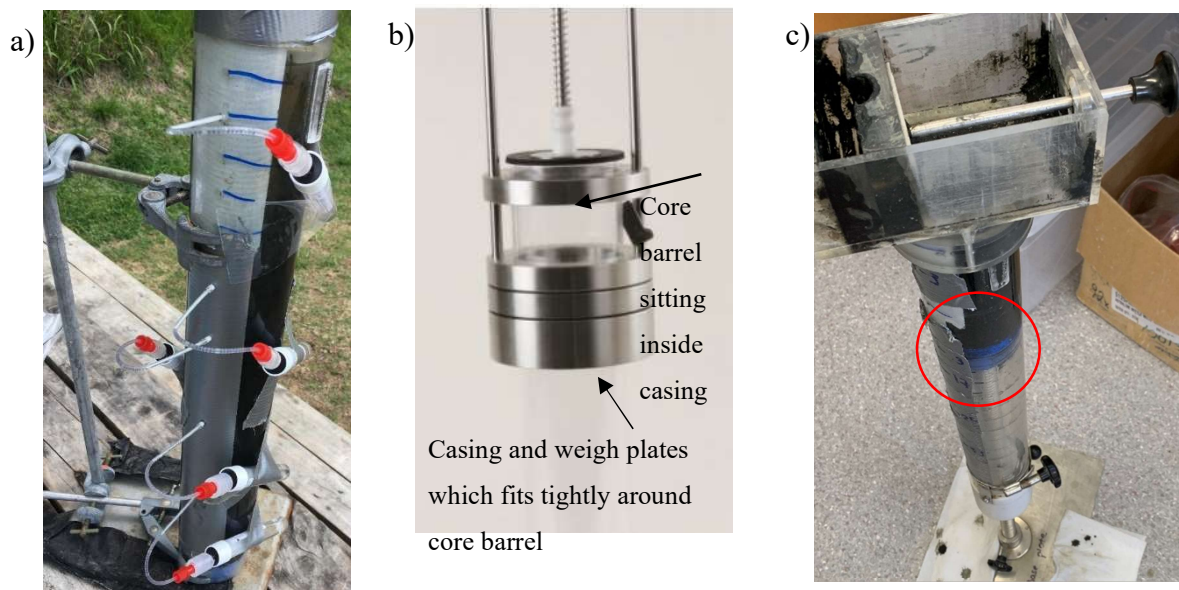


Figure 5-2. a) Sediment core held in barrel; rhizons are attached for extraction of pore water into vacutainers; b) image from Pylonex website⁹¹ depicting how the core barrel fits inside the gravity corer casing; c) barrel attached to core extruder with custom made segment extractor attached. Red circle shows where plug was unable to be wound further due to duct tape inside the core barrel.

The sediment core collected in December 2019 was extruded and analysed for total elemental concentrations (Section 2.5.2 and 2.5.3). The concentrations and trends with depth for As, Fe, and Mn were examined due to the relationship between these elements in redox dominated chemistry. The sediment was segmented into approximate 3 cm samples. The depth range and dry weights are reported in Table 5-5 and concentrations of As, Fe, and Mn are displayed in Figure 5-3.

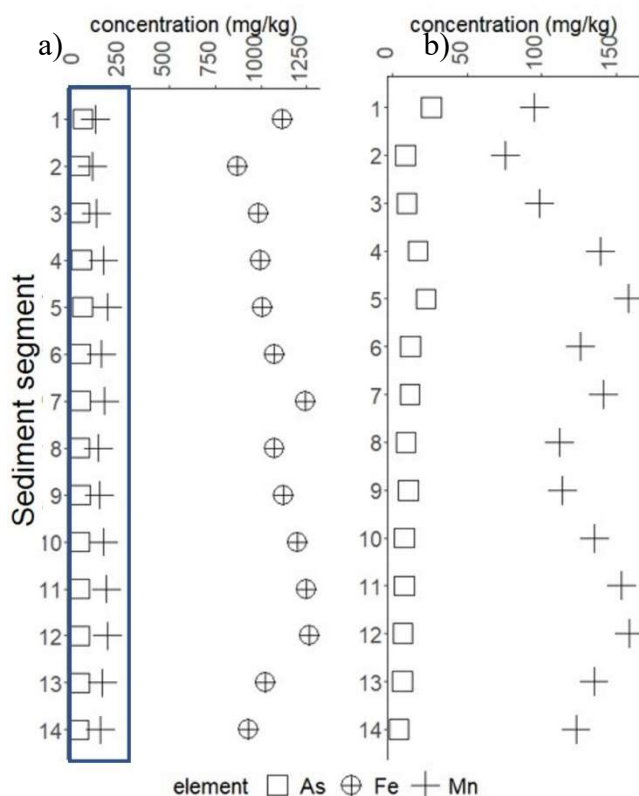


Figure 5-3. Arsenic (As), iron (Fe), and manganese (Mn) concentrations per dry weight (mg kg^{-1}) with depth, 1 being the surface segment of sediment (0-3 cm) and 14 the deepest (~ 40 cm). a) depicts Fe (circle), Mn (cross), and As (square), and b) blue box from (a) expanded to show the variation in Mn (cross) and As (square) concentrations with depth.

Similar trends were observed between elemental concentrations within the top 20 cm of sediment. All concentrations decreased with depth from the surface segment with surface segment concentrations of 26 mg kg^{-1} As (maximum As concentration), $1,119.7 \text{ mg kg}^{-1}$ Fe, and 95.0 mg kg^{-1} Mn. The decreases at segment 2 (depth 4-6cm) were 67% for As, 22 % for Fe, and 20% for Mn. A gradual increase was then observed from segment 2 to segment 5 for As, and to maximum concentrations at segment 7 for Fe, and segment 5 for Mn. The bottom 20 cm of the sediment showed similar trends between Fe and Mn, which both peak at segment 12 ($1,264$ and 158.9 mg kg^{-1} , respectively). However, As decreases with depth from segment 5 to segment 14 (4.3 mg kg^{-1}). The Fe and Mn concentration spikes could be due to long-term accumulation of redox sensitive elements, which can be indicative of changing redox conditions⁴⁴. Redox boundaries (i.e. reduction at low pE and ascent then oxidation in higher pE) as well as kinetic differences between oxidation rates of the redox sensitive metals contribute to the accumulation layers. Mn shows a concentration peak higher in the sediment layer than Fe

(segment 5 over segment 7 – approximately 6 cm difference in depth) because Mn oxidises more slowly and will be transported further towards the surface sediments before precipitating out.¹² A rate of oxidation for As (relative to Fe and Mn) was unable to be found; however, this information could help explain the great As concentrations at the surface if As oxidises more slowly and thus travels further.

The pore water and sediment concentration results taken offshore from HW1 (2019) differ to a sediment core analysed in 2012 at the equivalent TAs5 site.¹ The TAs5 As trend was similar to HW1. Maximum concentrations for As at TAs5 were found in the surface sediment segment (56 mg kg⁻¹) with a > 90% decrease within 7 cm and a continuous decrease until 2 mg kg⁻¹ in the deepest segment of sediment. The concentrations however, differed. TAs5 surface sediments contained 53% more As than HW1 and the deepest HW1 segment was 53% higher than deepest TAs5 (this could be a difference in sample depths – depending on the exact lengths of the core barrels). Fe was in lower concentration in the sediments at HW1 than TAs5, with the maximum recorded as 805 mg kg⁻¹; however, two peaks were recorded in segments 1 and 5 (compared with segments 1 and 7 in 2019 HW1 sediments). The maximum concentration of Fe in the sediment (TAs5 – 2012) is lower than the minimum concentration reported in the offshore HW1 (2019) sample (869 mg kg⁻¹ - segment 2). The 2012 Mn concentration was highest at a depth of 2-4 cm (420 mg kg⁻¹) which is 2.7x greater in concentration than Mn in any segment off HW1 (2019). The difference in depth of peak values indicate a difference in the depth of the redox boundary between the two sites, with anoxia occurring higher in the sediment profile in TAs5 than HW1.

The sedimentation rate for Lake Tarawera is unknown; however, it has been reported that volcanic materials from the 1886 Mount Tarawera eruption can be seen within 30 cm of sediment collected from TAs5, indicating a slow sedimentation rate.¹ It is hypothesised that sedimentation rates would not be homogenous throughout the lake. Sediments offshore from inlets (e.g., TAs1) which suspend particulates along the flow path may see a faster rate of sedimentation than sediments in deeper water bodies (e.g., TAs5) which would require particulates to remain suspended through transport from inlets to the deeper waters before settling out. The As concentrations in the deeper water sites (Figure

4-6) also suggests cycling occurs with overturning of the water column, which may involve re-partitioning of particulates to the dissolved phase and re-precipitation, compared with the introduction of new particulates settling into the sediments offshore from the inlets. Sedimentation rate and sediment cycling could explain the differences in concentrations and trends between the two coring locations. Long-term time series analysis of sediments would provide data to support this hypothesis and would help ascertain whether there were redox boundaries attributed to the multiple concentration spikes seen in Figure 5-3.

When comparing sediment concentrations to pore waters (Figure 5-1), there are similar trends with depth. The analysed pore waters are not from the digested sediment core; however, it is noted that when collecting pore waters with gaps in between it is likely that trends could be missed, such as the sediment concentrations in Figure 5-3 that show multiple troughs and peaks with depth.

Summary

The retention of As^{III} in vacutainers over time was seen from initial field samples where delayed analysis occurred. However, bench-top experiments in attempt to replicate these conditions and monitor the rate of As^{III} oxidation was unsuccessful, based on inconclusive results across two experiments; one using University of Waikato campus lake waters and the other using pore waters extraction from Lake Tarawera sediment core.

Pore water and sediment samples collected off-shore from HW1 showed higher levels of As concentrations than are dissolved in the water column. The sediments contained mg kg⁻¹ concentrations, an order of magnitude higher than the equivalent pore waters (µg L⁻¹), and they both showed highest concentrations in the surface sediments/pore waters and a decrease with depth. To correlate these trends; however, pore water samples should be taken from the same increments as the sediment, in lower volume to avoid drawing waters from elsewhere in the core.

CHAPTER SIX

CONCLUSIONS

6.1 Thesis summary

This thesis investigated physicochemical fluctuations within Lake Tarawera, particularly in relation to the presence, speciation, and movement of As and related elements such as Fe and Mn that through redox processes contribute to the presence and speciation of As. The thesis focused on the Wairua Arm of the lake, an area of known geothermal activity. The major findings of this thesis are summarised below.

Chapter 3 studied the physical parameters (variation in seasonal temperature and dissolved oxygen concentrations with depth in open-waters) of the water column of Lake Tarawera to be aid in explanation of seasonal changes in As concentration. Changes in physical parameters typical of a large, deep lake occur on an annual cycle, with a period of mixed waters and a period of thermal stratification causing separation of the hypolimnetic waters from the surface waters. The deepest measured site in the main body of the lake (~80 m) displayed hyperanoxic water from 76 m depth in the month of April which is near the end of the stratification period. Comparisons of physicochemical data through time (1996 – 2017) indicate a slight decrease in water dissolved oxygen in the benthic waters from 2011.

Chapter 4 examined the species of As that was present within the lake and concentrations (dissolved and total) from both inlets and open-water sites. Investigations by previous researchers (2018-February 2019) of the inlets into Lake Tarawera identified the Wairua Arm as a hotspot for As; with As concentrations ranging from 41.0 – 947 $\mu\text{g L}^{-1}$. These results led to this thesis focusing on sampling in the Wairua Arm and open-water sites leading out to the main water body. Results from the 2019-2020 sampling are as follows:

1. Arsenic speciation analysis was performed on all samples obtained from Lake Tarawera. Only one instance of the highly toxic As^{III} was reported throughout the course of this sampling which was located in a surface stream inlet (WR1). The appearance of As^{III} at this site was likely due to

coverage by lake weed causing a depletion in DO and was only found during one sampling trip. Current conditions of the open waters of Lake Tarawera favour the oxidised species of As (As^{V}) and the collected data indicates that As^{V} remains dissolved in the water column at high concentrations (exceeding WHO drinking water standards). This is an encouraging result, as As^{III} is more toxic to people; however, exposure to high concentrations of total As is still detrimental to humans.

2. The concentration of total As in Wairua Arm inlets ranged from 41.0 to 947 $\mu\text{g L}^{-1}$, indicating continuous loading of As into the water column. RMHW and HW1 are two inlets which contribute high concentrations of As to the system; RMHW through As loading ($16,400 \pm 2,660 \mu\text{g As s}^{-1}$), and HW1 through consistently high year-round As concentrations ($714 \pm 200 \mu\text{g L}^{-1}$). The concentration of As coming from these inlets is seasonally variable, but that variability depends on the inlet source. The higher concentrations from the (suspected) Rotomahana inlet sites correspond to cycling occurring in Lake Rotomahana, rather than the expected increase of As in summer months due to solubility in warmer waters.
3. Open-water As concentrations are influenced by thermal stratification, with benthic samples increasing during the stratified period, as well as with depth from $\text{TAs1} < \text{TAs5}$. During the mixed period, the open-water surface and benthic As concentrations are homogenous ($48.3 \pm 1.3 \mu\text{g L}^{-1}$ surface and $50.2 \pm 1.4 \mu\text{g L}^{-1}$ benthic, across all sites), in contrast to significantly different concentrations towards the end of the stratified period ($45 \pm 4.9 \mu\text{g L}^{-1}$ surface, and $76 \pm 31 \mu\text{g L}^{-1}$ benthic, in March). The accumulation of As in the benthic waters in TAs5 ($127 \mu\text{g L}^{-1}$, March) could be a combination of the gravity settling of As from the water column, as well as reductive dissolution of As from a sediment flux.
4. The mixing of As into Lake Tarawera was investigated at two different inlets: one with a high flow rate and high As concentration (RMHW) and one with a low flow rate and high As concentration (HW1). RMHW

($130 \pm 3 \text{ L s}^{-1}$ flow rate), on the day of sampling, was mixing in the southerly direction which could be influenced by local weather such as wind. The isotopic signatures from the RMHW grab samples show the waters are a combination of Lake Rotomahana and Lake Tarawera, as well as influence from rainfall and evaporation. The HW1 site shows a different pattern of mixing to that of RMHW. The lower flow rate (0.1 L s^{-1}) and high temperatures of HW1 causes a small-scale thermocline within wading depth off-shore and disperses As throughout the surface waters towards the open water site, TAs1. The deeper, cooler water at HW1 contained less As than the warmer surface waters (ranging between $149\text{-}340 \mu\text{g L}^{-1}$ surface, and $61\text{-}113 \mu\text{g L}^{-1}$ benthic) until the induced thermocline disappears and the surface and benthic waters have a more evenly mixed As concentration at TAs1 ($53 \mu\text{g L}^{-1}$ surface, and $41 \mu\text{g L}^{-1}$ benthic). This local surface mixing from HW1 to TAs1 is suggested to be the reason for the consistently higher surface than benthic concentrations at TAs1, which contradicts the other four open-water sites having higher benthic concentrations than equivalent surface concentrations. The isotopic signature of the grab samples taken near HW1 appear to be mostly mixed lake waters; indicating that the low flow of HW1 does not alter the isotope pattern of the mixed open-waters when mixing into the lake.

5. Suspended fractions of As, Fe, or Mn were low in the water column, and the concentration of particulate As exceeded the two metals; therefore, there is low likelihood that As will be removed from the system through adsorption reactions. The high concentrations of As, Fe and Mn in the sediments indicate the adsorption of As to Fe/Mn may be occurring until the sorbent is at capacity/consumed by As and unable to react any further. Fe and Mn are important in the cycling of As between sediments and benthic waters under the right conditions. Those conditions do not appear to have been met in Lake Tarawera, but long-term BoPRC data shows a decline in DO in the benthic waters at TAs5 from 2011 onwards. A continual decline may cause an increase in redox chemistry occurring in the waters; resulting in reduction of As and the related sorbents in a DO depleted hypolimnion during

stratification, leading to cycling of As between sediments and the hypolimnetic waters.

Chapter 5 explored the retention of As^{III} in samples stored in vacutainers over-time, and presented pore water and sediment data from samples taken off HW1. The collection and storage of pore waters using rhizons and vacutainers was tested for long-term preservation of As^{III} in laboratory and field-collected samples. A three-month delay in HPLC-ICP-MS analysis of field samples displayed a retention of As^{III}; however, laboratory spike recovery results for deliberate time series analysis were highly variable and with a low retention of As^{III}. An experiment using Type 1 water and UoW Chapel Lake water showed slow oxidation of As^{III} (i.e., As^{III} was detected after 55-days); however, stored pore waters collected from the Lake Tarawera sediment core showed complete oxidation of As^{III} within 29-days. Due to the contradicting nature of these results, additional experimentation is required to provide a better indication of the stability of As^{III} under different storage conditions. The pore water As data showed the greatest As^{III} and As^V concentrations in the surface, both decreasing with depth. This corresponded to the sediment trends; however, the pore water and sediment samples were from sediment cores collected at two different time points. The sediment As concentration in the surface (0-3 cm) was 26 mg kg⁻¹, which decreased with 40 cm depth to a minimum of 4.3 mg kg⁻¹, excluding a 22 mg kg⁻¹ spike at segment 5 (13-15 cm). This indicates a change over time in redox boundaries, however the rate of sedimentation is unknown, as are the pE/pH values of the pore waters, and for conclusions on this data, further sampling should be undertaken.

6.2 Recommendations for future work

The biological aspects which have been acknowledged as important but not pursued in this thesis would complement this research well in terms of overall health concern to recreational use of the lake (including fishing). This includes the accumulation of As in the fish occupying the lake, particularly the bottom dwellers, as well as the uptake by plants and how plant life can alter the speciation of As.

Future work could also include examining the kinetics of reaction rates for the oxidation of As^{III} to As^{V} as an indication of what is occurring in the deep open-water sites during stratification, where concentrations of As^{V} increase over the period of stratification and DO levels reach hyperanoxic levels. This could elucidate whether the source of the increased As measured in TAs5 is reduced As^{III} being advected through the pore waters and oxidised in the oxic hypolimnion, or an accumulation of dissolved As^{V} from the water column (gravity settling). These kinetic studies are also relevant to the further work on retention of As^{III} during storage in vacutainers over time.

Further work on the method development and validation of pore water collection and storage using rhizons and vacutainers is required to ascertain the cause of oxidation in the vacutainers. Relevant analyses for determining the source of oxidation could include pH, pE, and DO measurements of pore waters as well as speciation of Fe and Mn within the pore water samples.

Related to pore water As concentrations, the sediments could be examined for exchangeable fractions, to determine whether or not As is incorporated into mineral as constituent ions, effectively removing it from the redox cycling system. Comparing pore water concentrations to sediment concentrations would give a clearer indication of the difference in As concentrations in the layers of sediment. It is recommended that when collecting pore water samples, no overlying water is left in the sediment core, and sample volumes are minimal to reduce movement of water within the sediment core.

References

1. Pearson. L. K. Sediment-Pore Water Chemistry of Taupo Volcanic Zone Lakes and The Effect Trophic State has on Exchange with the Water Column. PhD Thesis, University of Waikato, New Zealand, **2012**.
2. Ongoing Water Quality Monitoring Undertaken at Lake Tarawera by the University of Waikato/Bay of Plenty Regional Council. 2018-2019.
3. Robinson. B. H. Pollution of the Aquatic Biosphere by Arsenic and other Elements in the Taupo Volcanic Zone. MSc Thesis, Massey University, New Zealand, **1994**.
4. Hettick, B. E.; Canas-Carrell, J. E.; French, A. D.; Klein, D. M. Arsenic: A Review of the Element's Toxicity, Plant Interactions, and Potential Methods of Remediation. *Journal of Agricultural Food Chemistry* **2015**, *63*, 7097-7107.
5. Lee, X. C.; Yalcin, S.; Ma, M. Speciation of Submicrogram per liter Levels of Arsenic in Water. On-Site Speciation Separation Integrated with Sample Collection. *Journal of Environmental Science Technology* **2000**, *34*, 2342-2347.
6. Elder. J. F. *Metal Biogeochemistry in Surface-Water Systems*; U.S Government: Denver, CO, 1988.
7. Torres, J.; Santos, P.; Ferrari, C.; Kremer, C.; Kremer, E. Solution Chemistry of Arsenic Anions in the Presence of Metal Cations. *Journal of Solution Chemistry* **2017**, *46*, 2231-2247.
8. Jain. C.; Ali. I. Arsenic: Occurance, Toxicity, and Speciation Techniques. *Journal of Water Research* **2000**, *34*, 4304-4312.
9. Boyle. R. W.; Jonassen. I. R. The Geochemistry of Arsenic and its use as an Indicator Element in Geochemical Prospecting. *Journal of Geochemical Exploration* **1973**, *2*, 251-296.
10. Lord, G.; Kim, N.; Ward, N. I. Arsenic Speciation of Geothermal Waters in New Zealand. *Journal of Environmental Monitoring* **2012**, *14*, 3192-3201.
11. McLaren, S. J.; Kim, N. D. Evidence for a Seasonal Fluctuation of Arsenic in New Zealand's Longest River and the Effect of Treatment on Concentrations in Drinking Water. *Journal of Environmental Pollution* **1995**, *90*, 67-73.
12. Webster. J. G.; Nordstrom. D. K. Geothermal Arsenic: The Source, Transport, and Fate of Arsenic in Geothermal Systems. In *Arsenic in Ground Water*; Welch. A. H. and Stollenwerk. K. G., Eds.; Springer: Boston, MA, **2003**; pp 101-125.
13. Terlecka, E. Arsenic Speciation Analysis in Water Samples: A Review of the Hyphenated Techniques. *Journal of Environmental Monitoring and Assessment* **2005**, *107*, 259-284.

14. Sugár, É.; Tatár, E.; Záray, G.; Mihucz, V. G. Field Separation - Based Speciation Analysis of Inorganic Arsenic in Public Well Water in Hungary. *Microchemical Journal* **2013**, *107*, 131-135.
15. Nicholas, D. R.; Ramamoorthy, S.; Palace, V.; Spring, S.; Moore, J. N.; F, R. R. Biogeochemical Transformations of Arsenic in Circumneutral Freshwater Sediments. *Journal of Biodegradation* **2003**, *14*, 123-137.
16. Watts, M. J.; O'Reilly, J.; Marcilla, A. L.; Shaw, R. A.; Ward, N. I. Field Based Speciation of Arsenic in UK and Argentinean Water Samples. *Journal of Environmental Geochemistry and Health* **2010**, *32*, 479-490.
17. Mason, B. H.; Moore, C. B. *Principles of Geochemistry*; Wiley, 1982.
18. Hartland, A.; Anderson, M. S.; Hamilton, D. P. Phosphorus and Arsenic Distributions in a Seasonally Stratified, Iron- and Manganese- Rich Lake: Microbiological and Geochemical Controls. *Journal of Environmental Chemistry* **2015**, *12*, 708.
19. Bednar, A. J.; Garbarino, J. R.; Burkhardt, M. R.; Ranville, J. F.; Wildeman, T. R. Field and Laboratory Arsenic Speciation Methods and Their Application to Natural-Water Analysis. *Journal of Water Research* **2004**, *38*, 355-364.
20. O'Day, P. Chemistry and Mineralogy of Arsenic. *Journal of Elements* **2006**, *2*, 77-83.
21. Ackermann, J.; Vetterlein, D.; Tanneberg, H.; Neue, H. U.; Mattusch, J.; Jahn, R. Speciation of Arsenic under Dynamic Conditions. *Journal of Engineering in Life Sciences* **2008**, *8*, 589-597.
22. Ferguson, J. F.; Gavis, J. A Review of the Arsenic Cycle in Natural Waters. *Journal of Water Research* **1972**, *6*
23. Rahdar, S.; Taghavi, M.; Khaksefidi, R.; Ahmadi, S. Adsorption of Arsenic^V from Aqueous Solution using Modified Saxaul Ash: Isotherm and Thermodynamic Study. *Journal of Applied Water Science* **2019**, *9*
24. Bostick, B. C.; Fendorf, S. Arsenite Sorption on Troilite (FeS) and Pyrite (FeS₂). *Journal of Geochimica et Cosmochimica Acta* **2003**, *67*, 909-921.
25. Anderson, L. C. D.; Bruland, K. W. Biogeochemistry of Arsenic in Natural Waters. *Journal of Environmental Science Technology* **1991**, *25*, 420-427.
26. Wilkie, J. A.; Hering, J. G. Adsorption of Arsenic onto Hydrous Ferric Oxide: Effects of Adsorbate/Adsorbent Ratios and Co-occurring Solutes. *Journal of Colloids and Surfaces A: Physicochemical and Engineering Aspects* **1996**, *107*, 97-110.
27. Arsenic: Medical and Biologic Effects of Environmental Pollutants. <https://www.ncbi.nlm.nih.gov/books/NBK231019/> (accessed 13/07/2019).
28. Varsányi, I.; Ó.Kovács, L. Distribution of Dissolved Arsenic in a Sedimentary Environment from the Near-Surface to a Depth of 2500 m, and Factors Controlling Distribution. *Journal of Applied Geochemistry* **2017**, *80*, 168-175.

29. Timperley. M H.; Vigor-Brown. R. J. Water chemistry of Lakes in the Taupo Volcanic Zone. *New Zealand Journal of Marine and Freshwater Research* **1986**, *20*, 173-183.
30. Manning, B. A.; Goldberg, S. Adsorption and Stability of Arsenic^{III} at the Clay Mineral– Water Interface. *Journal of Environmental Science & Technology* **1997**, *31*, 2005-2011.
31. Lin, L.; Song, Z.; Huang, Y.; Khan, Z. H.; Qiu, W. Removal and Oxidation of Arsenic from Aqueous Solution by Biochar Impregnated with Fe-Mn Oxides. *Journal of Water, Air, & Soil Pollution* **2019**, *230*
32. Stumm; Morgan, J. J. *Aquatic Chemistry : Chemical Equilibria and Rates in Natural Waters*; Somerset: John Wiley & Sons, Incorporated: Somerset, **1995**.
33. Farrell, J.; Chaudhary, B. K. Understanding Arsenate Reaction Kinetics with Ferric Hydroxides. *Journal of Environmental Science & Technology* **2013**, *47*, 8342-8347.
34. de Vitre. R.; Belzile. N.; Tessier. A. Speciation and Adsorption of Arsenic on Diagenetic Iron Oxyhydroxides. *Journal of Limnology and Oceanography* **1991**, *36*, 1480-1485.
35. Balistrieri. L. S.; Murray. J. W. The Surface Chemistry of δ -MnO₂ in Major Ion Seawater. *Journal of Cosmochimica Acta* **1982**, *46*, 1041-1052.
36. Takamatsu. T.; Kawashima. M.; M., K. The Role of Mn²⁺-rich Hydrous Manganese Oxide in the Accumulation of Arsenic in Lake Sediments. *Journal of Water Research* **1985**, *19*, 1029-1032.
37. Spycher. N. F.; Reed. M. H. As(III) and Sb(III) Sulfide Complexes: An Evaluation of Stoichiometry and Stability from Existing Experimental Data. *Journal of Geochimica et Cosmochimica Acta* **1989**, *53*, 2185-2194.
38. Grundl, T. J.; Haderlein, S.; Nurmi, J. T.; Tratnyek, P. G. Introduction to Aquatic Redox Chemistry. In *Aquatic Redox Chemistry*; American Chemical Society, **2011**; pp 1-14.
39. Day, J. A.; Montes-Bayon, M.; Vonderheide, A. P.; Caruso, J. A. A Study Of Method Robustness For Arsenic Speciation In Drinking Water Samples By Anion Exchange HPLC-ICP-MS. *Journal of Analytical and Bioanalytical Chemistry* **2002**, *373*, 664-668.
40. Davison. W. Iron and Manganese in Lakes. *Journal of Earth-Science Reviews* **1993**, *34*, 119-163.
41. Lehmann, M. K.; Nguyen, U.; Muraoka, K.; Allan, M. G. Regional Trends in Remotely Sensed Water Clarity over 18 Years in the Rotorua Lakes, New Zealand. *New Zealand Journal of Marine and Freshwater Research* **2019**, 1-23.
42. Outa, J. O.; Kowenje, C. O.; Plessl, C.; Jirsa, F. Distribution of Arsenic, Silver, Cadmium, Lead and other Trace Elements in Water, Sediment and Macrophytes in the Kenyan Part of Lake Victoria: Spatial, Temporal and Bioindicative Aspects. *Journal of Environmental Science and Pollution Research* **2020**, *27*, 1485-1498.

43. Eager. C. Biogeochemical Characterisation of an Alum Dosed Stream: Implications for Phosphate Cycling in Lake Rotoehu. MSc Thesis, University of Waikato, New Zealand, **2017**.
44. Aggett. J.; Kreigman. M. R. The Extent of Formation of Arsenic^{III} in Sediment Interstitial Waters and its Release to Hypolimnetic Waters in Lake Ohakuri. *Journal of Water Research* **1988**, 22, 407-411.
45. Pearson. L. K. The Nature, Composition and Distribution of Sediment in Lake Rotorua, New Zealand. MSc Thesis, University of Waikato, New Zealand, **2007**.
46. Moore, J. N.; Ficklin, W. H.; Johns, C. Partitioning of Arsenic and Metals in Reducing Sulfidic Sediments. *Journal of Environmental Science & Technology* **1988**, 22, 432-437.
47. Gao, F.; Deng, J.; Li, Q.; Hu, L.; Zhu, J.; Hang, H.; Hu, W. A New Collector for *in Situ* Pore Water Sampling in Wetland Sediment. *Journal of Environmental Technology* **2012**, 33, 257-264.
48. Xu, D.; Wu, W.; Ding, S.; Sun, Q.; Zhang, C. A High-Resolution Dialysis Technique for Rapid Determination of Dissolved Reactive Phosphate and Ferrous Iron in Pore Water of Sediments. *Journal of Science of The Total Environment* **2012**, 421-422, 245-252.
49. Gruzalski, J. G.; Markwiese, J. T.; Carriker, N. E.; Rogers, W. J.; Vitale, R. J.; Thal, D. I. Pore Water Collection, Analysis and Evolution: The Need for Standardization. In *Reviews of Environmental Contamination and Toxicology Volume 237*; W. P. de Voogt, Ed.; Springer International Publishing: Cham, **2016**; pp 37-51.
50. Meers, E.; Laing, G. D.; Unamuno, V. G.; Lesage, E.; Tack, F. M. G.; Verloo, M. G. Water Extractability of Trace Metals from Soils: Some Pitfalls. *Journal of Water, Air, and Soil Pollution* **2006**, 176, 21-35.
51. Chen, M.; Ding, S.; Chen, X.; Sun, Q.; Fan, X.; Lin, J.; Ren, M.; Yang, L.; Zhang, C. Mechanisms Driving Phosphorus Release During Algal Blooms Based on Hourly Changes in Iron and Phosphorus Concentrations in Sediments. *Journal of Water Research* **2018**, 133, 153-164.
52. Seeberg-Elverfeldt, J.; Schlüter, M.; Feseker, T.; Kölling, M. Rhizon Sampling of Porewaters Near the Sediment-Water Interface of Aquatic Systems. *Journal of Limnology and Oceanography: Methods* **2005**, 3, 361-371.
53. Brodecka-Goluch. A., S. P., and Bolątek J. Impact of Sampling Techniques on the Concentration of Ammonia and Sulfide in Pore Water of Marine Sediments. *Journal of Oceanological and Hydrobiological Studies* **2019**, 48, 184-195.
54. Steiner, Z.; Lazar, B.; Erez, J.; Turchyn, A. V. Comparing Rhizon Samplers and Centrifugation for Pore-Water Separation in Studies of the Marine Carbonate System in Sediments. *Journal of Limnology and Oceanography: Methods* **2018**, 16, 828-839.
55. Andreae. M. O. Arsenic Speciation in Seawater and Interstitial Waters: The Influence of Biological-Chemical Interactions on the Chemistry

- of a Trace Element. *Journal of Limnology and Oceanography* **1979**, *24*, 440-452.
56. Michalke, B. The Coupling of LC to ICP-MS in Element Speciation: I. General Aspects. *Journal of Trends in Analytical Chemistry* **2002**, *21*, 142-153.
 57. Gilmartin, G.; Gingrich, D. A Comparison of the Determination and Speciation of Inorganic Arsenic using General HPLC Methodology with UV, MS and MS/MS Detection. *Journal of Chromatography B* **2018**, *1083*, 20-27.
 58. Colon, M.; Hidalgo, M.; Iglesias, M. Arsenic Determination by ICP-QMS with Octopole Collision/Reaction Cell. Overcome of Matrix Effects Under Vented and Pressurized Cell Conditions. *Journal of Talanta* **2011**, *85*, 1941-1947.
 59. Wilson. C. J. N.; Houghton. B. F.; McWilliams. M. O.; Lanphere. M. A.; Weaver. S. D.; Briggs. R.M. Volcanic and Structural Evolution of Taupo Volcanic Zone, New Zealand: a Review. *Journal of Volcanology and Geothermal Research* **1995**, *68*, 1-28.
 60. Keam, R. F. The Tarawera Eruption, Lake Rotomahana, and the Origin of the Pink and White Terraces. *Journal of Volcanology and Geothermal Research* **2016**, *314*, 10-38.
 61. Nairn, I. A. The Te Rere and Okareka Eruptive Episodes — Okataina Volcanic Centre, Taupo Volcanic Zone, New Zealand. *New Zealand Journal of Geology and Geophysics* **1992**, *35*, 93-108.
 62. Burns. N.; McIntosh. J.; Scholes. P. Managing the Lakes of the Rotorua District, New Zealand. *Journal of Lake and Reservoir Management* **2009**, *25*, 284-296.
 63. Burns. N.; Bryers. G.; Bowman. E. *Protocol for Monitoring Trophic Levels of New Zealand Lakes and Reservoirs*. Ministry for the Environment: **2000**.
 64. Cherry. J. A.; Shaikh. A. U.; Tallman. D. E.; Nicholson. R. V. Arsenic Species as an Indicator of Redox Conditions in Groundwater. *Journal of Hydrology* **1979**, *43*, 373-392.
 65. Rotorua Lakes <https://www.rotorualakes.co.nz/lake-tarawera> (accessed 13/07/2019).
 66. Totally Tarawera <https://www.totallytarawera.com> (accessed 13/07/2019).
 67. Rotorua Tourism. <https://www.rotoruanz.com> (accessed 13/07/2019).
 68. Lake Tarawera Scenic Reserve, Places to Go <https://www.doc.govt.nz>, (accessed 13/07/2019).
 69. Gillon. N.; White. P.; Hamilton D.; Silvester. W. *Groundwater in the Okataina Caldera: Model of Future Nitrogen Loads to Lake Tarawera*. Environment Bay of Plenty: **2009**.
 70. Scholes P.; Hamill K. *Rotorua Lakes Water Quality Report 2014/2015*; **2016**; <http://www.rotorualakes.co.nz/vdb/document/150>.
 71. T.D. Martin, J. T. C., and C.A. Brockhoff Method 200.2, Sample Preparation Procedure for Spectrochemical Determination of Total Recoverable Elements. Revision 2.8. United States Environmental

- Protection Agency. https://www.epa.gov/sites/production/files/2015-08/documents/method_200-2_rev_2-8_1994.pdf (accessed 23/07/2020).
72. Environment, B. C.-M. o. Digestion for Total Metals in Water - Prescriptive. Revised 15/09/2017. British Columbia - Ministry of Environment https://www2.gov.bc.ca/assets/gov/environment/research-monitoring-and-reporting/monitoring/emre/methods/sept2017/bc_moe_total_metals_in_water_digestion_15sept2017.pdf (accessed 19/07/2019).
 73. Marcinkowska. M.; Komorowinz. I.; Baralkiewicz. D. New Procedure for Multielemental Speciation Analysis of Five Toxic Species: As^{III}, As^V, Cr^{VI}, Sb^{III}, and Sb^V in Drinking Water Samples by Advanced Hyphenated Technique HPLC/ICP-DRC-MS. *Journal of Analytica Chimica Acta* **2016**, *920*, 102-111.
 74. Zhang, Y.; Wu, Z.; Liu, M.; He, J.; Shi, K.; Zhou, Y.; Wang, M.; Liu, X. Dissolved Oxygen Stratification and Response to Thermal Structure and Long-Term Climate Change in a Large and Deep Subtropical Reservoir (Lake Qiandaohu, China). *Journal of Water Research* **2015**, *75*, 249-258.
 75. Liu, M.; Zhang, Y.; Shi, K.; Zhu, G.; Wu, Z.; Liu, M.; Zhang, Y. Thermal Stratification Dynamics in a Large and Deep Subtropical Reservoir Revealed by High-Frequency Buoy Data. *Journal of Science of The Total Environment* **2019**, *651*, 614-624.
 76. Davies - Colley, R. J. Mixing Depths in New Zealand lakes. *New Zealand Journal of Marine and Freshwater Research* **1988**, *22*, 517-528.
 77. De Crop, W.; Verschuren, D. Determining Patterns of Stratification and Mixing in Tropical Crater Lakes Through Intermittent Water-Column Profiling: A Case Study in Western Uganda. *Journal of African Earth Sciences* **2019**, *153*, 17-30.
 78. Brookes, J. D.; O'Brien, K. R.; Burford, M. A.; Bruesewitz, D. A.; Hodges, B. R.; McBride, C.; Hamilton, D. P. Effects of Diurnal Vertical Mixing and Stratification on Phytoplankton Productivity in Geothermal Lake Rotowhero, New Zealand. *Journal of Inland Waters* **2013**, *3*, 369-376.
 79. Nürnberg, G. K. Quantified Hypoxia and Anoxia in Lakes and Reservoirs. *The Journal of The Scientific World* **2004**, *4*, 276509.
 80. Jolly., V. H. The Comparative Limnology of some New Zealand Lakes. *New Zealand Journal of Marine and Freshwater Research* **1968**, *2:2*, 214-259.
 81. Renwick. R. New Zealand National Climate Summary - the Year 2008. The National Institute for Water and Atmospheric Research, Ltd (New Zealand). <https://niwa.co.nz/climate/summaries/annual/2008#:~:text=New%20Zealand's%20climate%20for%202008,to%20NIWA's%20National%20Climate%20Centre.&text=The%20national%20average%20tempe>

- [rature%20was,during%202008%2C%20milder%20than%20normal.](#)
(accessed 24/07/2020).
82. Fedaeff, N. New Zealand Climate Summary - 2019. The National Institute for Water and Atmospheric Research, Ltd (New Zealand). https://niwa.co.nz/sites/niwa.co.nz/files/2019_Annual_Climate_Summary_FINAL.pdf (accessed 24/07/2020).
 83. *Tarawera Lakes Restoration Plan (2015). Bay of Plenty Regional Council. 2015.*
 84. . Personal Communication, **2019**.
 85. Walker, S. L.; de Ronde, C. E. J.; Fornari, D.; Tivey, M. A.; Stucker, V. K. High-Resolution Water Column Survey to Identify Active Sublacustrine Hydrothermal Discharge Zones within Lake Rotomahana, North Island, New Zealand. *Journal of Volcanology and Geothermal Research* **2016**, *314*, 142-155.
 86. Palmer, M. J.; Chételat, J.; Richardson, M.; Jamieson, H. E.; Galloway, J. M. Seasonal Variation of Arsenic and Antimony in Surface Waters of Small Subarctic Lakes Impacted by Legacy Mining Pollution Near Yellowknife, NT, Canada. *Journal of Science of The Total Environment* **2019**, *684*, 326-339.
 87. Average Weather on March 3 in Rotorua, New Zealand. <https://weatherspark.com/d/144936/3/3/Average-Weather-on-March-3-in-Rotorua-New-Zealand#Sections-Wind> (accessed 11/09/2020).
 88. Geurts, J. J. M.; Smolders, A. J. P.; Banach, A. M.; van de Graaf, J. P. M.; Roelofs, J. G. M.; Lamers, L. P. M. The Interaction Between Decomposition, Net N and P Mineralization and Their Mobilization to the Surface Water in Fens. *Journal of Water Research* **2010**, *44*, 3487-3495.
 89. Gunduz, O., G. H., Cakir, A., Elci, A., Baba, A., Simsek, C. Sample Collection into Sterile Vacuum Tubes to Preserve Arsenic Speciation in Natural Water Samples. *Journal of Environmental Engineering* **2013**, *139*, 1080-1088.
 90. Arai, Y.; Sparks, D. L. Residence Time Effects On Arsenate Surface Speciation At The Aluminum Oxide-Water Interface. *Journal of Soil Science* **2002**, *167*
 91. . <https://www.pylonex.com/The-HTH-Gravity-Corer>
 92. McBride, C. G.; Abell, J.; Baisden, T. *Assessing effects of changes to nutrient loads on Lake Tarawera water quality: Model simulations for 2010 to 2020 (draft report in preparation)*. . Environmental Research Institute prepared by University of Waikato for Bay of Plenty Regional Council: **2020**.
 93. Baisden, T. Water Isotopes - Lakes, Inflows, and ... groundwater. Presented at Rotorua Te Arawa Lakes Technical Advisory Group Meeting, May 2020, Online (Zoom).

Appendix

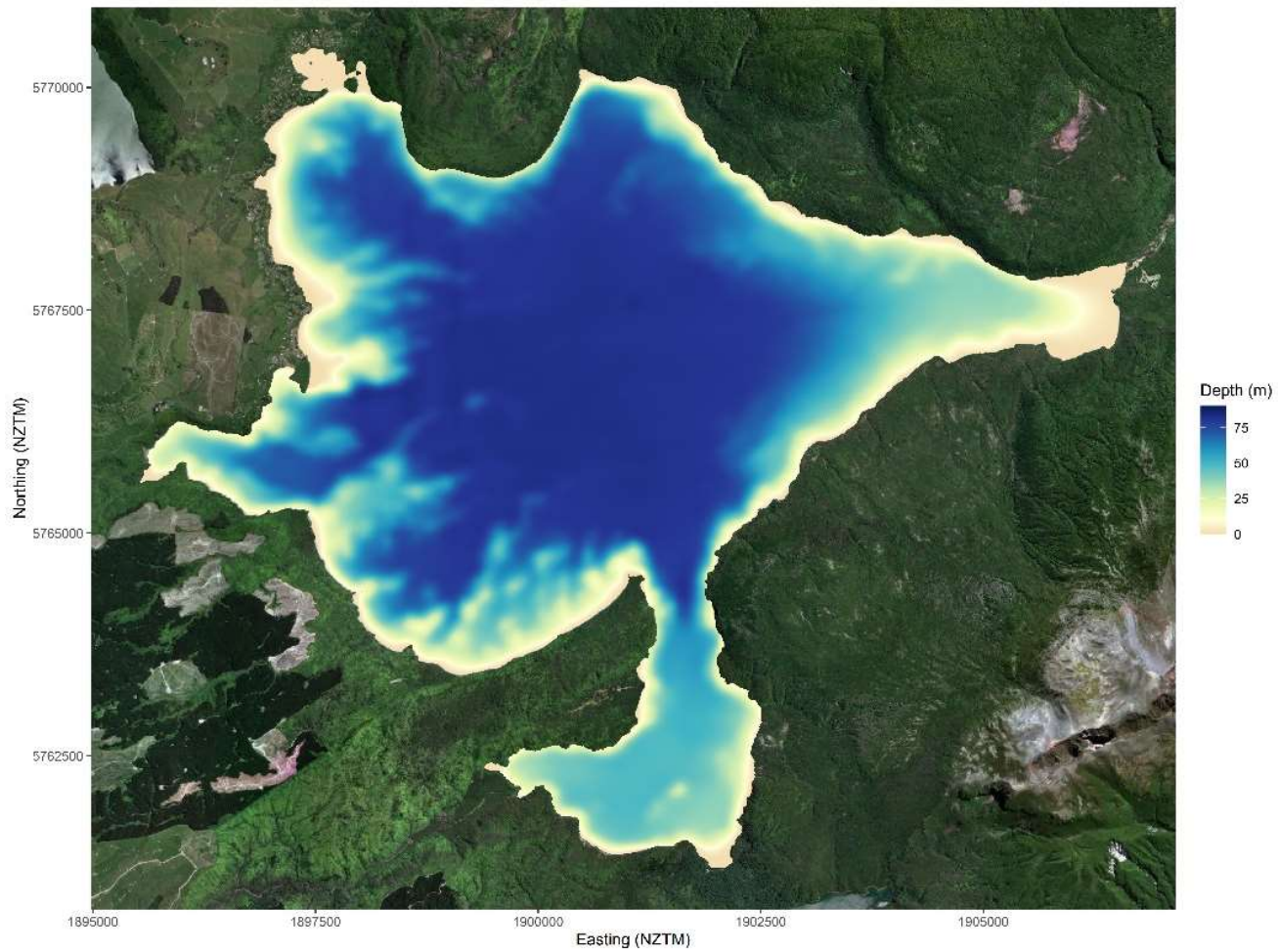


Figure A-1. Bathymetry map of Lake Tarawera. Copied from McBride *et. al.* 2020⁹²

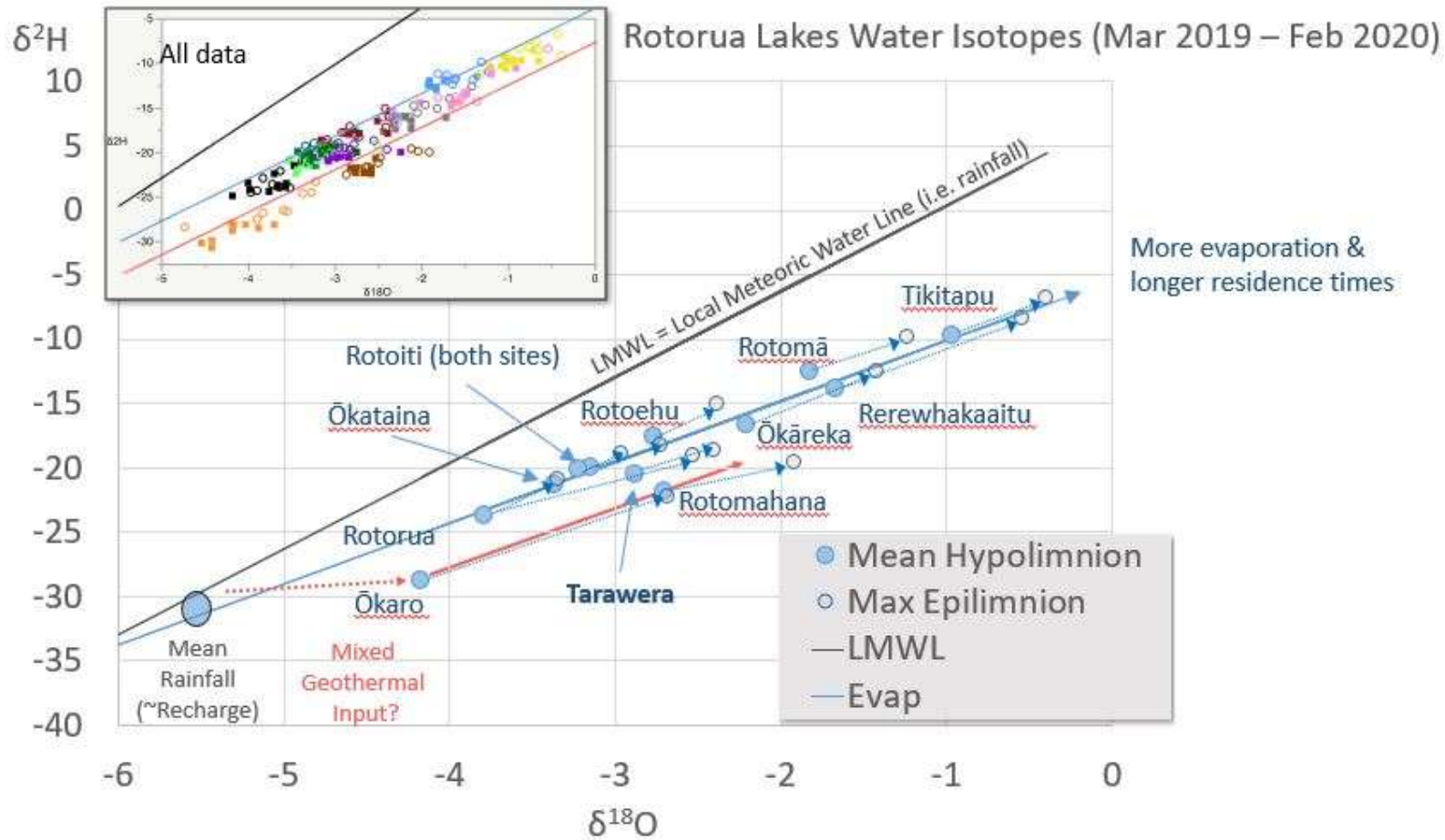


Figure A-2. Rotorua Lakes Water Isotopes (March 2019 – February 2020). Taken from Baisden, 2020.⁹³

Table A-1. Summary of all sites mentioned in this thesis. Identifies who the samples were collected by, and what they were for. Indicates sites which overlapped and used as combined data. BoPRC denotes continuous monitoring programme, and UoW means for this thesis.

Sample Name	Samples collected			
	by:	for:	on:	type:
Craig Armstrong	BoPRC	ICP-MS	2018/2019	Inlet
Island Waterfall	BoPRC	ICP-MS	2018/2019	Inlet
Main Twin Creek	BoPRC	ICP-MS	2018/2019	Inlet
Main Waterfall	BoPRC	ICP-MS	2018/2019	Inlet
Maori Reserve	BoPRC	ICP-MS	2018/2019	Inlet
Middle Flax B	BoPRC	ICP-MS	2018/2019	Inlet
Peter Thodie	BoPRC	ICP-MS	2018/2019	Inlet
Orchard	BoPRC	ICP-MS	2018/2019	Inlet
Peter Thodie NW	BoPRC	ICP-MS	2018/2019	Inlet
Ramp 4 Jetty Stream	BoPRC	ICP-MS	2018/2019	Inlet
Rotomahana Rockslide	BoPRC	ICP-MS	2018/2019	Inlet
Small Spring	BoPRC	ICP-MS	2018/2019	Inlet
Small Twin Creek	BoPRC	ICP-MS	2018/2019	Inlet
Te Wairoa St	BoPRC	ICP-MS	2018/2019	Inlet
WA1	BoPRC	ICP-MS	2018/2019	Inlet
Wairea Hotpool	BoPRC	ICP-MS	2018/2019	Inlet
Wairua	BoPRC	ICP-MS	2018/2019	Inlet
Wairua Arm Dancing Sands	BoPRC	ICP-MS	2018/2019	Inlet

Waitangi Stream	BoPRC	ICP-MS	2018/2019	Inlet
Corner Pool	BoPRC	ICP-MS	2018/2019	Inlet
HW1	BoPRC, UOW	ICP-MS, HPLC, totals	2018/2019, 2019/2020	Inlet
HW2	BoPRC, UOW	ICP-MS, HPLC, totals	2018/2019, 2019/2020	Inlet
Middle Flax A	BoPRC, UOW	ICP-MS, HPLC, totals	2018/2019, 2019/2020	Inlet
Outlet	BoPRC, UOW	ICP-MS, HPLC, totals	2018/2019, 2019/2020	Outlet
Rotomahana Siphon	BoPRC, UOW	ICP-MS, HPLC, totals	2018/2019, 2019/2020	Inlet
Rotomahana Spring	BoPRC, UOW	ICP-MS, HPLC, totals	2018/2019, 2019/2020	Inlet
Rotomahana Waterfall	BoPRC, UOW	ICP-MS, HPLC, totals	2018/2019, 2019/2020	Inlet
WR1	UoW	ICP-MS, HPLC, totals	2019/2020	Inlet
TAs1	UoW	ICP-MS, HPLC, totals	2019/2020	open-water
TAs2	UoW	ICP-MS, HPLC, totals	2019/2020	open-water
TAs3	UoW	ICP-MS, HPLC, totals	2019/2020	open-water
TAs4	UoW	ICP-MS, HPLC, totals	2019/2020	open-water
TAs5	UoW	ICP-MS, HPLC, totals	2019/2020	open-water